

# **RAMAIAH INSTITUTE OF TECHNOLOGY**

(Autonomous Institute, Affiliated to Visvesvaraya Technological University, Belagavi)

Bangalore-560054



Major Project Report On

## **DESIGN AND MANUFACTURE OF ANTENNA DEPLOYMENT MECHANISM OF 2U VOLUME FOR CUBE SATELLITES**

Submitted in Partial Fulfilment of the Requirement for the award  
of

**Bachelor of Engineering in Mechanical Engineering**

By:

1MS17ME008            Achintya S

1MS17ME011            Aditya K N

1MS17ME103            N Ria Bopanna

1MS17ME133            Rajatsurya M

Under the guidance of

**Dr. K Lokesh**

Assistant Professor, Department of Mechanical Engineering

Ramaiah Institute of Technology, Bangalore-560054

2020-21

# **RAMAIAH INSTITUTE OF TECHNOLOGY**

**(Autonomous Institute, Affiliated to Visvesvaraya Technological University, Belgagavi)**

**Bangalore-560054**



## **CERTIFICATE**

This is to certify that the project work titled "**Design and Manufacture of Antenna Deployment Mechanism of 2U Volume for Cube Satellites**" is a Bonafide work carried out by: **Achintya S (1MS17ME008), Aditya K N (1MS17ME011), N Ria Bopanna (1MS17ME103) and Rajatsurya M (1MS17ME133)** in partial fulfillment of the award of the Degree of Bachelor of Engineering in Mechanical Engineering during the year 2020-21. It is certified that all corrections/suggestions indicated for continuous internal assessment have been incorporated in the report submitted to the department. To the best of our knowledge, this report does not contain any work which has been previously carried out by others and the report has been approved as it satisfies the academic requirements in respect of Project work prescribed for the Bachelor of Engineering Degree.

**DR. K LOKESHA**

**Guide**

**DR RAJI GEORGE**

**Head of Department**

**DR NVR NAIDU**

**Principal, RIT**

Name & Signature of External Examiner: -

- 1) \_\_\_\_\_
- 2) \_\_\_\_\_
- 3) \_\_\_\_\_

# **RAMAIAH INSTITUTE OF TECHNOLOGY**

**(Autonomous Institute, Affiliated to Visvesvaraya Technological University, Belgaum)**

**Bangalore-560054**

## **DEPARTMENT OF MECHANICAL ENGINEERING**

### **DECLARATION**

We hereby declare that the entire work embodied in this project has been independently carried out by us under the supervision of internal guide **Dr. K Lokesh**, Assistant Professor, Department of Mechanical Engineering, **Ramaiah Institute of Technology, Bangalore** in partial fulfillment of the requirement of the **Bachelor of Degree in Mechanical Engineering**. We further declare that the report has not been submitted either in part or in full to any other university for the award of any Degree.

#### **Signature of Students:**

**1. Achintya S (1MS17ME008)**

**2. Aditya K N (1MS17ME011)**

**3. N Ria Bopanna (1MS17ME103)**

**4. Rajatsurya M (1MS17ME133)**

# **RAMAIAH INSTITUTE OF TECHNOLOGY**

**(Autonomous Institute, Affiliated to Visvesvaraya Technological University, Belagavi)**

**Bangalore-560054**

## **DEPARTMENT OF MECHANICAL ENGINEERING**

### **ACKNOWLEDGEMENT**

First and foremost,

We would like to express our deepest gratitude for the invaluable guidance of our Guide Dr. K Lokesh, Assistant Professor, Department of Mechanical Engineering, Ramaiah Institute of Technology, Bangalore, for all his guidance and help. We are immensely grateful to Dr. Raji George, Professor and Head, Department of Mechanical Engineering, Ramaiah Institute of Technology, Bangalore, for his invaluable support. We are extremely thankful to Dr. NVR Naidu, Principal, Ramaiah Institute of Technology, for creating an atmosphere of Research and Development in the College and encouraging us to initiate research activities. Additionally, we would like to thank Nihal S Manvi, student at IIT Madras for his inputs. We are also grateful to Suresh Kumar H N, employee at ISRO for his feedback throughout the project.

## **ABSTRACT**

The valuable data provided by satellites are of paramount importance in applications like achieving sustainability, climate goals, defense, telecommunications, etc. The size of these satellites has decreased, reducing their costs. CubeSats are 4-inch cubes and weigh about 3 pounds. Such basic CubeSat units can be combined to form slightly larger spacecraft while conforming to the same configurations and constraints. Multiples of the basic CubeSat unit are combined together to establish larger CubeSats. For example, a 1-Unit CubeSat measures one single basic CubeSat unit as described above, while a 3-Unit CubeSat consists of 3 standard CubeSat units stacked vertically. The CubeSat concept has become very popular, both in university groups, as well as for researchers, space agencies, governments, and companies. CubeSats offer a fast and affordable way for a wide array of stakeholders to be active in space and allow for a fast innovation cycle.

This project seeks to address the limited availability of an efficient and easy-to-manufacture deployment system of satellite booms that can be integrated into CubeSats through the design and fabrication of a novel mechanism. A two-stage deployment scheme is developed to thrust the boom to the outside of the spacecraft via compression springs, then unfurl the petals with a tether.

# Table of Contents

<b>1</b>	<b>Introduction .....</b>	<b>1</b>
1.1	Context of the Project .....	1
1.2	What is a CubeSat?.....	1
1.3	Deployable Boom of Satellite .....	2
<b>2</b>	<b>Literature Survey .....</b>	<b>3</b>
<b>3</b>	<b>Problem Definition .....</b>	<b>4</b>
<b>4</b>	<b>Objectives.....</b>	<b>5</b>
<b>5</b>	<b>Methodology.....</b>	<b>6</b>
5.1	Design of Parts of Mechanism.....	6
5.2	Design of Locking Mechanism .....	6
5.3	Virtual Assembly and Interference Analysis.....	6
5.4	Static and Dynamic Analysis .....	6
5.5	Design and Manufacture of Electronic Actuators .....	6
5.6	Additive Manufacturing and Assembly .....	7
5.7	Testing and Validation of Proof of Assembly .....	7
<b>6</b>	<b>Components of the Assembly .....</b>	<b>8</b>
<b>7</b>	<b>Design and Function of the Components.....</b>	<b>10</b>
7.1	Design of Box.....	10
7.2	Design of Lid .....	11
7.3	Design of Hinges.....	12
7.3.1	Female Hinge .....	12
7.3.2	Male Hinge.....	13
7.3.3	Hinge Pin.....	14
7.3.4	Previous Design Iterations.....	14
7.4	Design of Torsion Spring.....	15
7.4.1	Calculations for Design of Torsion Spring.....	16
7.5	Design of Compression Springs .....	18
7.5.1	Calculation for Design of Compression Spring .....	19
7.6	Radio Frequency Plates .....	22
7.7	Antenna Hub.....	23
7.7.1	Base of the Antenna Hub.....	24
7.7.2	Slits of the Antenna Hub.....	25
7.8	Guiding Columns in the Box .....	26
7.9	Blocking Part.....	27
7.9.1	Alternate Design considerations for the Blocking part .....	27
7.10	Locking Mechanism .....	28

7.10.1	Male Locking Part .....	29
7.10.2	Female Locking Part.....	29
7.10.3	Alternate Design of Locking Mechanism .....	30
<b>8</b>	<b>Assembly and Kinematic Simulation of Components.....</b>	<b>32</b>
8.1	Assembly of Hinge .....	32
8.2	Assembly of Torsion Spring .....	32
8.3	Assembly of the Box .....	33
8.4	Assembly of Guiding Columns .....	33
8.5	Assembly of Antenna Hub on base .....	35
8.6	Assembly of Antenna Hub on columns .....	36
8.7	Assembly of Blocking Plate.....	36
8.8	Assembly of Male Locks .....	37
8.9	Assembly of Female Locks.....	38
8.10	Kinematic Simulation.....	39
8.10.1	Brief introduction of DMU Kinematic Catia V5.....	39
8.10.2	Wireframe environment of Catia V5 .....	40
8.10.3	Application of DMU Kinematic and Wireframe Modeling.....	40
8.11	Antenna Deployment Mechanism - Design 2.....	47
8.11.1	Columns - Design 2 .....	47
8.11.2	Antenna Hub Design 2 .....	47
8.11.3	Spring Design 2 .....	48
8.11.4	Assembly of Different Components - Design 2.....	49
8.11.5	Reasons for Failure of Design 2 .....	50
8.12	Alternate Booming Mechanism.....	50
<b>9</b>	<b>Dynamic Analysis of Spring Forces .....</b>	<b>52</b>
<b>10</b>	<b>Contact Analysis and Finite Element Analysis .....</b>	<b>57</b>
10.1	Introduction to Contact Analysis .....	57
10.1.1	Contact Analysis of Antenna Bub, Base and Blocking Part.....	59
10.1.2	Contact Analysis between Columns and Base of the Antenna Hub .....	60
10.1.3	Contact Analysis between Columns and Blocking Part .....	61
10.1.4	Contact Analysis between Flexible Plate and Female Locks.....	61
10.1.5	Contact Analysis between Box and Lid.....	62
10.2	Finite Element Analysis.....	63
10.2.2	FEA of the lid.....	67
10.2.3	FEA of the pin .....	68
10.2.4	FEA of Torsion Springs .....	70
10.2.5	FEA of the Box.....	74

10.2.6	Antenna Hub FEA.....	76
10.2.7	FEA of the Compression Springs.....	77
10.2.8	FEA of the Blocking Part .....	79
10.2.9	Analysis of Contact Regions.....	81
10.2.10	FEA of Locking Mechanism.....	82
<b>11</b>	<b>Fabrication of Antenna Deployment Mechanism .....</b>	<b>85</b>
11.1	FEA of PLA – Polylactic acid .....	85
11.2	Additive Manufacturing & Assembly of Components.....	88
<b>12</b>	<b>Result and Discussion .....</b>	<b>91</b>
<b>13</b>	<b>Conclusion and Scope for Future Work.....</b>	<b>92</b>
<b>14</b>	<b>References.....</b>	<b>93</b>

## LIST OF TABLES

TABLE 6.1: COMPONENTS.....	8
6.2 9	
TABLE 7.1: INCH TO MILLIMETRE CONVERSIONS 1.....	17
TABLE 7.2: INCH TO MILLIMETRE CONVERSION TABLE 2 .....	20

## LIST OF FIGURES

FIGURE 1.1: CUBESAT CONFIGURATIONS 1 .....	1
FIGURE 1.2: CONFIGURATIONS 2.....	2
FIGURE 1.3: DEPLOYABLE BOOM .....	2
6.1: LABELLED COMPONENTS .....	8
7.1: 3D MODEL OF BOX.....	11
7.2: 2D DRAWING OF BOX .....	11
7.3: 2D DRAWING OF LID.....	12
7.4: 3D MODEL OF LID .....	12
FIGURE 7.5: 3D MODEL OF FEMALE HINGE .....	13
FIGURE 7.6: 3D MODEL OF MALE HINGE .....	13
FIGURE 7.7: 2D DRAWING OF MALE HINGE.....	13
FIGURE 7.8: 2D DRAWING OF HINGE PIN .....	14
FIGURE 7.9: 3D MODEL OF HINGE PIN .....	14
FIGURE 7.10: PREVIOUS MALE HINGE DESIGN DRAWING .....	15
FIGURE 7.112 - 3D MODEL OF TORSION SPRING .....	16
FIGURE 7.12 - DRAWING OF COMPRESSION SPRING .....	19
FIGURE 7.13 - 3D MODEL OF COMPRESSION SPRING.....	19
FIGURE 7.14 - FEA OF COMPRESSION SPRING .....	22
FIGURE 7.15-RF PLATES WRAPPED AROUND THE ANTENNA HUB.....	23
FIGURE 7.16-COMPOSITION OF THE RF PLATES .....	23
FIGURE 7.17: 3D MODEL OF ANTENNA HUB .....	24
FIGURE 7.18: 2D DRAWING OF ANTENNA HUB .....	24
FIGURE 7.20.19: 3D MODEL OF BASE PLATE.....	25
FIGURE 7.20: 2D DRAWING OF BASE PLATE AND HUB .....	25
FIGURE 7.21: TOP VIEW OF HUB .....	25
FIGURE 7.22: PROFILE VIEW OF HUB SHOWING SLITS .....	25
FIGURE 7.23: 3D MODEL OF GUIDING COLUMNS .....	26
FIGURE 7.24: 2D DRAWING OF GUIDING COLUMNS.....	26
FIGURE 7.25: 2D DRAWING OF BLOCKING PLATE.....	27

FIGURE 7.26: 3D MODEL OF BLOCKING PLATE .....	27
FIGURE 7.27-2D DRAFT OF ALTERNATE DESIGN .....	28
FIGURE 7.28: 3D MODEL OF ALTERNATE BLOCKING PART.....	28
FIGURE 7.29-2D DRAFT OF THE MALE LOCKING PART.....	29
FIGURE 7.30-ISOMETRIC VIEW OF MALE LOCKING PART.....	29
FIGURE 7.31-FLEXIBLE PLATE PRESENT INSIDE THE FEMALE LOCKING PART .....	30
FIGURE 7.32-2D VIEW OF THE FEMALE LOCKING PART .....	30
FIGURE 7.33-ISOMETRIC VIEW OF THE FEMALE LOCKING PART .....	30
FIGURE 7.35-MALE LOCKING PART OF ALTERNATE DESIGN .....	31
FIGURE 7.34-FEMALE LOCKING PART OF THE ALTERNATE DESIGN.....	31
FIGURE 8.1: ASSEMBLY OF HINGE .....	32
FIGURE 8.2: TORSION SPRING ON MATING PIN.....	32
FIGURE 8.3: ASSEMBLED TORSION SPRING.....	32
FIGURE 8.4 - ASSEMBLY OF BOX .....	33
FIGURE 8.5-M3 SCREW FOR MOUNTING THE COLUMNS .....	34
FIGURE 8.6-BASE OF THE BOX WITH M3 SCREW HOLES.....	34
FIGURE 8.7-BASE OF THE COLUMNS WITH SCREW HOLES.....	34
FIGURE 8.8-M3 SCREW HOLES TO MOUNT ANTENNA HUB.....	35
FIGURE 8.9-M3 SCREWS TO MOUNT ANTENNA HUB .....	35
FIGURE 8.10-ASSEMBLY OF THE ANTENNA HUB AND COLUMNS .....	36
FIGURE 8.11: ALIGNMENT OF BLOCKING PLATE WITH COLUMN .....	36
FIGURE 8.12: ASSEMBLY OF BLOCKING PART IN BOX .....	36
FIGURE 8.13-M1.6 SCREWS TO MOUNT THE MALE LOCKS.....	37
FIGURE 8.14: SCREW HOLES ON BASE.....	38
FIGURE 8.15-MALE LOCKS ASSEMBLED ON BASE .....	38
FIGURE 8.16-M1.6 SCREW HOLES TO MOUNT THE FEMALE LOCKS.....	39
FIGURE 8.17-FEMALE LOCKS ASSEMBLED UNDERNEATH THE BLOCKING PART .....	39
FIGURE 8.18: SCREWHOLES OF THE FEMALE LOCK .....	39
FIGURE 8.19-THE DIFFERENT TYPES OF JOINTS PRESENT IN DMU KINEMATIC .....	40
FIGURE 8.20: JOINT 1 IN ANTICLOCKWISE DIRECTION TO SIMULATE THE LID OPENING .....	41
FIGURE 8.21: REVOLUTE JOINT 2 IN ANTICLOCKWISE DIRECTION.....	41
FIGURE 8.22: PRISMATIC JOINT .....	42
FIGURE 8.23: THE LID OPENING .....	42
FIGURE 8.24: 90 DEGREES .....	43
FIGURE 8.25: 180 DEGREES .....	43
FIGURE 8.26: LID OPENED.....	43
FIGURE 8.27-SPECIFICATIONS OF THE PRISMATIC JOINT TO SIMULATE THE DEPLOYMENT OF ANTENNA HUB .....	44
FIGURE 8.28: START OF DEPLOYMENT OF THE ANTENNA HUB .....	45
FIGURE 8.29: INTERMEDIATED POSITION .....	45
FIGURE 8.30: FINAL POSITION OF THE ANTENNA HUB AFTER DEPLOYMENT .....	45

FIGURE 8.31: BOOMING PROCESS UNDERWAY.....	46
FIGURE 8.32: BEFORE BOOMING .....	46
FIGURE 8.33: FULLY BOomed PLATES .....	46
FIGURE 8.34: 3D MODEL OF DESIGN 2 COLUMN.....	47
FIGURE 8.35: 2D DRAWING OF COLUMN - DESIGN 2 .....	47
FIGURE 8.36: 2D DRAWING OF DESIGN 2 HUB.....	47
FIGURE 8.37: 3D MODEL OF DESIGN 2 HUB.....	47
FIGURE 8.38: 3D MODEL OF SPRING - DESIGN 2 .....	48
FIGURE 8.39: 2D DRAWING OF SPRING - DESIGN 2 .....	48
FIGURE 8.40: DESIGN 2 ASSEMBLY OF HUB ON COLUMN .....	49
FIGURE 8.41: DESIGN 2 ASSEMBLY OF SPRING ON COLUMN.....	49
FIGURE 8.42: RADIAL BOOMING.....	51
FIGURE 8.43: TANGENTIAL BOOMING.....	51
9.1ds55	
FIGURE 10.10.1: BONDE10.2D CONTACT .....	58
FIGURE 10.10.3: NO SEPARATION CONTACT .....	58
FIGURE 10.10.4: FRICTIONLESS CONTACT .....	58
FIGURE 10.10.5-ROUGH CONTACT DEPICTION.....	59
FIGURE 10.6-FRICTIONAL CONTACT DEPICTION .....	59
FIGURE10.10.7: CONTACT ANALYSIS BETWEEN BASE AND BLOCKING PART .....	60
FIGURE 10.10.8: CONTACT ANALYSIS BETWEEN COLUMNS AND ANTENNA HUB .....	60
FIGURE10.10.9: CONTACT ANALYSIS BETWEEN COLUMNS AND BLOCKING PART.....	61
FIGURE 10.10.10: CONTACT ANALYSIS BETWEEN FEMALE LOCK AND FLEXIBLE PLATE.....	62
FIGURE 10.10.11: CONTACT ANALYSIS BETWEEN FLEXIBLE PLATE'S BOTTOM END AND FEMALE LOCK .....	62
FIGURE 10.10.12: CONTACT ANALYSIS BETWEEN BOX AND LID .....	63
FIGURE10.10.13: PROPERTIES OF ALUMINIUM ALLOY 7705 .....	64
FIGURE10.10.14: PROPERTIES OF STRUCTURAL STEEL S460 .....	65
FIGURE10.10.15: PROPERTIES OF BERYLLIUM COPPER .....	66
FIGURE10.10.16-APPLICATION OF FORCE AND SUPPORT STRUCTURES ON LID.....	67
FIGURE 10.10.17: RESULTS OF FEA OF LID MADE OF ALUMINIUM .....	67
FIGURE10.10.18: RESULT OF FEA OF LID MADE OF STRUCTURAL STEEL .....	68
FIGURE 10.10.19-APPLICATION OF TORQUE ON HINGE PIN.....	69
FIGURE10.10.20: RESULTS OF FEA OF HINGE PIN USING STRUCTURAL STEEL .....	69
FIGURE10.10.21: RESULT OF FEA OF PIN MADE OF BERYLLIUM COPPER.....	70
FIGURE 10.10.22: APPLICATION OF TORQUE AND FIXED SUPPORTS ON TORSION SPRINGS .....	73
FIGURE10.10.23: RESULT OF FEA OF TORSION SPRINGS MADE OF BERYLLIUM COPPER .....	73
FIGURE10.10.24: RESULT OF FEA OF TORSION SPRING MADE OF STRUCTURAL STEEL.....	74
FIGURE 10.10.25: SUPPORT STRUCTURES AND APPLICATION OF FORCE ON BOX.....	74
FIGURE10.10.26: RESULT OF FEA OF BOX MADE OF ALUMINIUM.....	75
FIGURE10.10.27: RESULT OF FEA OF BOX MADE OF STRUCTURAL STEEL.....	75

FIGURE 10.10.28: APPLICATION OF SUPPORT STRUCTURES AND FORCE ON ANTENNA HUB .....	76
FIGURE 10.10.29: STRUCTURAL SUPPORT AND FORCES ON COMPRESSION SPRINGS.....	78
FIGURE 11.1: MATERIAL PROPERTIES OF PLA .....	85
FIGURE 11.2: FEA OF LID USING PLA .....	86
FIGURE 11.3: FEA OF HINGE PIN USING PLA .....	86
FIGURE 11.4: FEA OF BOX USING PLA.....	86
FIGURE 11.5: FEA OF ANTENNA HUB USING PLA .....	87
FIGURE 11.6: FEA OF BLOCKING PLATE USING PLA.....	87
FIGURE 11.7: FEA OF CONTACT REGIONS USING PLA.....	87
FIGURE 11.8: FEA OF CONTACT REGIONS USING PLA 2.....	88
FIGURE 11.9: FDM PRINTER.....	88
FIGURE 11.10: PRINTING OF BOX .....	88
FIGURE 11.11: PRINTING OF BASE .....	89
FIGURE 11.12: FABRICATED HINGE PIN.....	89
FIGURE 11.13: FABRICATED BOX W/ MALE HINGE.....	89
FIGURE 11.14: FABRICATED LID W/ FEMALE HINGE .....	89
FIGURE 11.15: FABRICATED BLOCKING PLATE .....	90
FIGURE 11.16: FABRICATED COMPONENTS.....	90
FIGURE 11.17: FABRICATED ANTENNA HUB.....	90
FIGURE 11.18: ASSEMBLED BOX & LID .....	90

# 1 Introduction

## 1.1 Context of the Project

Since the advent of space science and exploration, the uses and applications of space technology has been an expanding frontier. Having found crucial roles in such applications as telecommunications, defense, intelligence, meteorology, climate science, space exploration and others, space science and technology is an area of constant research and development. Among the many areas of improvement, concerning many engineering disciplines, is the design and material science of mechanisms of the satellite, including construction of the container, design of communication mechanisms – antenna, transponders, etc., and development of applications of the satellite. In this regard, this project is an attempt at rethinking the deployment booming mechanism of the antenna hub of a cube-satellite with a 2U configuration.

## 1.2 What is a CubeSat?

Satellites come in varying sizes. Of these, a small satellite is typically one that weighs less than 300 kg. A CubeSat is one such satellite with definite criteria controlling its shape, size, and weight. These conformity requirements help standardize the satellites, reducing costs and making it easy to create off-the-shelf parts.

They come in configurations that are multiples of a unit configuration, called 1U – for example 1U, 1.5U, 2U, 3U, 6U, etc. – as defined by NASA. A 1U CubeSat is 10 cm cube weighing between 1 kg and 1.33 kg. A 3U, therefore has dimensions 10×10×34 cubic centimeters, and so on.



*Figure 1.1: CubeSat Configurations 1*

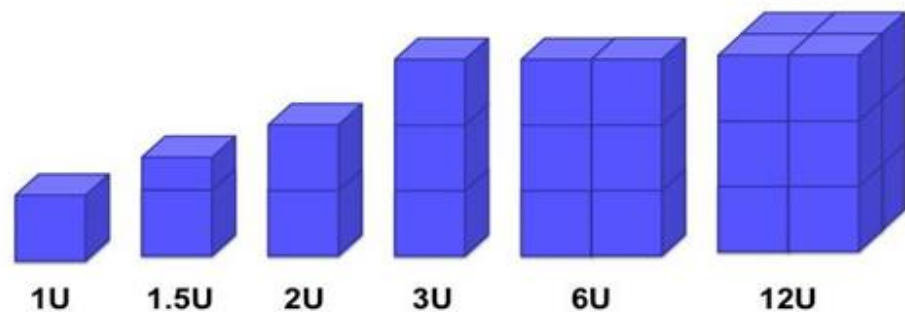


*Figure 1.2: Configurations 2*

### 1.3 Deployable Boom of Satellite

Since avionics have been miniaturized, satellites have grown smaller in size. Due to this, antennae, solar sails, etc. have to be compacted and deployed as booms. These booms can then be incorporated into small satellite systems. The deployment of such a booming mechanism is the subject of this project.



*Figure 1.3: Deployable Boom*

## 2 Literature Survey

A portion of the instigating information was contained in “The 42<sup>nd</sup> Aerospace Mechanism Symposium”, which provides a forum for those active in the design, production and use of aerospace mechanisms. A major focus is the reporting of problems and solutions associated with the development and flight certification of new mechanisms. The fields of current interest and development, including the project’s subject matter were included there. The configurations and standardizations were obtained in the official NASA website, included in their e-pamphlet titled “CubeSat101: Basic Concepts and Processes for First-Time CubeSat Developers”, as well as their design guides “CubeSat Design Specification (CDS)” at [www.cubesat.org](http://www.cubesat.org). Further contextualization, and updates on the current technologies were provided by other technical articles and scientific papers published presently. Details regarding the specificities of the requirements were ironed out in these papers, making the focusing of this project accurate and precise.

An alternate mechanism present in the 42<sup>nd</sup> Aerospace mechanical symposium, which yielded the same result as this project, deployed differently. The deployment used two sets of torsion springs for both the de-containment and deployment procedures. This project uses one set of torsion springs for de-containment and a set of compression springs for the deployment, to achieve the same desired outcome. The problem with the former is the presence of unbalanced forces and expensive mitigating mechanisms. As a result, the idea to develop a simpler, effective design was seeded.

All the sources are mentioned in the “References” section.

### **3 Problem Definition**

One of the principal issues with the design, manufacture and launching of CubeSats is the accommodation of hardware in them that can undertake their required functions. Due to the large volume of such key equipment as antennae, sails, etc. (of the order of 10 sq meters to 100 sq. meters), they need to be compacted and stowed away in the relatively small CubeSats (multiples of 100 sq. centimeters). When this problem is taken on, it gives rise to another challenge – of deploying the boom. In other words, there is a limited availability of mechanisms that can inexpensively, efficiently and effectively deploy these booming systems to the outside of the satellite at the required point in space and time after being launched.

This project seeks to address this limited availability of deployment systems by designing, manufacturing and demonstrating the proof of concept of a novel Antenna Deployment System.

## 4 Objectives

The broad objective of the project is to design a mechanism within a CubeSat of 2U configuration that, upon instigation, opens up and thrusts out the antenna hub stowed within for boozing. In order to achieve the same, the project was divided into a number of smaller sequential objectives, namely:

- Development of Suitable Mechanism
- Design of Mechanism and Incorporation into 2U CubeSat
- Static and Dynamic Condition Analysis for Various Materials
- Fabrication of Preliminary Model
- Testing and Validation of Proof of Concept

## 5 Methodology

In order to accomplish the aforementioned objectives, the methodology of the project was sequentially divided as follows.

### 5.1 Design of Parts of Mechanism

The different parts of the mechanism are to conform to the 2U configuration as well as be mechanically sound. In addition, the tolerances and spacing between and among parts were to comply with the requirements of the additive manufacturer for fabrication.

### 5.2 Design of Locking Mechanism

In addition to the parts of the mechanism itself, a locking mechanism to hold the satellite closed until time of deployment was necessary. This was to conform to the spatial restrictions outside the CubeSat, as well as be able to withstand loading.

### 5.3 Virtual Assembly and Interference Analysis

The separate designs of the parts and mechanisms were then to be put together in a logical way such that the intended function was performed. Also, the meshing of the parts was to be in such a way that no interference between materials occurs.

### 5.4 Static and Dynamic Analysis

The designs were then to be analyzed for soundness of structure under static and dynamic loading conditions. Finite Element Method was done to closely approximate the effects of loading.

### 5.5 Design and Manufacture of Electronic Actuators

Electronic actuators were required to release the locking mechanism of the satellite lid and push the antenna hub outward. These were to be designed and manufactured accordingly.

## 5.6 Additive Manufacturing and Assembly

The 3D models of part assemblies were to be converted to 3D Printing supported formats and outsourced for additive manufacturing. The printed parts were then to be put together into a functional assembly.

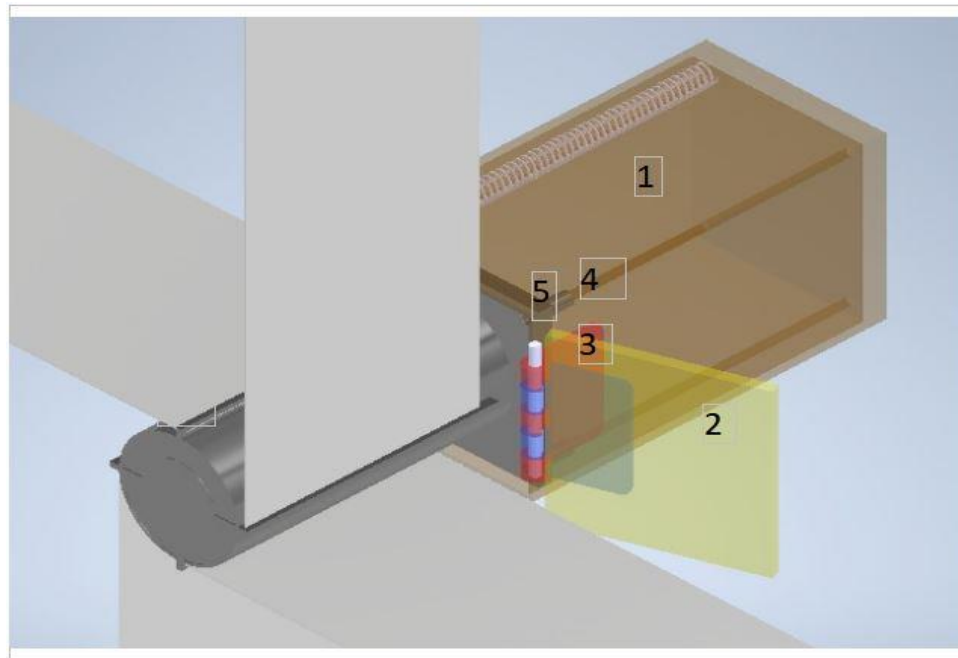
## 5.7 Testing and Validation of Proof of Assembly

The assembly was to be tested for functionality and mechanical soundness and validated as a Proof of Concept.

## 6 Components of the Assembly

The assembled satellite containing the mechanism is shown in the figure below.

Corresponding component parts are labelled in the table following the same.



*6.1: Labelled Components*

*Table 6.1: Components*

Part Name	Part Number	Material Composition
1	Box	Aluminium
2	Lid	Aluminium
3	Hinge (Female)	Beryllium Copper
4	Hinge (Male)	Beryllium Copper
5	Hinge Pin	Beryllium Copper / Steel
6	Compression Spring	Beryllium Copper
7	Torsion Spring	Beryllium Copper
8	RF Plate	Beryllium Copper

9	Antenna Hub	Aluminium
10	Guide Columns	Aluminium
11	Blocking Plate	Aluminium
12	Lock	Aluminium

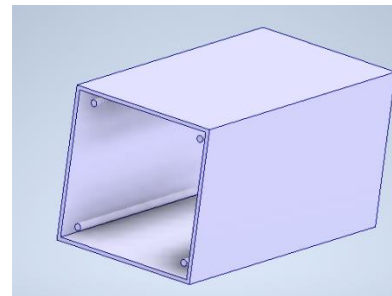
6.2

## 7 Design and Function of the Components

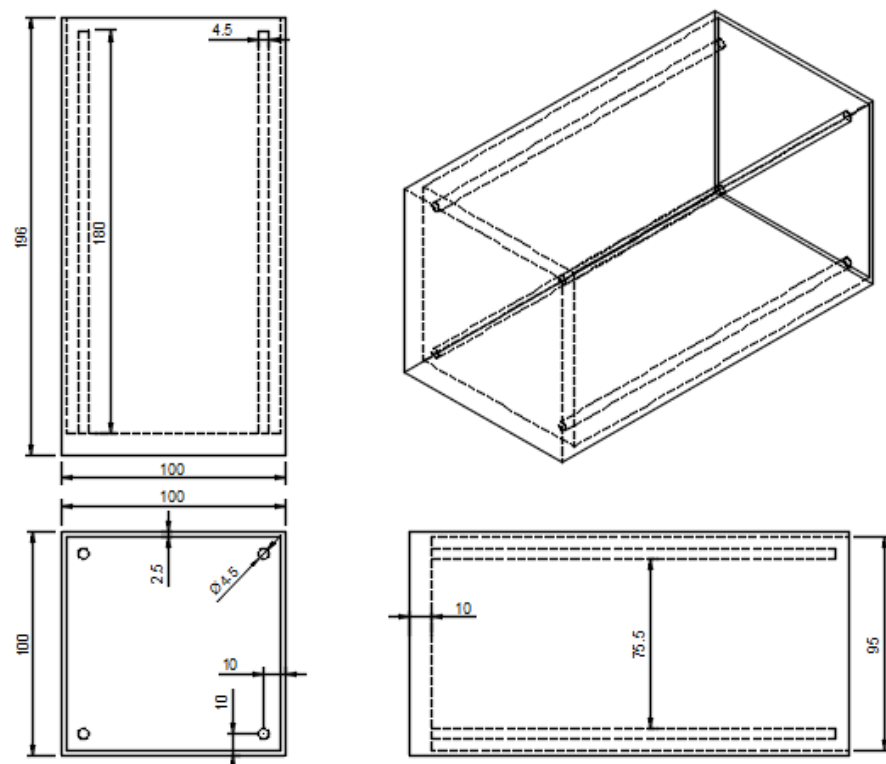
### 7.1 Design of Box

The box is the outer container in which the entire mechanism is stowed, along with other avionics. Its main function is to contain the antenna hub and its associated mechanism within a restricted space. Additionally, it also absorbs part of the impulse forces imparted by the lid. The antenna hub, RF plates and compression springs are contained within the box until the entire booming mechanism is actuated. It also contains smooth cylindrical rods attached vertically to the base of the box which is used to guide the motion of the antenna hub out of the box. The electronics required for the actuation of the booming mechanism is also housed inside the box and on its base. The design of the box is critical as it defines the outer limits of the mechanism which ultimately decides the type and size of antenna that can be integrated into the mechanism and hence the type of data the satellite can receive and transmit.

The dimensions of the base of the box are 100 X 100 mm. The total height of the box is 196 mm. This is in keeping with the 2U volume limit. It is made of Aluminium to reduce the weight of the box. The thickness of the walls of the box is 2.5 mm. Thickness is kept to a minimum in order to reduce the amount of material which, in turn, reduces both material costs and weight. However, it is ensured that sufficient material is present on the walls of the box to absorb the impulsive forces imparted by the swinging of the lid. The thickness of the base of the box is 10 mm. The base provides a strong foundation for the cylindrical rods. It also provides a base for the mounting of the various electronic components and sensors required for the actuation of the mechanism. These components will sit between the base of the box and the base plate of the antenna hub. The four cylindrical rods of 4.5 mm diameter present on the base are used to guide the extension of the compression springs and thereby the motion of the antenna hub. The hub slots onto these rods with the help of holes present in its base plate and is therefore constrained to move linearly upwards. The box acts as an anchoring point for the male hinge which is used in the opening of the lid.



7.1: 3D Model of Box

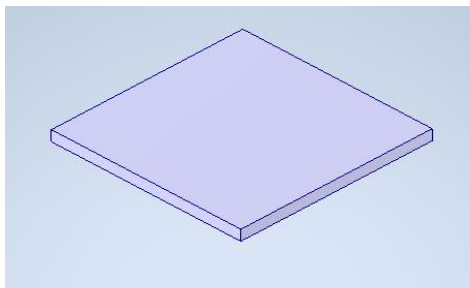


7.2: 2D Drawing of Box

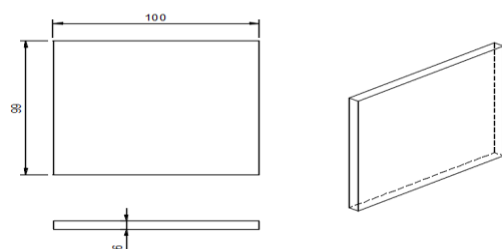
## 7.2 Design of Lid

The lid is a component present on the open face of the box whose main function is to contain the antenna hub until it is ready for deployment. It also ensures that no external environmental factors like dust and moisture hamper the functioning of the sensitive electromechanical components present within the box. It is mated to the box by means of a revolute joint comprising of a male and female hinge. The motion of these hinges and, by extension, the motion of the lid is actuated by means of a torsion spring present on the hinge pin.

The lid has a simple cuboidal design of dimensions 100 X 99 X 6 mm. It is made of Aluminium. It can be observed that one of the sides of the lid is shorter than the other by the other by 1mm. This is done order to accommodate the hinge



7.4: 3D Model of Lid



7.3: 2D Drawing of Lid

## 7.3 Design of Hinges

Hinges are used to couple the lid to the box by means of a revolute joint. The design of hinges can be divided into two types, male, and female hinges. The male hinge is mated to the box while the female hinge is mated to the lid. The male and female hinges are, themselves, couple using a hinge pin. The pin allows the two hinges to rotate about a common axis and ensures smooth movement of the lid. The motion of these hinges is actuated by means of a torsion spring. The hinges are made of Beryllium-Copper.

### 7.3.1 Female Hinge

The design of the female hinge can be further divided into two parts, a rectangular plate and two concentric cylinders with holes. The rectangular plate is 60 X 36 mm and has 4 mm radius fillet on two vertices. It is 3 mm thick. The function of this plate is to provide a large area of contact for the mounting of the hinge onto the lid.

The concentric cylinders have a diameter and length of 12 mm with holes of diameter 6 mm through their centers and are placed 12 mm apart. These cylinders are aligned coaxially with the cylinders of the male hinge. The hinge pin then passes through the 6 mm holes to complete the revolute joint.

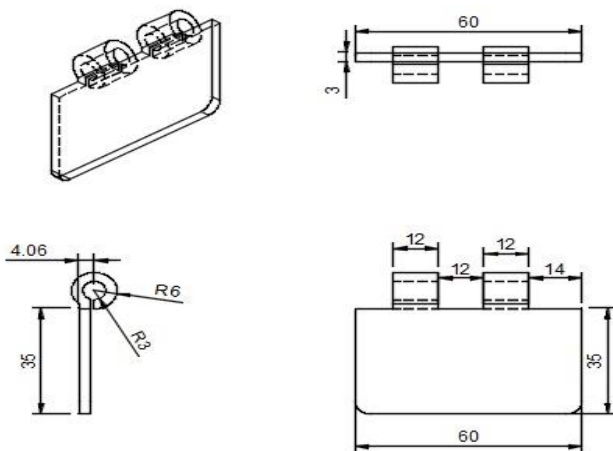


Figure 7.4: 2D Drawing of Female Hinge

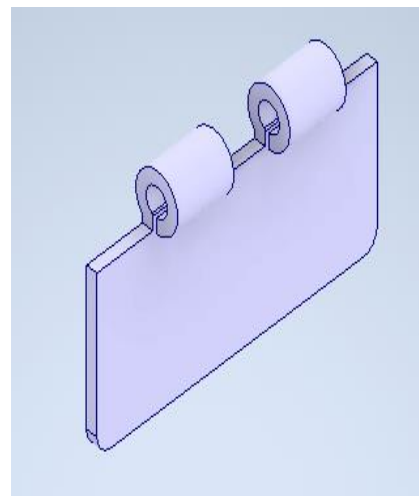


Figure 7.5: 3D Model of Female Hinge

### 7.3.2 Male Hinge

The design of the male hinge is broadly similar to that of the female hinge but for a few notable differences. The rectangular plate is increased in dimension to 60 X 36 mm. This ensures that the lid aligns perfectly with the top surface of the box when it is closed. The male hinge also has three cylindrical elements instead of just two like the female hinge. The distance between these cylinders has also been increased to 13 mm to provide a 1 mm clearance between the male and female hinges. Also, one of these cylinders has a further 3 mm extrusion that covers its hole completely on one side. This ensures that the pin is constrained within the hinges and does not move or dislodge during operation. Furthermore, the plane of the rectangular plate is tangential to the circumference of the cylinder, unlike the female hinge. This ensures that there is adequate space between the wall of the box and the female hinge so that it can fold back completely when opened. This also prevents interference between the lid and the RF plates when they are opened.

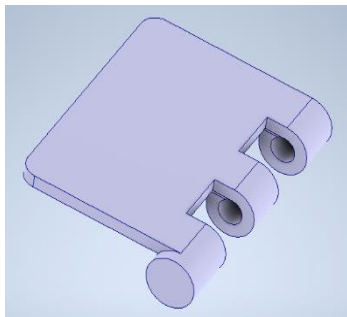


Figure 7.6: 3D Model of Male Hinge

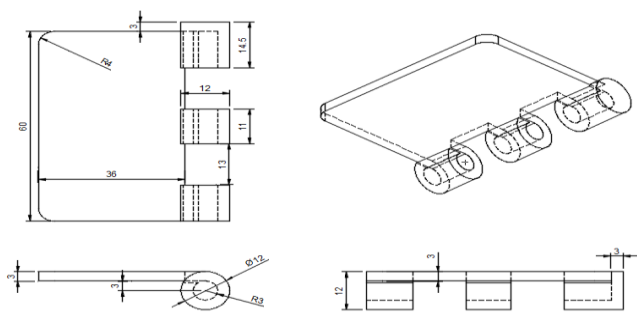


Figure 7.7: 2D Drawing of Male Hinge

### 7.3.3 Hinge Pin

The hinge pin is used to couple the male and female hinges. The female hinge rotates about the axis of the hinge pin while the male hinge remains fixed on the box which results in the opening motion of the box. It is also the part on which the torsion spring is mounted.

The hinge pin consists of a cylinder of diameter 5 mm and length 60 mm. This part passes through the holes of the cylindrical elements in the hinges. It also has a disc of diameter 12 mm and 3 mm thick on one of its ends. When, the cylinder passes through the hinges, the disc acts as a stopper and constrains the motion of the pin on one side. The other side is constrained by the male hinge. It is made of Aluminium.

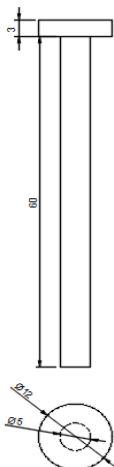


Figure 7.8: 2D Drawing of Hinge Pin



Figure 7.9: 3D Model of Hinge Pin

### 7.3.4 Previous Design Iterations

The initial design of the male hinge was identical to the female hinge. However, there was constant interference between the plate of the male hinge and the female hinge. This prevented the lid from opening out completely which, in turn, caused the edge of the lid to interfere with RF plates when they were deployed. The width of the hinge was also reduced from 80 mm to 60 mm as there was interference between RF plates and cylindrical elements of the hinges. As a result, this design was rejected, and the current design was adopted.

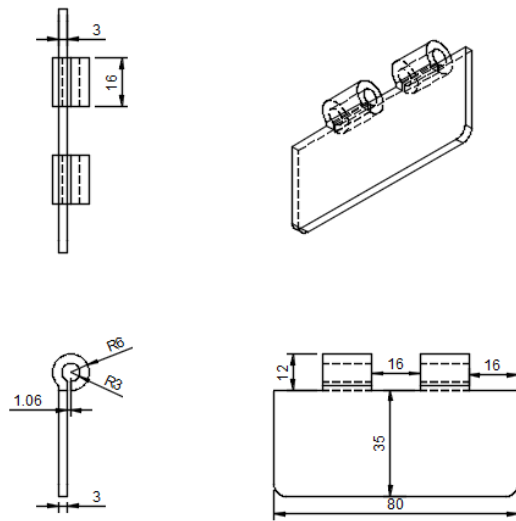


Figure 7.10: Previous Male Hinge Design Drawing

## 7.4 Design of Torsion Spring

A torsion spring is present on the hinge pin and is used to actuate the motion of the female hinge and lid. One end of the torsion spring is connected to the female hinge while the other is connected to the male hinge. When the lid is closed the torsion spring is in loaded condition. Thus, when the deployment mechanism is actuated, the torsion spring imparts a torque on the lid about the axis of the hinge pin which results in the opening of the lid. The torsion spring sits in the position as the cylindrical elements of the female hinge on the hinge pin. The torsion spring is made of Beryllium-Copper.

The torsion spring has a spring index of 7 in order to make it easier to manufacture. It has a wire diameter of 1.016 mm and a mean diameter of 7.112 mm. It has an internal diameter of 6.096 mm and therefore can easily fit around the pin of diameter 5 mm with a clearance of about 0.5 mm. This ensures reduced contact between hinge pin and torsion spring and therefore results in smoother operation of the lid assembly as a whole and also increases the operational life of the torsion spring. The angle traversed by lid from closed to open position is  $270^\circ$ . This results in a total deflection of 16.75 mm. Furthermore, it has been calculated to provide a torque of 131.308 N-mm and possesses a stiffness of 0.0278 Nm / rad.

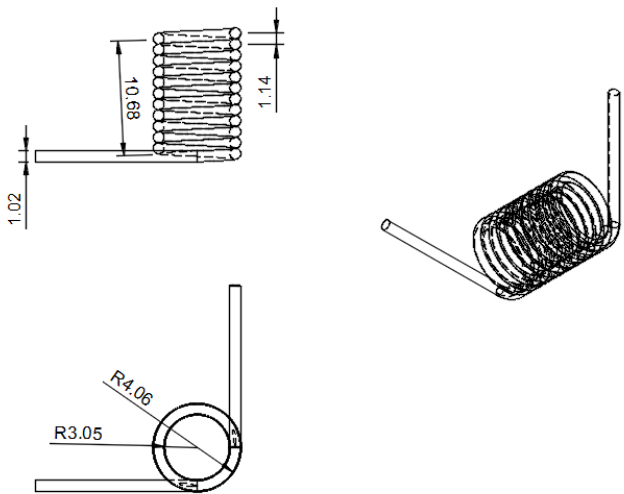


Figure 7.11 - Drawing of Torsion Spring

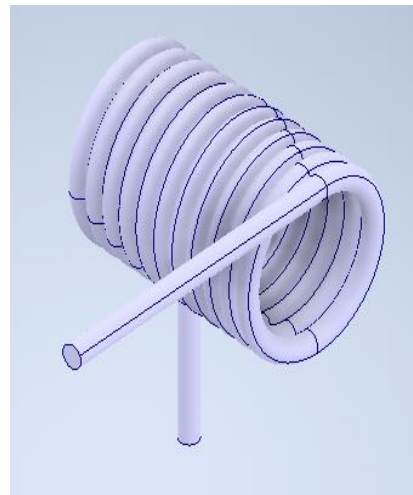


Figure 7.112 - 3D Model of Torsion Spring

#### 7.4.1 Calculations for Design of Torsion Spring

In order to come up with a practical design for the torsion spring, certain assumptions were made,

A spring index of 7 was assumed as spring indices between 6 and 12 are easy to manufacture for Beryllium-Copper material.

The inner diameter of the spring was assumed to be greater than or equal to 6 mm so that there would be a clearance of at least 0.5 mm between the spring and hinge pin when assembled. Also, the length is assumed to be 12 mm for the spring to fit between the hinges on the pin.

The material Beryllium-Copper was assumed to be isotropic and possessing uniform density.

Let,  $d$  = Wire diameter of Spring (mm)

$D$  = Mean diameter of Spring (mm)

$Di$  = Inner diameter of the spring (mm)

From assumptions we know that,

$$\text{Spring Index} = C = 7$$

$$\text{Length of Spring} = L = 12 \text{ mm}$$

$$Di \geq 6$$

Equation 7.4.1.1

$$C = D/d$$

Equation 7.4.1.2

$$Di = D - d$$

Equation 7.4.1.3

The values of wire diameter were substituted into equations 7.4.1.1, 7.4.1.2, 7.4.1.3 from the below table of wire diameters for Beryllium-Copper such that all three equations are satisfied.

0.033"	0.838 mm
0.034"	0.864 mm
0.035"	0.889 mm
0.036"	0.914 mm
0.037"	0.940 mm
0.038"	0.965 mm
0.039"	0.991 mm
0.040"	1.016 mm
0.041"	1.041 mm
0.042"	1.067 mm
0.043"	1.092 mm
0.044"	1.118 mm
0.045"	1.143 mm
0.046"	1.168 mm

Table 7.1: Inch to Millimeter Conversions I

We find the value of spring wire diameters is found to be 1.016 mm. We substitute this value in equation 7.4.1.2,

$$D = 7 \times 1.016 = 7.112$$

$$\text{Moment of Inertia } (I) = \frac{\pi d^4}{64} = \frac{\pi \times 1.016^4}{64} = 0.0523 \text{ mm}^4$$

$$\text{No. of active turns } (i) = \frac{L}{d} = \frac{12}{1.016} \approx 11$$

$$\text{Angle of Rotation } (\theta) = \frac{3\pi}{2} \text{ rad}$$

$$\text{Young's Modulus } (E) = 131 \text{ Gpa}$$

$$\text{Total Deformation } (y) = \frac{\theta D}{2} = \frac{\frac{3\pi}{2} \times 7.112}{2} = 16.75 \text{ mm}$$

$$y = \frac{M_t (\pi Di)D}{2EI}$$

Equation 7.4.1.4

$$\text{Torque } (M_t) = \frac{16.75 \times 2 \times 13000.38 \times 0.0523}{7.112^2 \times 11 \times \pi} = 131.38 \text{ N - mm}$$

$$\text{Stiffness } (K) = \frac{M_t}{\theta} = 27.864 \text{ N} - \frac{\text{mm}}{\text{rad}} = 0.0278 \text{ N} - \text{m/rad}$$

Equation 7.4.1.5

Thus, the designed torsion spring possesses a stiffness of 0.0278 N-m/rad and transmits a torque of 0.1318 N – mm.

## 7.5 Design of Compression Springs

Helical compression springs are used to actuate the upward motion of the antenna hub to the outside the box. There are four compression springs in total. Each of these springs are fitted coaxially around each of the guiding columns present on the base of the box. These columns constrain the extension and compression of the springs to a single upward direction. The ends of each of these springs are connected to the base plate of the antenna hub and base of the box. The ends of the springs are square ended, and ground ended. When the lid is closed, and the antenna hub is pushed to the base of the box and the springs are thereby loaded. When the lid is opened, the extension of the springs exerts equal forces symmetrically on the corners of the base plate of the antenna hub causing the hub to deploy out of the box. The springs are made of Beryllium-Copper.

Each spring has a mean diameter of 10.43 mm and a length of 235 mm when there is no compression. On compression the length of the spring reduces to 25 mm. The wire

diameter of the springs is 1.499 mm. A spring index of 7 has been assumed in order to make the manufacturing of the spring easier. The compressive force acting on the spring is equal to the weight of the antenna hub and its base plate. A factor of safety of two is considered in order ensure efficient functioning of springs in cases of increased load. The inner diameter of the spring is assumed to be greater than or equal to 4.5 mm. This is done in order to ensure a clearance of at least 0.5 mm between the coils of the spring and the columns when they are fitted coaxially. This will reduce wear on the surface of the columns and ensure that the antenna hub moves upwards with uniform acceleration.

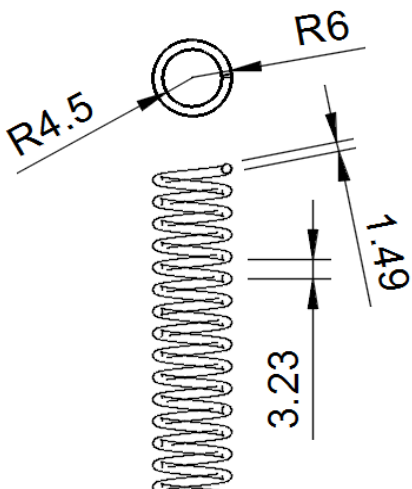


Figure 7.12 - Drawing of Compression Spring

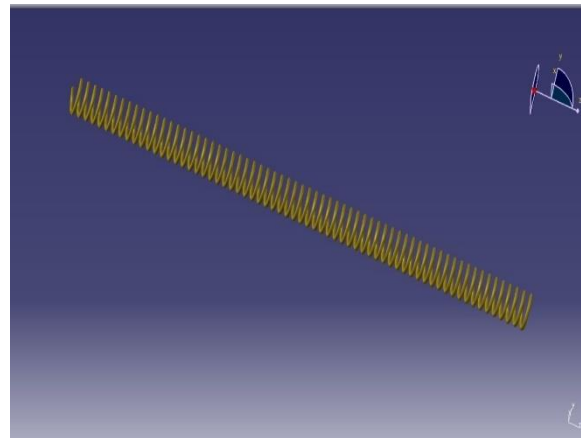


Figure 7.13 - 3D Model of Compression Spring

### 7.5.1 Calculation for Design of Compression Spring

In order to come up with a practical design for the compression spring, certain assumptions were made.

A spring index of 7 was assumed as spring indices between 6 and 12 are easy to manufacture for Beryllium-Copper material.

The inner diameter of the spring was assumed to be greater than or equal to 4.5 mm so that there would be a clearance of at least 0.5 mm between the spring and guiding columns when assembled. Also, the length is assumed to be 230 mm for the spring to fit within the box with adequate amount of compression to deploy the antenna hub.

The material Beryllium-Copper was assumed to be isotropic and possessing uniform density.

Let,  $d$  = Wire diameter of Spring (mm)

$D$  = Mean diameter of Spring (mm)

$Di$  = Inner diameter of the spring (mm)

From assumptions we know that,

$\text{Spring Index} = C = 7$

$\text{Length of Spring without compression} = L = 230 \text{ mm}$

$\text{Length of Spring after compression} = 25 \text{ mm}$

$\text{Total spring deflection (y)} = 230 - 25 = 205 \text{ mm}$

$\text{Force (F)} = FOS \times \text{Wt. of Hub} = 2 \times 19.62 = 39.24 \text{ N}$

$Di \geq 6$

Equation 7.5.1.1

$C = D/d$

Equation 7.5.1.2

$Di = D - d$

Equation 7.5.1.3

The values of wire diameter were substituted into equations 1.5.1.1, 1.5.1.2, 1.5.1.3 from the below table of wire diameters for Beryllium-Copper such that all three equations are satisfied.

0.053"	1.346 mm
0.054"	1.372 mm
0.055"	1.397 mm
0.056"	1.422 mm
0.057"	1.448 mm
0.058"	1.473 mm
0.059"	1.499 mm
0.060"	1.524 mm
0.061"	1.549 mm
0.0625"	1.588 mm
0.063"	1.600 mm
0.064"	1.626 mm
0.065"	1.651 mm
0.066"	1.676 mm

Table 7.2: Inch to Millimetre Conversion Table 2

We find the value of spring wire diameters is found to be 1.499 mm. We substitute this value in equation 1.5.1.2,

$$D = 7 \times 1.499 = 10.493$$

$$K = \frac{4C-1}{4C-4} + \frac{0.651}{C} = \frac{(4 \times 7)-1}{(4 \times 7)-4} + \frac{0.651}{7} = 1.218$$

*Equation 7.5.1.4*

$$\text{Outside Diameter } (D_o) = D + d = 10.493 + 1.499 = 11.992 \text{ mm}$$

$$\text{Inside Diameter } (D_i) = D - d = 10.493 - 1.499 = 8.99 \text{ mm}$$

$$\text{Modulus of Rigidity } (G) = 4.4 \times 10^4 \text{ Mpa (Beryllium - Copper)}$$

$$y = \frac{8FD^3i}{d^4G} = 205 \text{ mm}$$

*Equation 7.5.1.4*

$$\text{No. of active turns } (i) = \frac{205 \times 1.499^4 \times 4.4 \times 10^4}{8 \times 39.24 \times 10.493} = 125.57 \approx 126$$

$$i' = i + n = 126 + 2 = 128 \quad (n = 2 \text{ for Square, Ground ended})$$

$$\text{Max. Deflection } (y_{max}) = \frac{8FD^3i}{d^4G} = \frac{8 \times 39.24 \times 10.493^3 \times 126}{1.499^4 \times 4.4 \times 10^4} = 205.69 \text{ mm}$$

*Equation 7.5.1.5*

$$a = 0.25y_{max} = 0.25 \times 205.69 = 51.424 \text{ mm}$$

$$\text{Solid Length} = i'd = 128 \times 1.499 = 191.872 \text{ mm}$$

$$l_o \geq (i + n)d + y_{max} + a$$

$$l_o = (128) \times 1.499 + 205.69 + 51.424 = 448.982 \text{ mm}$$

$$\text{Pitch } (p) = \frac{l_{o-2d}}{i'} = \frac{448.98 - (2 \times 1.499)}{128} = 3.4825 \text{ mm}$$

*Equation 7.5.1.*

A helical compression spring of the above dimensions is designed and the finite element analysis of the same is performed and the results are obtained as shown in below figure.

It can be observed from the above the analysis that the maximum shear stress is 880.8 MPa.

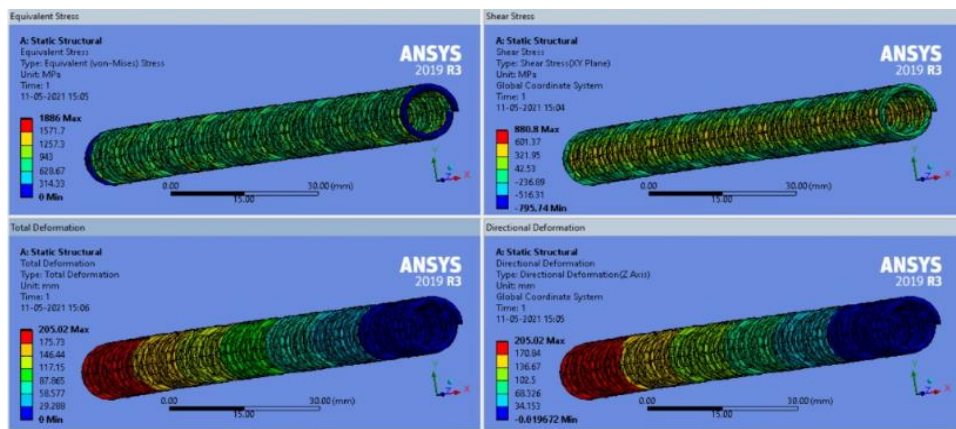


Figure 7.14 - FEA of Compression Spring

Hence,

$$\tau = \frac{8FDK}{\pi D^3} = 880.8 \text{ Mpa}$$

Equation 7.5.1.7

$$F = \frac{\pi \times 1.499^3 \times 880.8}{8 \times 10.493 \times 1.218} = 91.15 \text{ N}$$

$$\text{Required Stiffness } (k_o) = \frac{F}{y} = \frac{91.15}{205} = 444.63 \text{ N/m}$$

$$\text{Actual Stiffness } (k_a) = \frac{d^4 G}{8 i D^3} = \frac{1.499^4 \times 4.4 \times 10^4}{8 \times 126 \times 10.493^3} = 437.026 \text{ N/m}$$

Thus, a spring of required dimensions is designed possessing a stiffness of 437.08 N/m and a pitch of 3.4825 mm.

## 7.6 Radio Frequency Plates

Radio Frequency plates or RF plates are used to transmit radio frequency signals. There are strips of radio frequency components lined up on the RF plates as shown in fig 5.1 which help in transmitting and receiving the Radio frequencies. RF plates are used in satellites when the signals have to be transmitted in the lower frequency ranges of the electromagnetic spectrum. The signal/energy losses are also very minimal when transmission takes place in the radio frequency range hence RF plates are of paramount importance when it comes to construction of antenna's. The material used to construct the RF plate is Copper Beryllium this is because Copper Beryllium has an excellent

electrical conductive performance, the ability to withstand high strains and it is inexpensive.

The dimensions of our RF plates are as follows length-510mm breath-310mm thickness-0.5mm (hence these RF plates are thin sheets which have high structural rigidity and low stiffness). Due to this unique property RF plates can be stored in small volumes by rolling them or folding them which in turn reduces the housing size of the satellite. The antenna which has to be deployed has 4 RF plates which are held together with the help of an antenna hub which is a cylinder as shown in fig 5.2, the RF Plates are rolled around the cylindrical hub and they are held together with the help of an electrical tether which untethers itself when an electrical signal is passed the 4 RF plates are released tangentially with respect to the antenna hub (this is known as tangential deployment).

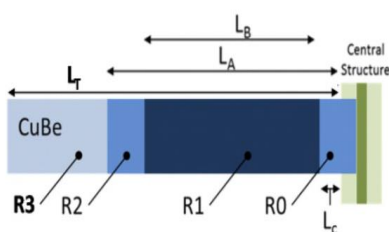


Figure 7.166-Composition of the RF Plates



Figure 7.15-RF Plates Wrapped around the Antenna Hub

## 7.7 Antenna Hub

The main function of an antenna hub is to hold the RF plates firmly. It acts as a housing for the RF plates when they are in their stowed state. The antenna hub is one of the most important parts of the mechanism as it has to hold the RF plates in position to ensure there is a smooth transmission of signals after deployment. It also has to withstand the harsh environment of space. Therefore, it has to be designed in such a way that it has the ability to be robust at all times. It was decided thus, that the antenna hub be constructed using Aluminium, as it is a metal having high strength and is light and durable. It is also fire resistant. These properties make it an important material in the field of space science, and is important here.

The antenna hub is a cylinder which has a height of 153 mm and a diameter of 66.04 mm. It has 4 slits which are 0.5 mm thick in which the RF plate sits in place. The RF plates are rolled around the antenna hub. The RF plates also consists of electronic components which are essential for the working of the antenna. The figures below shows the isometric view and the 2D drafts of the antenna hub.

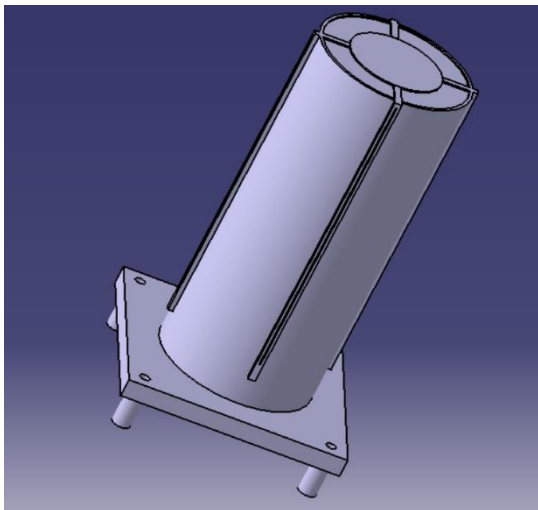


Figure 7.17: 3D Model of Antenna Hub

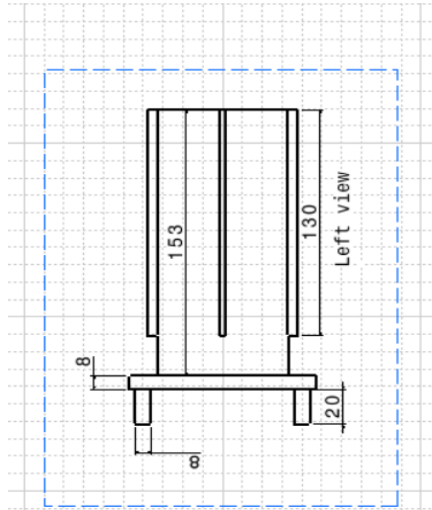


Figure 7.18: 2D Drawing of Antenna Hub

### 7.7.1 Base of the Antenna Hub

The antenna hub sits on a base which is a square of length 94 mm and has a thickness of 8 mm. The base holds the antenna hub and it has threaded holes which accommodate the male locking part. The base has to be sturdy enough to withstand the forces from the blocking part. It also consists of four 5.5 mm diameter holes. These holes are used to assemble the base of the antenna hub with the smooth columns. Underneath the base there is a hollow cylinder of height 10 mm and an inner diameter of 5.5 mm and outer diameter of 8 mm. The thickness of this cylinder is 2.5 mm. The compression springs are attached to these protrusions and this design feature ensures that the antenna hub and the compression springs are always attached and the compression springs are guided in a unidirectional manner.

The base plate is also made of Aluminium the same material which is used to manufacture the antenna hub. The base is comparatively thin. Having to withstand large forces from the blocking plate, Aluminium is deemed a suitable material. Since Aluminium has a high resistance to impact loading, the forces generated during the collision does not produce

any built-up stresses and hence the blocking part is safe from failure. A detailed note of this will be shown in the FEA of the base.

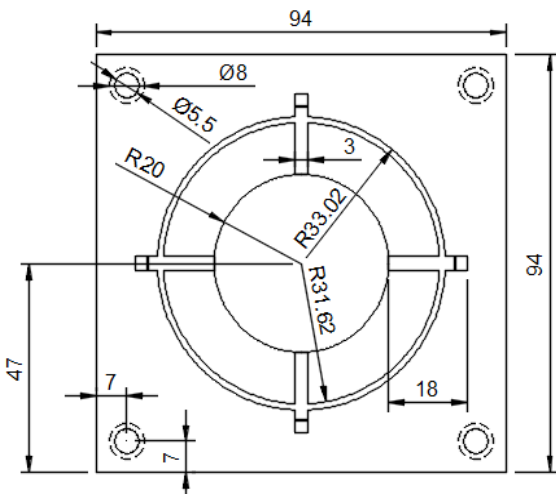


Figure 7.20: 2D Drawing of Base Plate and Hub

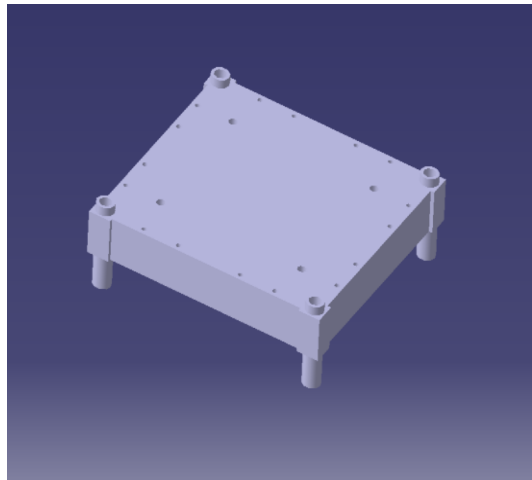


Figure 7.207.19: 3D Model of Base Plate

### 7.7.2 Slits of the Antenna Hub

The slits play an important role in accommodating the RF plates. There are four, equidistant protrusions of 5 mm from the surface of the hub which is each 3 mm thick. From a distance of 2.5 mm from the surface of the cylinder a slit of 0.5mm is made through each of these, through which the RF plate is furled into the antenna hub.

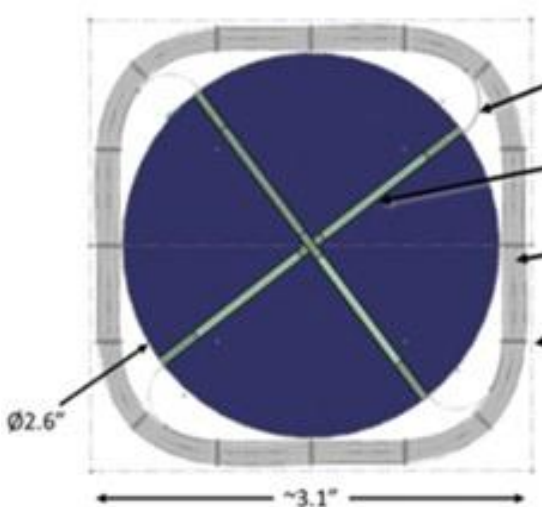


Figure 7.21: Top View of Hub

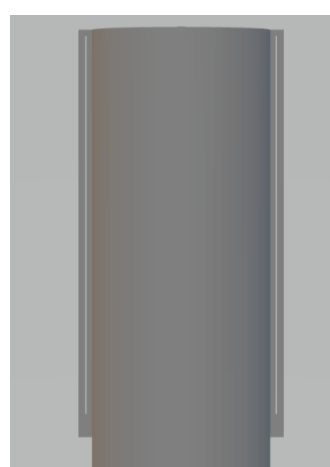


Figure 7.22: Profile View of Hub Showing Slits

## 7.8 Guiding Columns in the Box

The columns play an important role in guiding the antenna hub and the springs in the Z (vertical) direction. They constrain the hub and the springs in the X and Y directions to ensure proper contact with the locking parts on the blocking plate. The columns limit the chances of improper collision and improve the efficiency with which the mechanism works. The columns are cylinders of 4.5 mm diameter and have a height of 180 mm. They are thin and tall because the column on its own does not experience any force, as the design of the antenna hub and the column is done in such a way that forces are not experienced in the X and Y directions. But if such a force were to act on the column it must be robust and sturdy enough to withstand it. So the material chosen to build the columns is Aluminium. It's light and robust and can withstand large impact and undesirable forces without issue. There are no frictional forces acting on the columns because of the presence of DU bushes. These are cylindrical objects which have their outer diameter equal to the diameter of the holes present on the antenna hub and their inner diameter equal to the column diameter. These DU bushes are used to prevent frictional stresses on sliding objects in space. This is very important because liquid lubricants cannot be used in space due to surface tension forces outweighing the gravitational force of attraction of the Earth due to this condition the liquid lubricant assumes the shape of a sphere as it is the shape which has the least surface tension so in order to protect the column from frictional forces a solid object like DU bush is used.

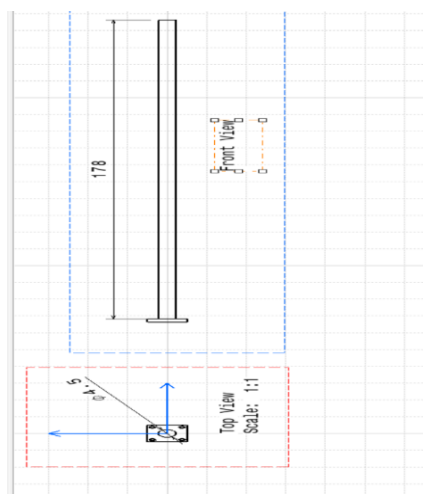


Figure 7.24: 2D Drawing of Guiding Columns

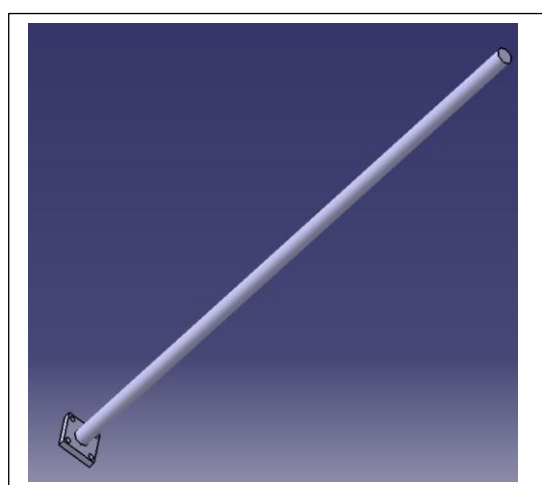


Figure 7.23: 3D Model of Guiding Columns

## 7.9 Blocking Part

The blocking part is a simple yet a very important component in the booming mechanism which deploys the antenna containing the RF plates to its final form. The main function of the blocking part is to stop the antenna hub from flying away to outer space. The dimensions of the blocking part are as follows, it is a square plate which has a side length of 96mm and a thickness of 6mm. A circular hole of 82 mm diameter is blanked on the surface of the blocking part. This hole allows the antenna hub to pass through it but the blocking action takes place when the base hits the blocking part. The blocking part also acts as a housing for the female locks which is an important part of the locking mechanism.

There is a large force generated when the base of the antenna hub hits the blocking part (a detailed expiation of how this force is generated will be given in the FEA and the physical calculations). For the blocking part to withstand these large forces a robust and a strong material which protects it from undesirable stresses must be used. For these reasons Aluminium is used to construct the blocking part as it is strong, robust and it can withstand stresses the below figures show the isometric and 2D drafts of the blocking part.

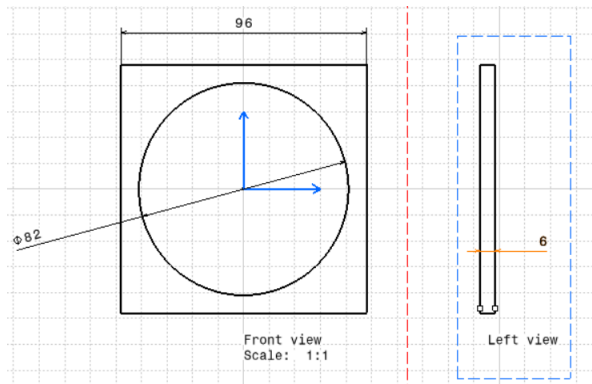


Figure 7.25: 2D Drawing of Blocking Plate

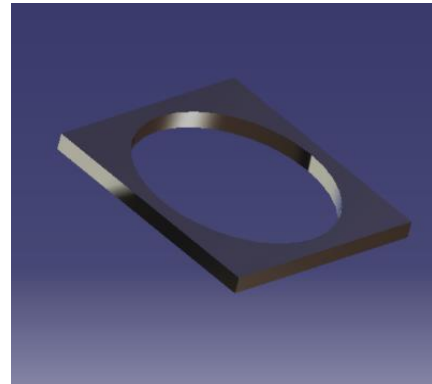


Figure 7.26: 3D Model of Blocking Plate

### 7.9.1 Alternate Design considerations for the Blocking part

There were several other designs used to block the antenna hub from being ejected, some of the notable ones are as follows:

1. Providing a small protrusion near the columns to bock the antenna hub. The problem with this design was that the protections provided were not strong enough to withstand the impulsive forces generated by the collision between the antenna hub and the protrusions.

2. Instead of a circular hole a square hole of side length 85 mm was blanked on to the blocking part. Though the designs were promising with respect to the ability of the designs to handle large forces there was a space constraint. The blocking part also acts as a housing for the female locking part which is an important part of the locking mechanism and this particular design did not have enough space to accommodate it and had to be rejected. The stresses developed at the edge of the cube was also relatively greater and hence a higher stress concentration was seen in this design.

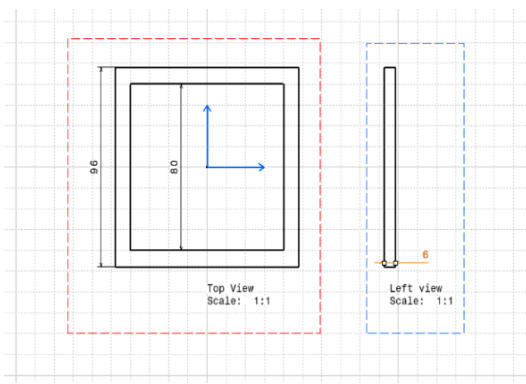


Figure 7.27-2D Draft of Alternate Design

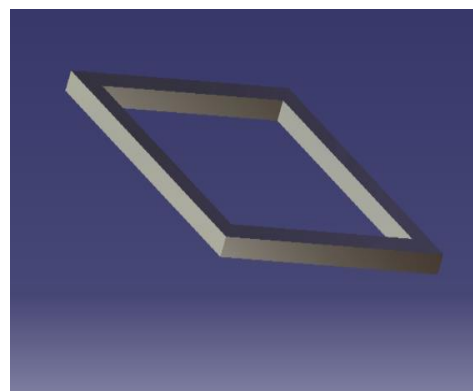


Figure 7.28: 3D Model of Alternate Blocking Part

## 7.10 Locking Mechanism

The last part of the mechanism is the sub-mechanism present in it, that is the locking mechanism. The antenna hub has to be simultaneous blocked and locked at the same time. The blocking part stops the antenna hub from being ejected to outer space and fixes the antenna hub firmly to the box so that if any undesirable forces act on the satellite the antenna doesn't dislodge. It also allows for the smooth transmission of the signals from the antenna to the receivers on Earth by stabilizing the antenna.

The locking mechanism has two components - the female locking part and the male locking part. These two parts couple together due to the forces generated by the compression springs to snap together. These types of locks are also known as snap-fit locks. They are commonly used in light bulbs. This is a miniaturized version of the same. As there is a large force acting on the locking parts, they have to be robust and sturdy and to save weight they have to be light. So the perfect material to manufacture their housing is Aluminium.

As mentioned earlier there are two components which constitutes the locking mechanism the two components are

1. Male locks which are placed on the base of the antenna hub
2. Female locks which are placed on the blocking part.

There are eight locks which constitute the complete locking mechanism. A detailed description of the same will be given in the next chapter which deals with the assembly of the different components of the deployment mechanism. Here, a detailed description of the design of male and female locks are shown

#### 7.10.1 Male Locking Part

The male locking part is present on the base plate of the antenna hub. This hits the female lock and snaps together. The male lock consists of guide pins that help in guiding the male locks when it is snapping with the female locks. These locks have protrusions which push a flexible plate present inside the female locks to snap in place. These locks are small but very effective. The dimensions of the locks are as follows. It has a length of 13.6 mm and a height of 3 mm the protrusions are 1.5 mm thick. The stresses and the forces acting on the locks are shown in the FEA of the locks.

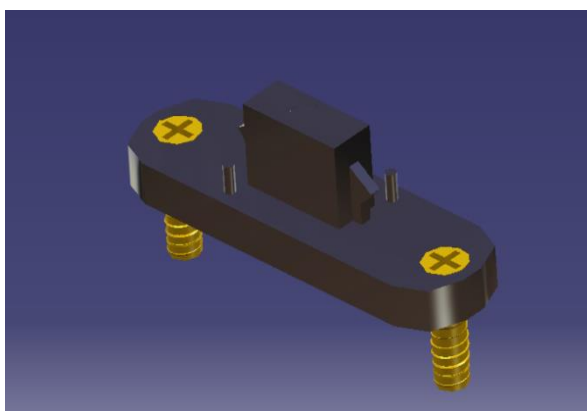


Figure 7.30-Isometric View of Male Locking Part

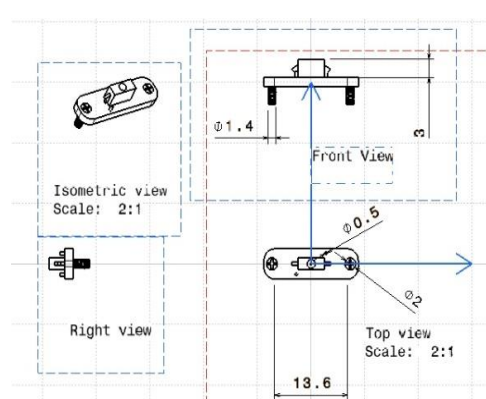


Figure 7.29-2D Draft of The Male Locking Part

#### 7.10.2 Female Locking Part

The female locking part is present on the stationary part that is the blocking plate. There are contours on the female locking part along which the male locking part snaps in place. A flexible plate is present which is made out of Beryllium Copper. When the male locks strike this part the protrusions in the male lock flex the plates and then the snapping

action occurs. A detailed description of the locking mechanism with relevant images will. The flexible sheet is shaped like the protrusions of the locking mechanism.

The dimensions of the female locking part are as follows. Length is 18.95 mm, thickness is 6 mm, contours to accommodate the male locks are 3 mm.

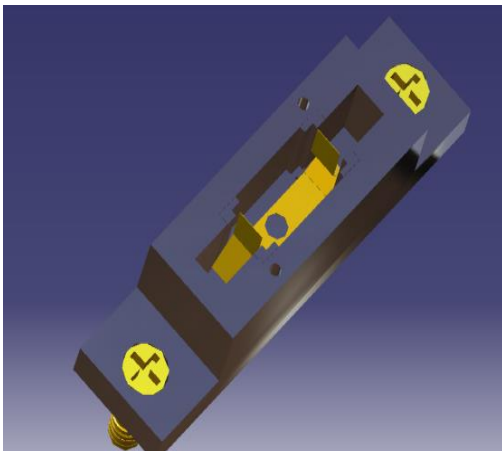


Figure 7.33-Isometric View of the female locking part

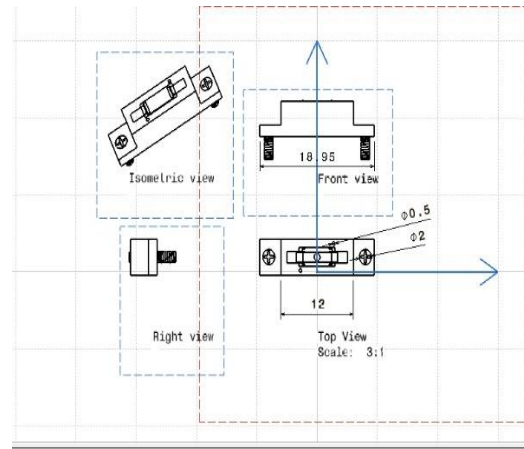


Figure 7.32-2D view of the Female locking part

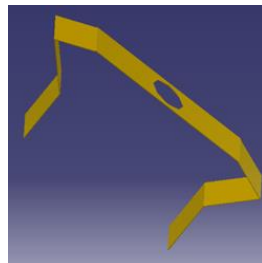


Figure 7.31-Flexible plate present inside the female locking part

### 7.10.3 Alternate Design of Locking Mechanism

There are different types of locks which work on the principle of snap fit. There were a few other designs considered for the locking mechanism which also worked on the principle of snap fit. The reason the first design prevailed over the others is because of the following.

1. The alternate design was too bulky to be integrated into the antenna deployment mechanism. Space and weight are the most important constraints for any satellite. As the design was too bulky, it weighed considerably more than the design which was chosen, increasing the total weight of the 2U cube sat box which further increases the cost to build and as well as launch the satellite.

2. The space required to integrate these locks was much larger than the designs considered to build the locking mechanism.

The design of the locks are as follows. The protrusions on the male locks are made of Beryllium Copper sheets they flex and compress once they hit the female locks. The difference between the design chosen and the design considered here is that the snapping action takes place at the side of the male locks in the latter, and in the former the snapping action takes place at the front of the male lock.

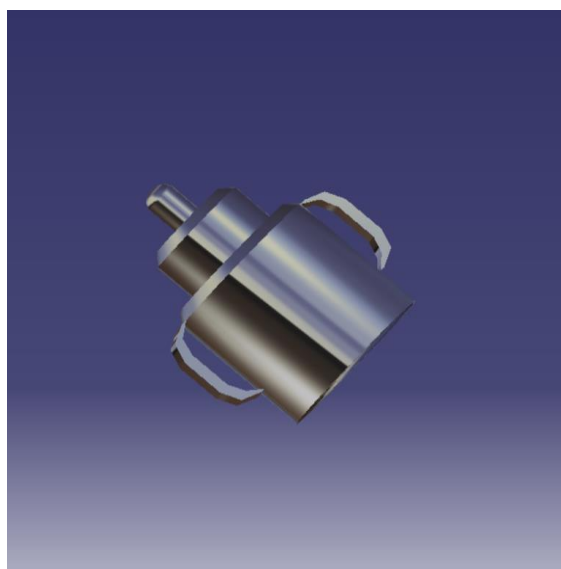


Figure 7.35-Male locking part of alternate design

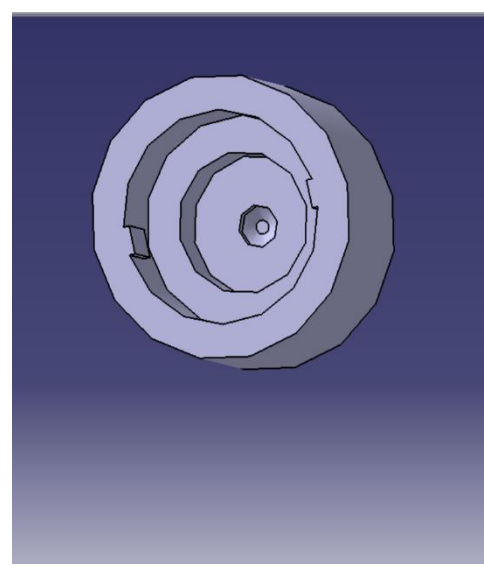
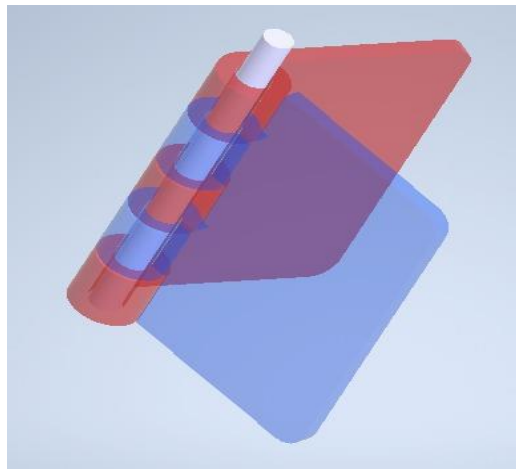


Figure 7.34-Female locking part of the alternate design.

## 8 Assembly and Kinematic Simulation of Components

### 8.1 Assembly of Hinge



*Figure 8.1: Assembly of Hinge*

The hinges comprise two halves, namely the male and female halves. When the coupling holes of both the halves are coaxially aligned alternately, with the female half (shown as blue in fig.8.1) between the male half (shown as red in fig.8.1), and subsequently held in place using the mating pin, they are mated, and are functional as hinges. This is used to allow the lid to have one degree of freedom in rotating about one of its edges.

### 8.2 Assembly of Torsion Spring

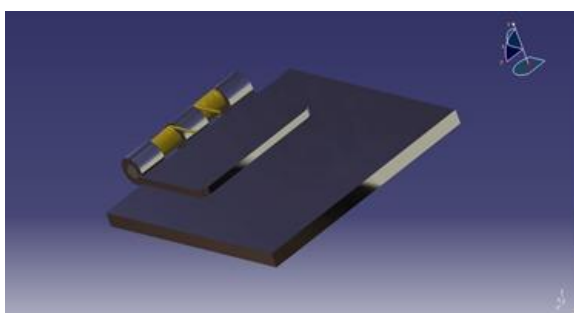


*Figure 8.3: Assembled Torsion Spring*

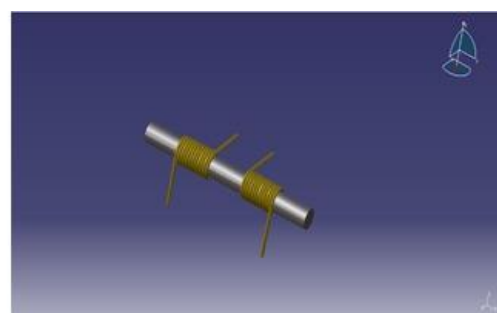


*Figure 8.2: Torsion Spring on Mating Pin*

The torsion springs in the assembly are used to open the lid of the box in order to allow the hub to be thrust out by the compression springs. These torsion springs are wound around the mating pin of the halves of the hinges, and joined with both, the lid and the box. In the assembly, they occupy the space between the coupling through-holes of the male half of the hinge.

### 8.3 Assembly of the Box

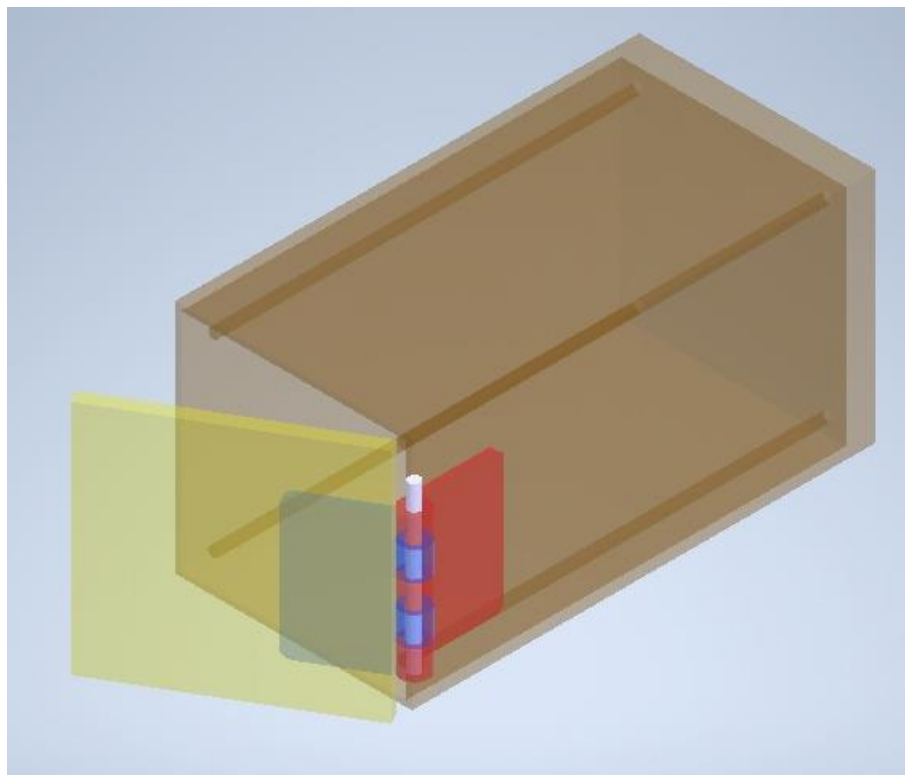


*Figure 8.4 - Assembly of box*

The box contains the antenna hub and other required circuitry and avionics within it. It is enclosed by the lid; to which it is connected using the hinges. Along one edge of the box, which it is to share with the lid, the male half of the hinge is joined as a lap joint. Similarly, the female half of the hinge is joined on the lid. The torsional spring on the hinge is made to undergo angular displacement, and the lid is closed on the box. To hold it in place the locking mechanism is used. This can be released, and the stored torsional energy is used to open the lid when required.

### 8.4 Assembly of Guiding Columns

The columns can be either 3D printed to the base of the box or mounted to the box with the help of screws. But if the columns have to be mounted with screws the design of the screw to mount the columns are as follows. The screws used are M3 screws and the design of the screws are as follows

Fine series UNF M3 Screws

Material- stainless steel

*major dia d = 3mm pitch = 0.5mm*

*Tensile stress area(At) = 4.264 mm<sup>2</sup>*

*Minor dia area(Ar) = 3.6516 mm<sup>2</sup>*

*Pitch dia = 2.675 mm (if thread has circular cross section)*

*External thread d1 = 2.38 mm*

*Internal Thread D1 = 2.458 mm*

*Lead angle = 3°24'*

$$\text{Size of set screws} = d = \frac{D}{8} + 8 = 8.375 \text{ mm}$$

*Max safe holding force =  $54254 \times (8.375 \times 10^{-3})^{2.31}$*

$$F = 0.86402 \text{ KN} = 864.02 \text{ N}$$

$$\text{Torque} = Mt = 0.2Fa = 0.2 \times 0.86402 = 0.172804 \text{ KNm} = 172.804 \text{ Nm}$$



Figure 8.5-M3 Screw for mounting the columns

There are four M3 holes on each column's base; so sixteen M3 screws are manufactured to assemble the columns on to the base.

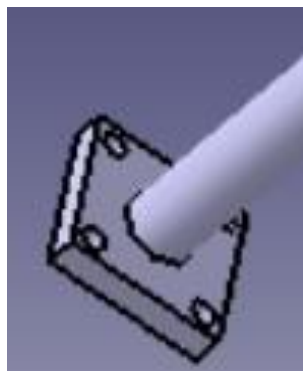


Figure 8.7-Base of the columns with screw holes

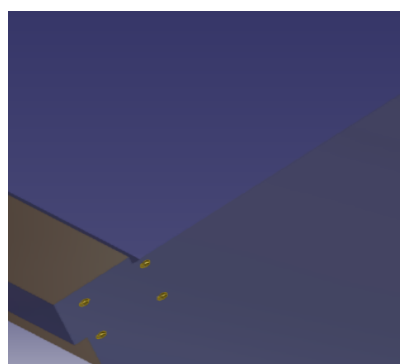


Figure 8.6-Base of the box with M3 screw holes

## 8.5 Assembly of Antenna Hub on base

The antenna hub is 3D printed with the base but if conventional machining processes are used screws are designed to mount the antenna hub onto the base. The M3 screws are used to mount the antenna hub onto the base the design specifications of the M3 screws are shown below.

Fine series UNF M3 Screws,

Material- stainless steel

*major dia d = 3mm pitch = 0.5mm*

*Tensile stress area(At) = 4.264mm<sup>2</sup>*

*Minor dia area(Ar) = 3.6516mm<sup>2</sup>*

*Pitch dia = 2.675mm (if thread has circular cross section)*

*External thread d1 = 2.38mm*

*Internal Thread D1 = 2.458mm*

*Lead angle = 3°24'*

$$\text{Size of set screws} = d = \frac{D}{8} + 8 = 8.375\text{mm}$$

*Max safe holding force =  $54254 \times (8.375 \times 10^{-3})^{2.31} F = 0.86402\text{KN} = 864.02\text{N}$ .....7.5.2*

*Max.Torque = Mt =  $0.2Fa = 0.2 \times 0.86402 = 0.172804\text{KNm} = 172.804\text{Nm}$ .....7.5.3*



Figure 8.9-M3 screws to mount antenna hub

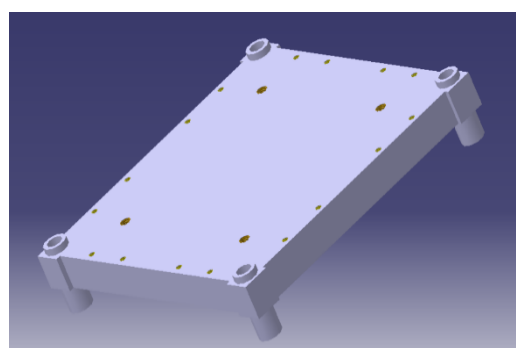
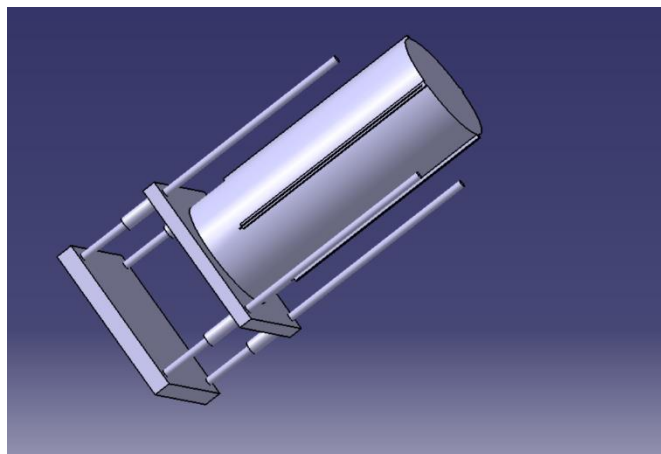


Figure 8.8-M3 screw holes to mount antenna hub

## 8.6 Assembly of Antenna Hub on columns

The antenna hub has 4 holes of 5.5 mm diameter which fit with the 4 columns that protrude from the base of the box. These columns are cylinders having a diameter of 4.5 mm and a height of 180 mm. As there is relative motion between the base of the antenna hub and the columns, a tolerance of 0.5 mm is given. There are no frictional forces acting on the columns or the base due to the presence of DU bush, but pressure forces act on the columns and a detailed explanation of this will be given in the FEA.



*Figure 8.10-Assembly of the antenna hub and columns*

## 8.7 Assembly of Blocking Plate

The blocking part has four grooves which are aligned with the columns. These grooves sit on the columns and a snapping mechanism exists between the walls of the box and the blocking part. This mechanism firmly holds the blocking part. Alternatively, locking part can be directly 3D printed with the box.

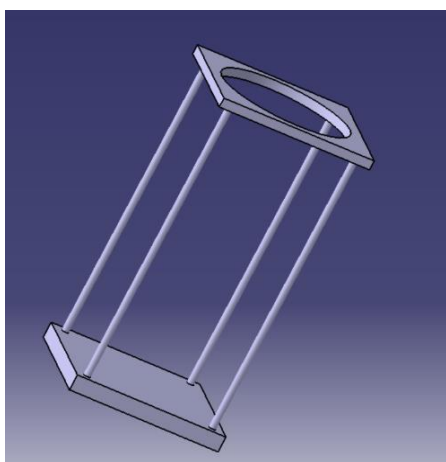


*Figure 8.11: Alignment of Blocking Plate with Column*

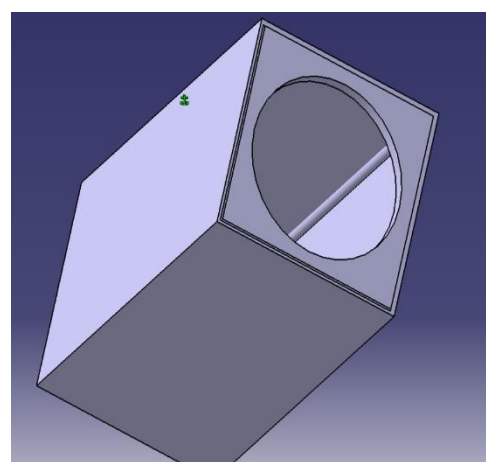


*Figure 8.12: Assembly of Blocking Part in Box*

## 8.8 Assembly of Male Locks

The male locks are assembled on top of the base of the antenna hub. These locks are really small so high precision 3D printers are required to print these parts directly onto the base of the Antenna hub and this process is very expensive. So in order to cut costs the locking mechanism can be 3D printed separately and then mounted on to the base there are M1.6 screws developed for this purpose and threaded holes are present on the base of the antenna hub. The design specifications of the M1.6 screws are as follows

## Fine series UNF, Material - Stainless steel

*Major dia d = 1.6mm Pitch = 0.35 mm*

$$\text{Tensile stress area} (At) = 1.161 \text{ mm}^2 \quad \text{Major dia area} (Ar) = 0.9741 \text{ mm}^2$$

*Pitch dia = 0.87 mm (if pitch is circular) External threads d1 = 0.754 mm*

*Internal threads D1 = 0.783 mm Lead angle = 4°11'*

$$F = 0.8228 \text{ } KN = 822.8 \text{ } N$$

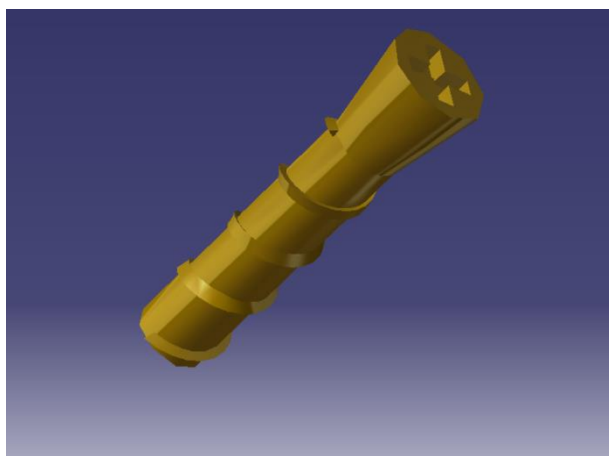


*Figure 8.13-M1.6 screws to mount the male locks*

There are eight male locks which are assembled on the base of the antenna hub two on each side of the base this is done to make sure that a secured lock is obtained and also to make sure that the locks do not experience a high value of equivalent stress when the snapping mechanism takes place therefore we need sixteen M1.6 screws to mount all the locks.

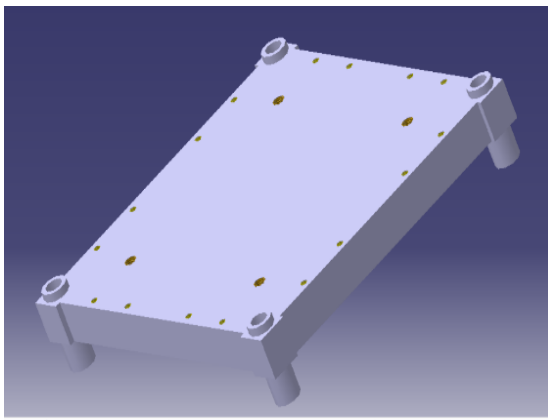


Figure 8.14: Screw Holes on Base

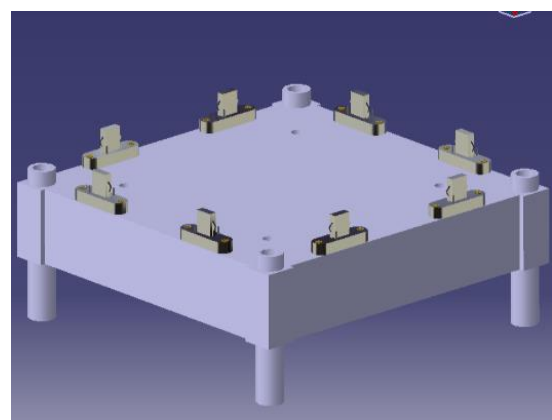


Figure 8.15-Male Locks Assembled on Base

## 8.9 Assembly of Female Locks

The female locking part in the locking mechanism is a stationary part that is mounted underneath the blocking part. There are eight female locks ready to catch the male locks to snap. To mount the female locks the same M1.6 screws are used, and threaded holes are present underneath the blocking part to mount the female locks underneath the blocking part. The design specifications of the M1.6 screws are as follows.

Fine series UNF, material - Stainless steel

*Major dia d = 1.6 mm ; Pitch = 0.35 mm*

*Tensile stress area(At) = 1.161 mm<sup>2</sup> Major dia area (Ar) = 0.9741 mm<sup>2</sup>*

*Pitch dia = 0.87 mm (if pitch is circular); External threads d1 = 0.754 mm*

*Internal threads D1 = 0.783 mm Lead angle = 4°11'*

*Size of set screws = d =  $\frac{D}{8} + 8 = \frac{1.6}{8} + 8 = 8.2 \text{ mm}$ .....7.9.1*

*Max safe holding force F =  $54254 \times (8.2 \times 10^{-3})^{2.31}$  .....7.9.2*

*F = 0.8228 KN = 822.8 N*

*Max torque = Mt = 0.2Fa = 0.1645KNm = 164.5Nm.....7.9.3*

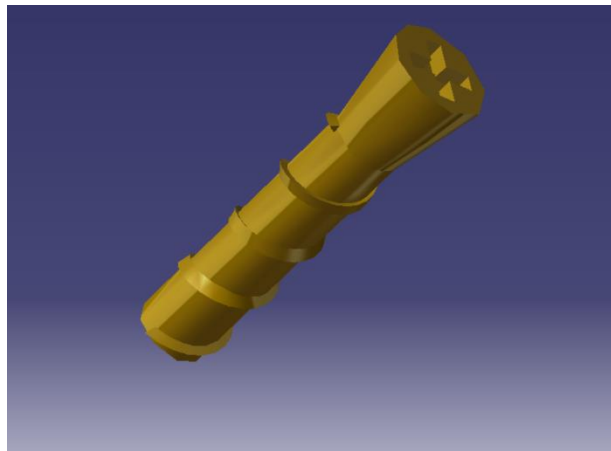


Figure 8.16-M1.6 Screw Holes to Mount the Female Locks

As there are eight female locks a total of sixteen M1.6 screws are required to mount the female locks the below figures show the assembly of the female locks underneath the blocking part.

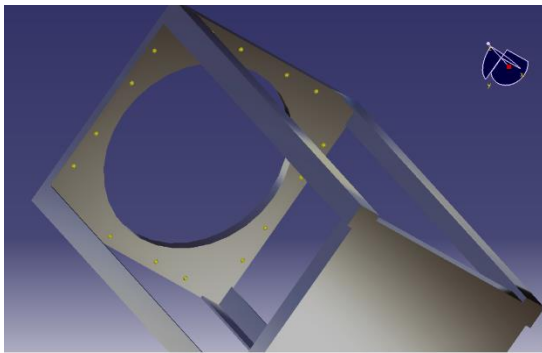


Figure 8.18: Screw Holes of the Female Lock



Figure 8.17-Female Locks Assembled Underneath the Blocking Part

## 8.10 Kinematic Simulation

The kinematic simulation of the antenna deployment mechanism was done using DMU kinematic on Catia V5. These simulations show how the mechanism works and it also analyzes the contact between the moving parts.

### 8.10.1 Brief introduction of DMU Kinematic Catia V5

This environment in Catia is used to simulate moving parts in a particular design. In order to do this, assembly of all the different parts of the design is done. After the assembly is done all the parts that are stationary in the design are fixed. After this step, a new mechanism is created. This allows the environment to create any simulation the user needs. In DMU Kinematic there are different joints which help in simulating different types

of motions present in a particular design. Some of the joints which are present are as follows.

1. Revolute joint helps in simulation of revolving motions
2. Prismatic Joint helps in simulation of linear motion
3. Cylindrical joint helps to create a joint between two cylindrical surfaces
4. Screw joint helps in simulation of screw rotation
5. Spherical joint helps in simulating motions like the ball and socket joint
6. Planar joint helps in simulating the sliding motion between two planes
7. Rigid joint helps in simulating movement between two surfaces where the coefficient of friction is very high



*Figure 8.19-The different types of joints present in DMU kinematic*

### 8.10.2 Wireframe environment of Catia V5

The wire frame environment is used to simulate the variation of different shapes in a particular design. For example, in this environment the compression of springs, the action of forces acting on sheet metals, folding and unfolding of sheet metal, provide different configurations for sheet metal etc., can be simulated.

### 8.10.3 Application of DMU Kinematic and Wireframe Modeling

The simulation of the antenna deployment mechanism has three different stages. These are the following ways the three stages were simulated using DMU kinematic:

To simulate the lid opening two Revolute joints were used and one prismatic joint was used. The revolute joint simulates the revolution of the lid on the hinge axis. A small offset

which occurred on the revolute joint. So a prismatic joint was also inserted to nullify this offset. The details of the prismatic and revolute joints are shown in the figures below.

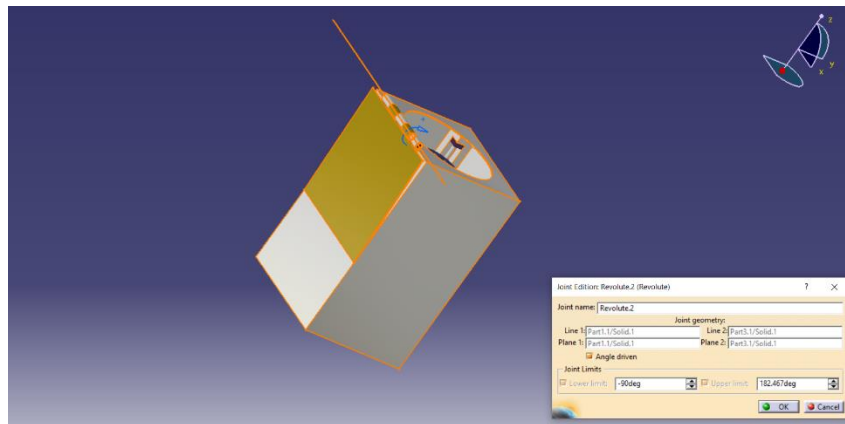


Figure 8.20: Joint 1 in Anticlockwise Direction to Simulate the Lid Opening

In order to create the revolute joint, two lines have to be chosen (these are the axes of the male and female hinges) and then two planes have to be selected (these are the mating surfaces of the two hinge surfaces).

Revolute joint 2 simulates the same action but in the opposite direction, which helps in closing the lid and replaying the simulation.

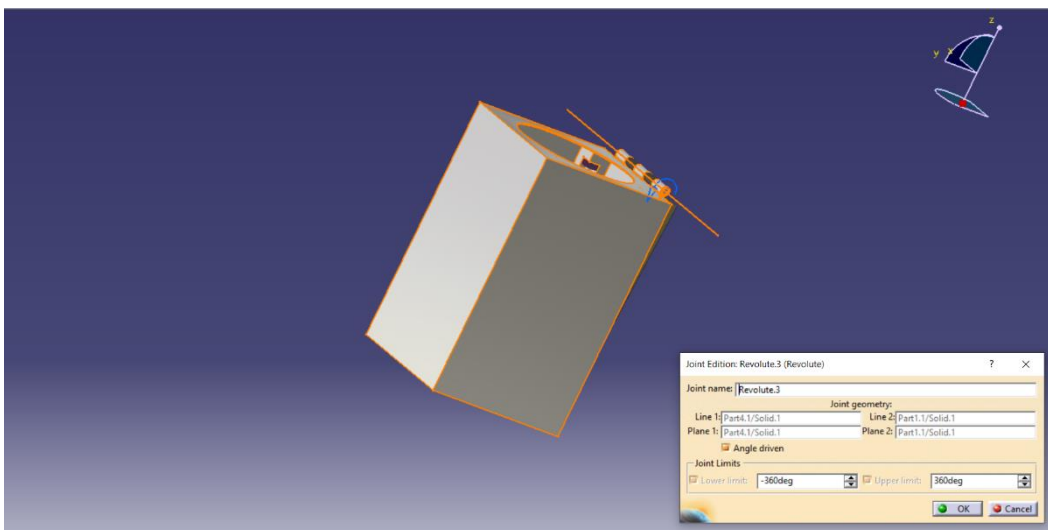


Figure 8.21: Revolute Joint 2 in clockwise Direction

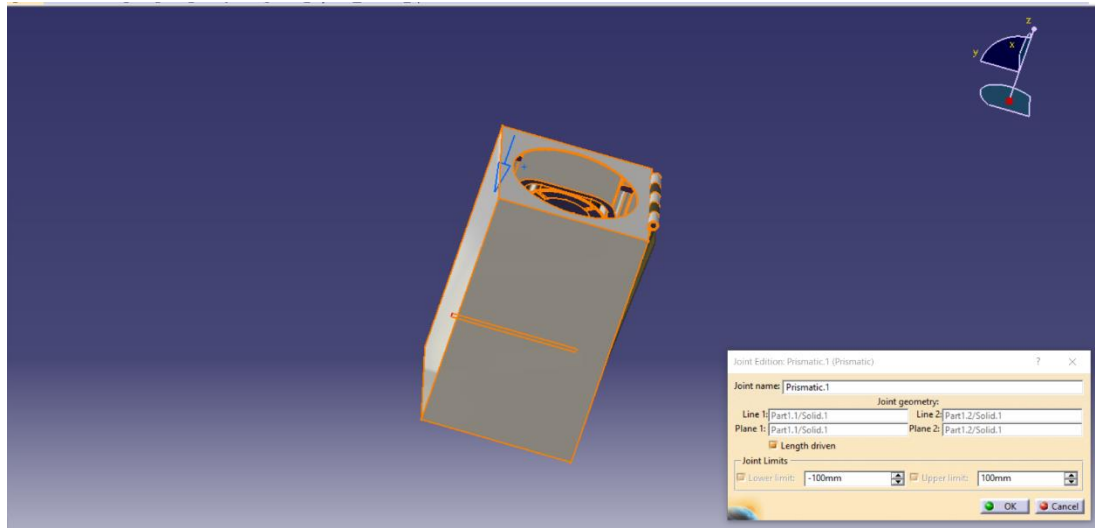


Figure 8.22: Prismatic Joint

After the creation of these joints it is possible to simulate the mechanism and different parameters can be set. The parameter set in our simulation is that the lid has to move from 0 degrees (closed position) to 270 degrees (completely opened position).

The simulation of the lid opening is shown by these series of figures shown below.

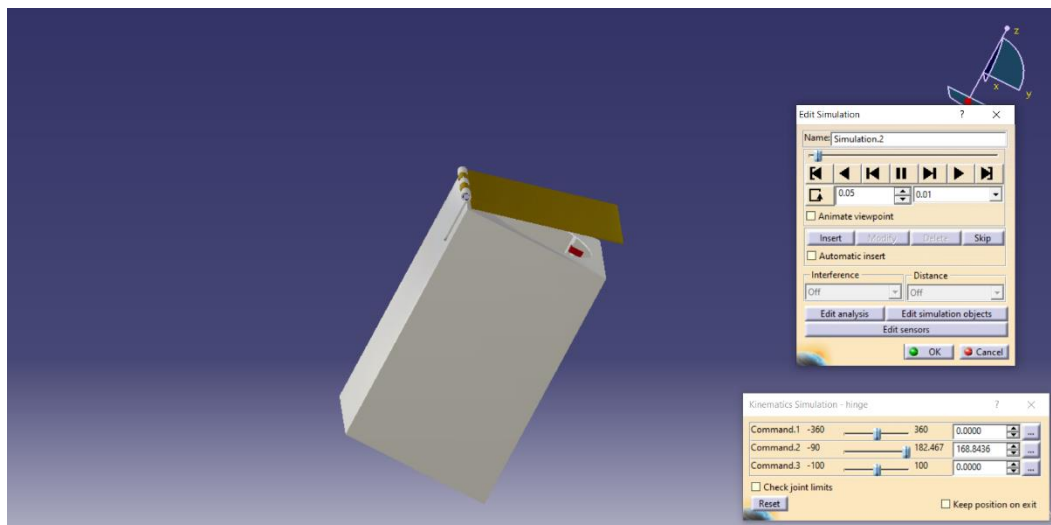


Figure 8.23: The Lid Opening

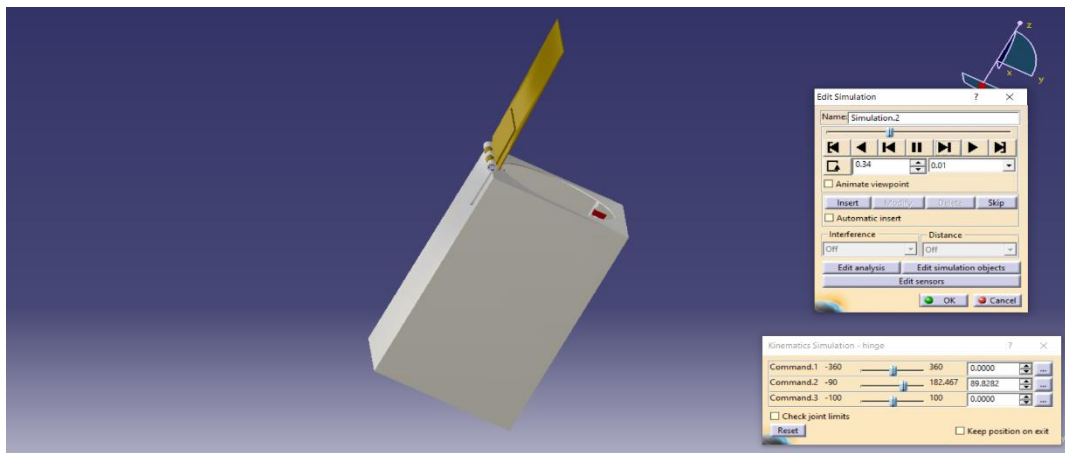


Figure 8.24: 90 Degrees

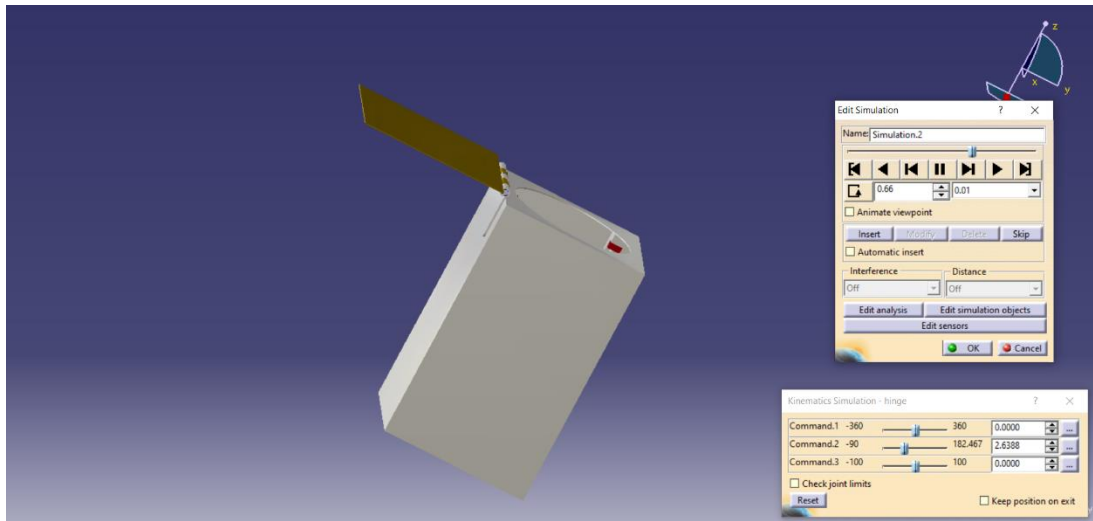


Figure 8.25: 180 Degrees

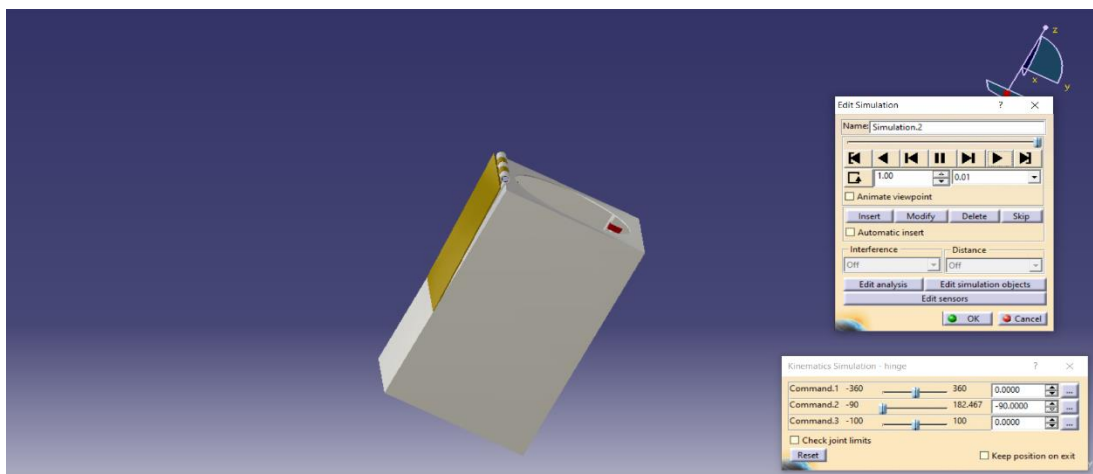
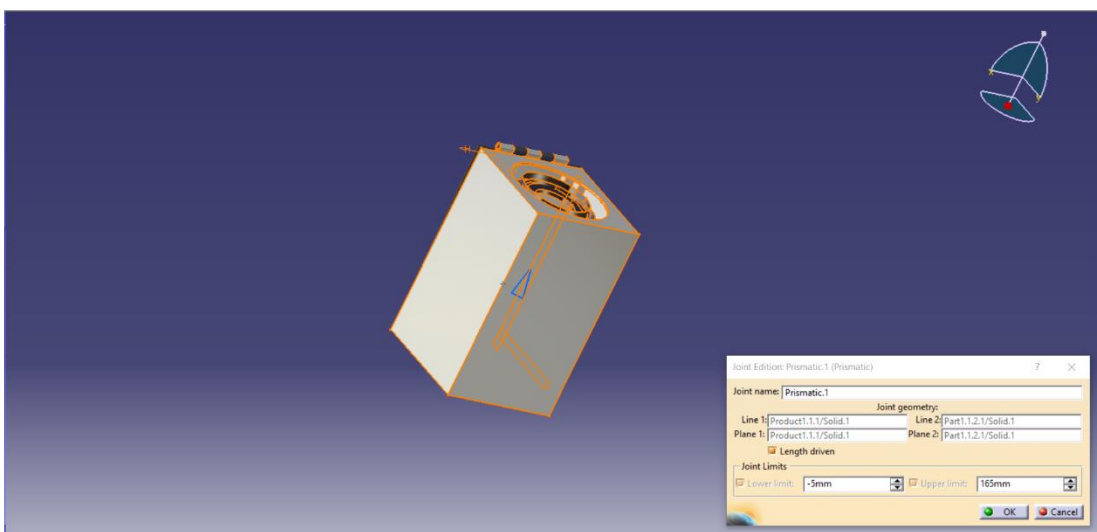


Figure 8.26: Lid Opened

Contact analysis: there is contact between the lid and the left side, resulting in forces acting on the lid and the box due to this collision. The effect of this impulsive force is shown in the FEA of the lid and the box.

The prismatic joint is used to simulate the deployment of the antenna hub from the box as mentioned earlier. It helps in simulating linear motion in a single direction. The specifications of the prismatic joint are shown in the figure below.



*Figure 8.27-Specifications of the prismatic joint to simulate the deployment of antenna hub*

The prismatic joint is created between two lines (the two lines are the edges which are in contact with each other during the linear motion - the base of the antenna hub and the walls of the box). The joint also requires two planes - these two are the planes that are in contact with each other. After the creation of this joint it is possible to simulate the deployment of the antenna hub from the box. The following figures show the simulation of the antenna hub deploying from the box:

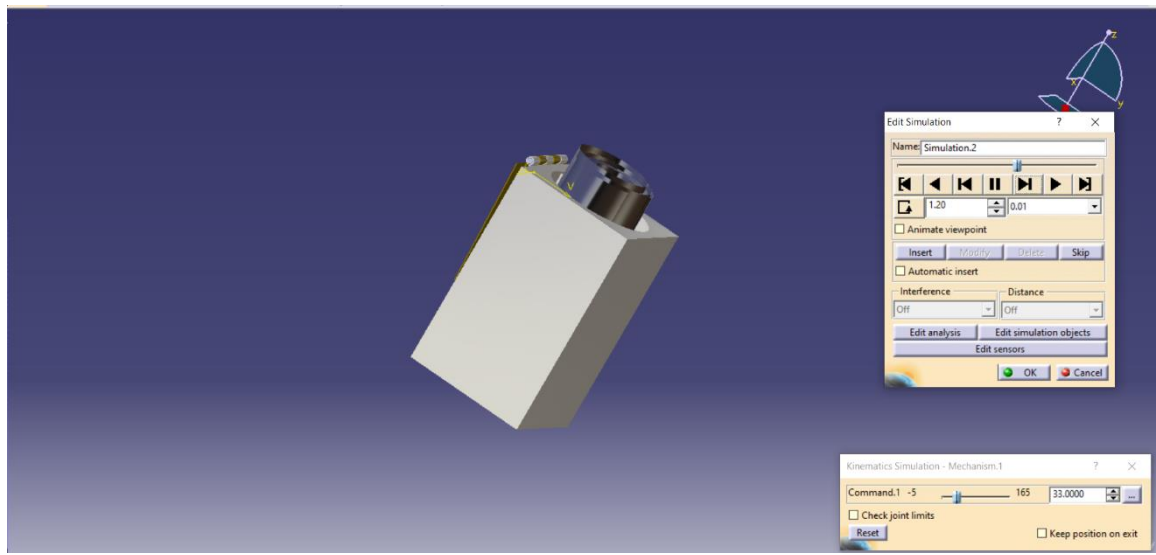


Figure 8.28: Start of Deployment of the Antenna Hub

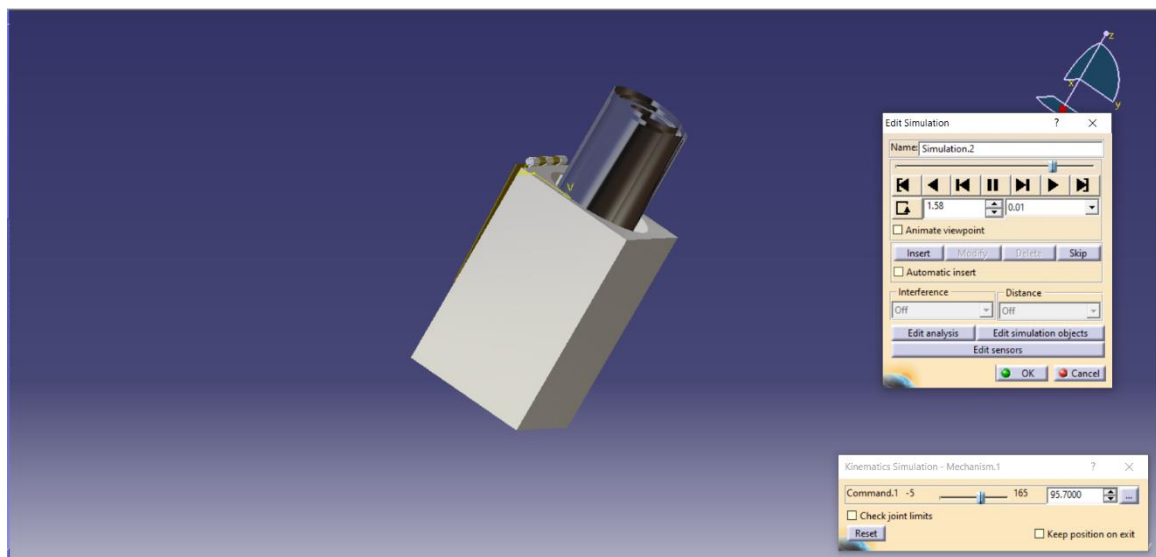


Figure 8.29: Intermediated Position

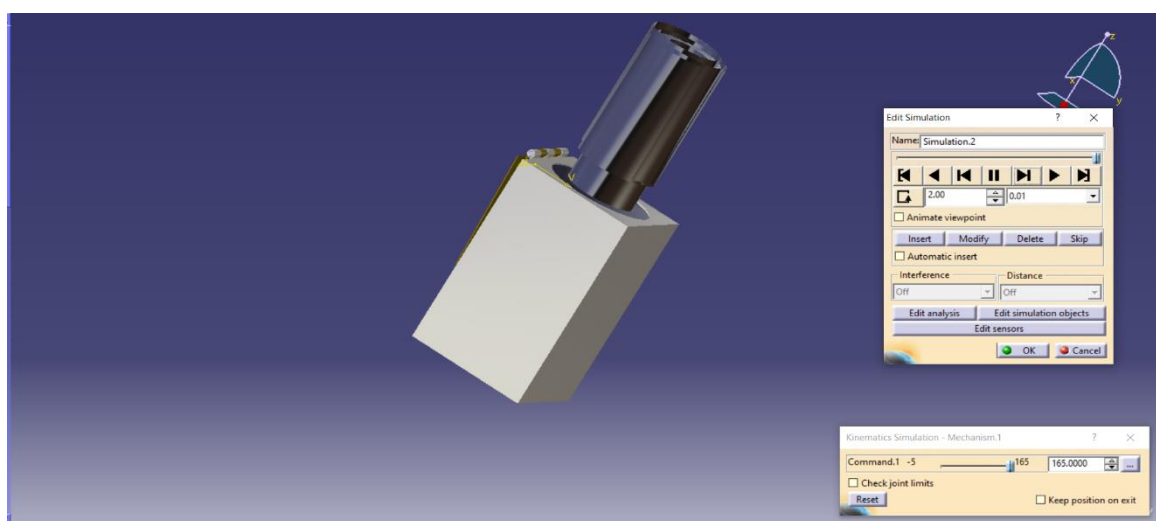


Figure 8.30: Final Position of the Antenna Hub After Deployment

Contact analysis – From this simulation we found out that the base of the antenna hub and the blocking part collide with each other. From this, the force acting on the blocking part and the reaction force acting on the base of the antenna hub were calculated. The value of these forces and the effect of these forces are shown in the FEA of the antenna deployment mechanism.

The third part of the simulation of the unfolding of RF plates also known as boozing. It is simulated using wireframe modeling. The sheet metal feature was used to represent the unfolding of RF plates. The RF plates are held together with the help of an electronic tether which release when the sensor senses that the antenna hub is out of the box (the release mechanism itself being an existing technology and out of the scope of the project). The figures below show the step by step boozing of the RF plates.



Figure 8.32: Before Boozing

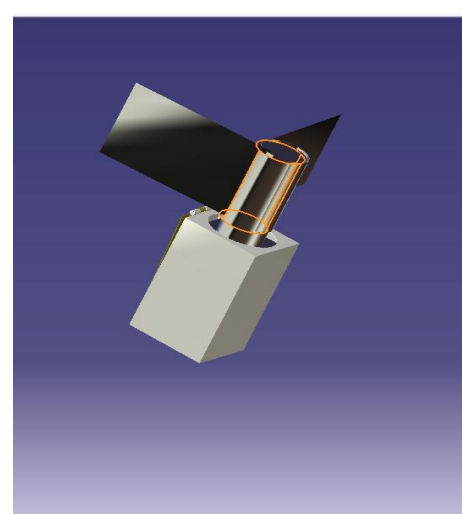


Figure 8.31: Boozing Process Underway

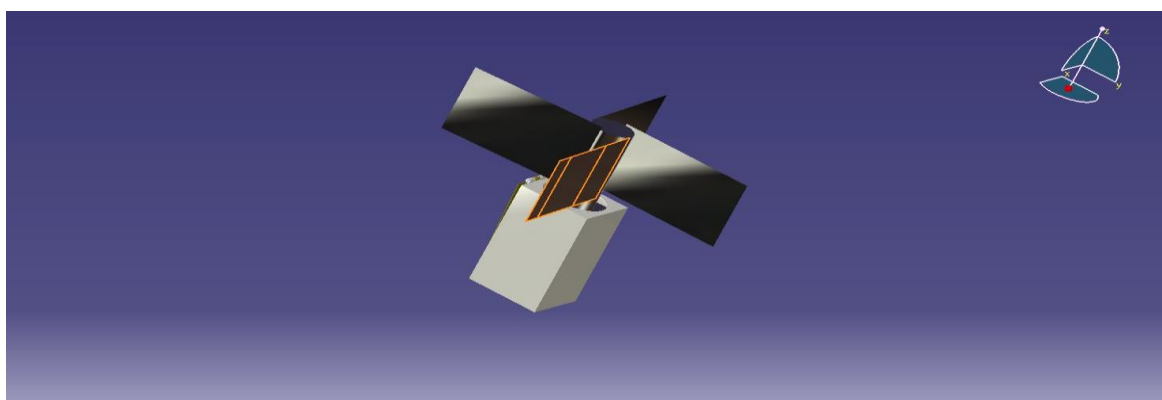


Figure 8.33: Fully Boozed Plates

## 8.11 Antenna Deployment Mechanism - Design 2

Another design was under consideration for the antenna deployment mechanism. The only changes in this design with respect to the design is w.r.t the antenna hub, the columns and the springs. A brief explanation of why these designs were rejected is explained.

### 8.11.1 Columns - Design 2

In design 2, instead of four columns there was one column present in the middle of the box. This column was made of Aluminium and was a cylinder of height 180 mm and the diameter was 40 mm.

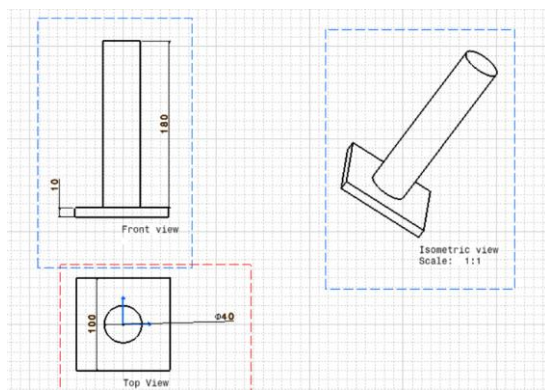


Figure 8.35: 2D Drawing of Column - Design 2

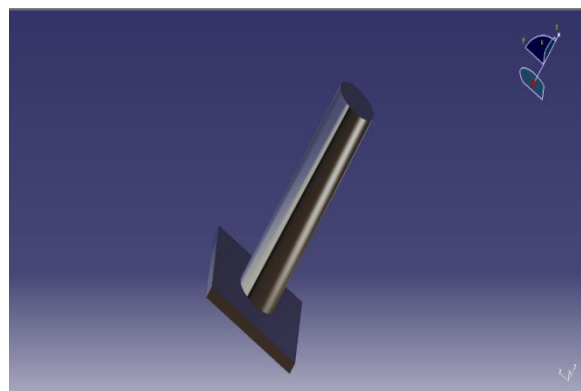


Figure 8.34: 3D Model of Design 2 Column

### 8.11.2 Antenna Hub Design 2

In order to accommodate a column of such a large diameter a hollow antenna hub had to be designed. This antenna hub was to be made of Aluminium and had the same dimensions except a hollow cylinder of ID 41 mm and OD of 66.04 mm along the axis.

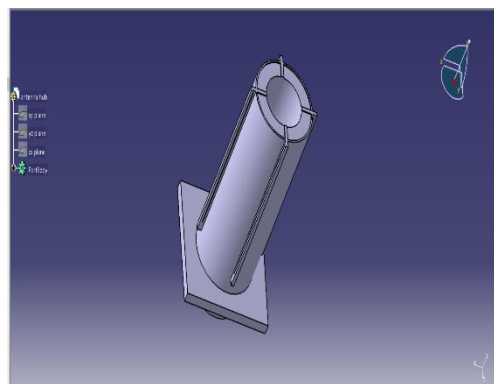


Figure 8.37: 3D Model of Design 2 Hub

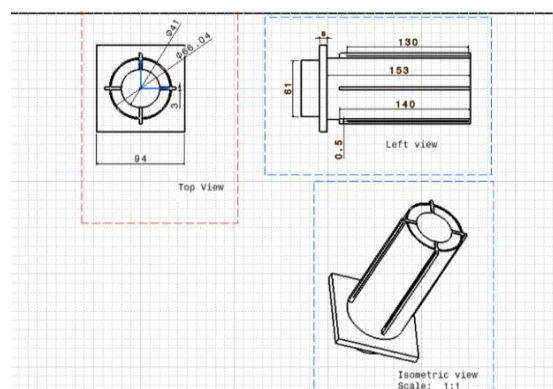


Figure 8.36: 2D Drawing of Design 2 Hub

### 8.11.3 Spring Design 2

A single helical compression spring was to be used to actuate the upward motion of the antenna hub to the outside the box. The spring is fitted coaxially around the guiding column present on the base of the box. This column constrains the extension and compression of the spring to a single upward direction. The end of the spring is connected to the base plate of the antenna hub and base of the box. The ends of the spring are square ended, and ground ended. When the lid is closed, the antenna hub is pushed to the base of the box and the spring is thereby loaded. When the lid is opened, the extension of the spring exerts a force on the base plate of the antenna hub causing the hub to deploy out of the box. The springs are made of Beryllium-Copper.

The spring has a mean diameter of 69.696 mm and a length of 235 mm when there is no compression. On compression the length of the spring reduces to 25 mm. The wire diameter of the spring is 8.712 mm. A spring index of 8 has been assumed in order to make the manufacturing of the spring easier. The compressive force acting on the spring is equal to the weight of the antenna hub and its base plate. A factor of safety of two is considered in order ensure efficient functioning of springs in cases of increased load. The inner diameter of the spring is assumed to be greater than or equal to 40 mm. This is done in order to ensure a clearance of at least 0.5 mm between the coils of the spring and the column when they are fitted coaxially. This will reduce wear on the surface of the column and ensure that the antenna hub moves upwards with uniform acceleration.

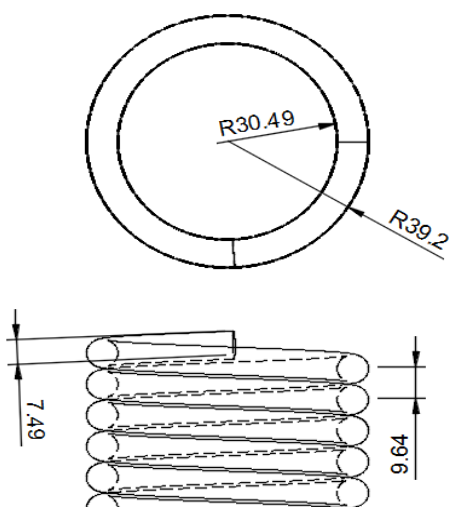


Figure 8.39: 2D Drawing of Spring - Design 2

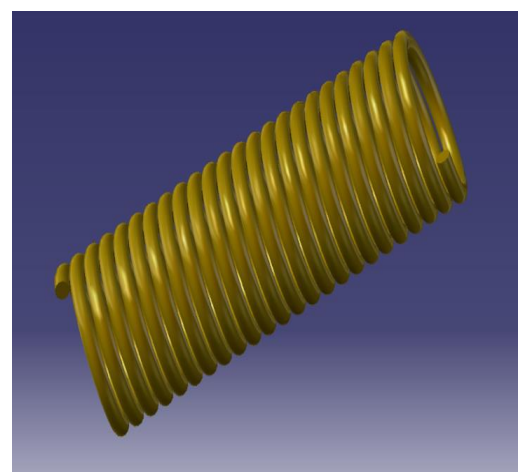


Figure 8.38: 3D Model of Spring - Design 2

#### 8.11.4 Assembly of Different Components - Design 2

The assembly of different parts of design 2 is similar to that of the chosen one. There is, however, a change in the assembly of the spring's antenna hub and columns and these changes are shown here.

In the assembly of column and antenna, hub the antenna hub is hollow and the column is inserted through the antenna hub, which is constrained to move linearly upwards along these columns. A protrusion is given to the underside of the antenna hub and this protrusion is used to support the spring. The below image shows the assembly of the column and the antenna hub.

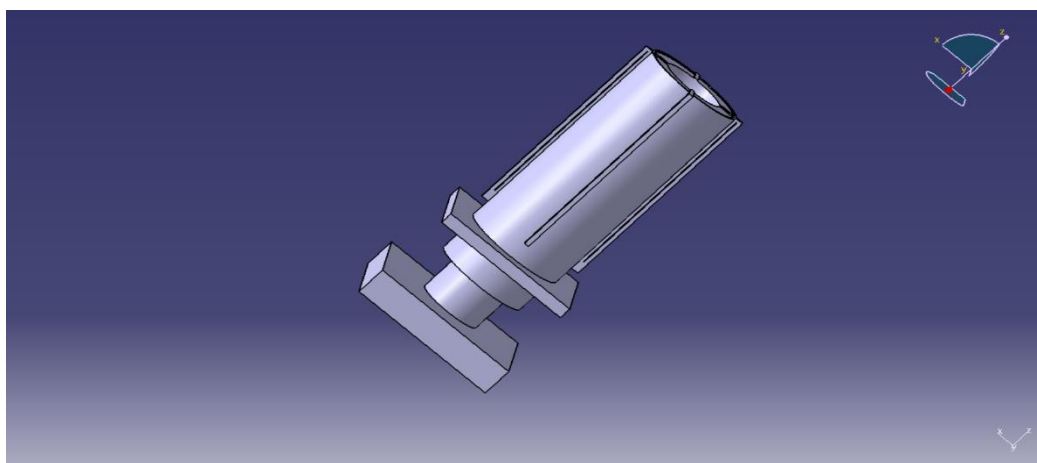


Figure 8.40: Design 2 Assembly of Hub on Column

The spring sits on the single column as shown in the figure. The springs are square and ground ended and they are attached to the base of the box.

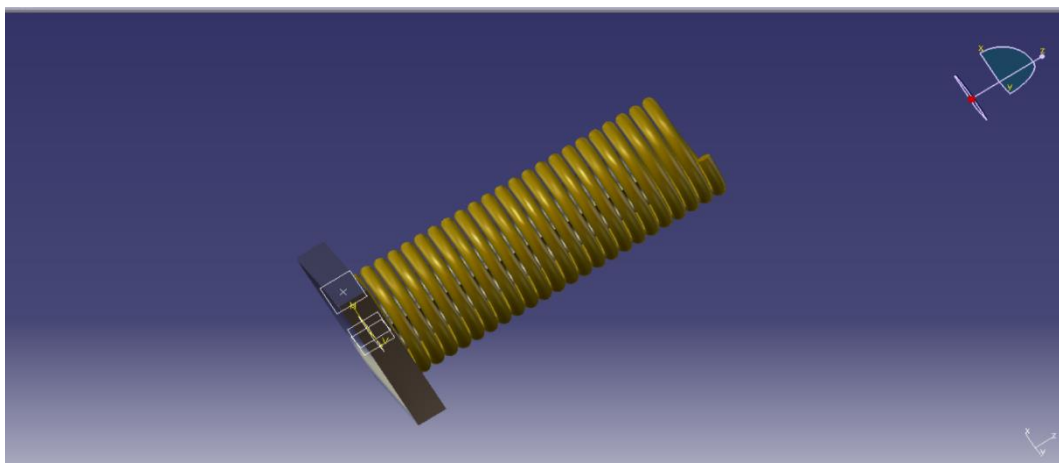


Figure 8.41: Design 2 Assembly of Spring on Column

In the above figure it can be seen that the diameter of the spring is considerably greater than the columns. This is because the protrusions underneath the antenna hub have diameters of 62 mm. In order to accommodate this diameter, the springs ID is equal to the diameter of the protrusion.

#### 8.11.5 Reasons for Failure of Design 2

The following flaws in design 2 led to its rejection:

1. The antenna hub was hollow which is not recommended. This is because the antenna hub houses the RF plates which is an important component of the antenna. Making the hub hollow makes it vulnerable as it cannot handle high forces acting on it in undesirable situations. Therefore, this design had to be rejected.
2. There was not enough space for electronics as the columns were occupying considerably more space than the chosen designs. Electronic components are important as they are responsible for the deployment of compression springs opening of locks, and other satellite-specific avionics.
3. The impulsive force on the blocking part in this design was very high. This is because the spring deployed the antenna hub in very high velocities, and these forces created very high stresses on the blocking part which led to the failure of the blocking part (the force generated by it was 261 N which was two times greater than the first design).

### 8.12 Alternate Booming Mechanism

There are two ways in which the RF plate can be boomed (i.e. Released). They are tangential deployment and radial deployment. In radial deployment the RF plates boom in the perpendicular direction with respect to the antenna hub, whereas in tangential deployment the RF plates boom in the tangential direction with respect to the antenna hub. Both the designs provide the same end result. The configuration of the RF plates in its stowed position occupies less space when the RF plates are deployed tangentially therefore tangential deployment was considered over radial deployment as the availability of space in CubeSats is limited.

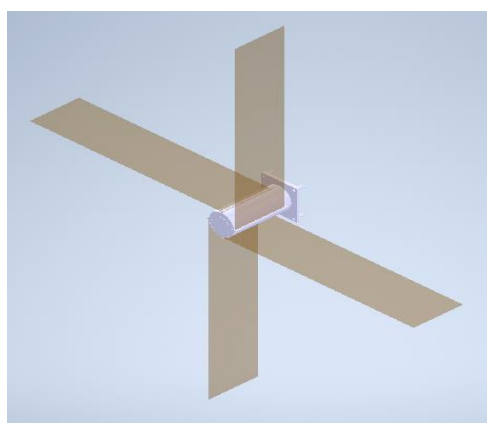


Figure 8.43: Tangential Booming

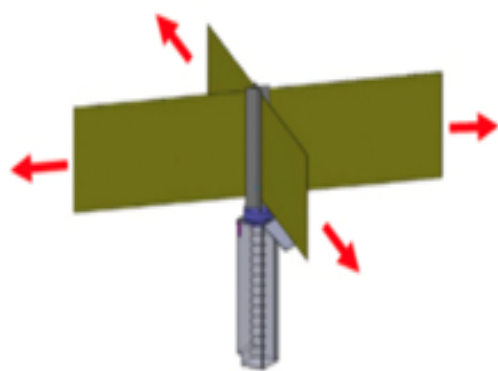
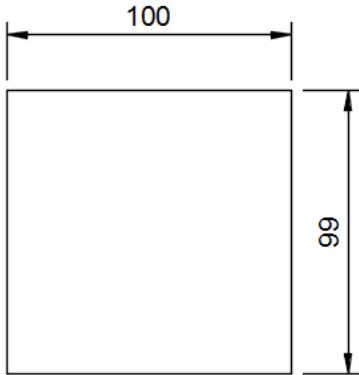


Figure 8.42: Radial Booming

## 9 Dynamic Analysis of Spring Forces

### 9.1 Torsional Spring



Consider the following properties of the lid.

$$\text{Length } (L) = 100 \text{ mm} = 0.1 \text{ m}$$

$$\text{Breadth } (b) = 99 \text{ mm} = 0.099 \text{ m}$$

$$\begin{aligned} \text{Distance from centre of lid to hinge axis } (e) \\ = 56.405 \text{ mm} = 0.056405 \text{ m} \end{aligned}$$

$$\text{Mass of Lid } (M) = 160.38 \text{ g} = 0.16038 \text{ kg}$$

$$\begin{aligned} \text{Mass per unit length of the lid } (M/L) \\ = 0.16038 / 0.1 \text{ kg/m} \end{aligned}$$

$$\text{Stiffness of Torsion Spring} = 0.027864 \text{ N/m}$$

$$\text{Moment of Inertia of lid about hinge axis } (I) = \frac{ML^2}{12} + Mb^2 + Me^2$$

$$I = \frac{0.16038 \times 0.1^2}{12} + (0.16038 \times 0.099^2) + (0.16038 \times 0.056405^2)$$

$$I = 6.8521 \times 10^{-4} \text{ kgm}^2$$

$$\text{Torque on Lid } (\tau) = \int dm g x = \int \frac{0.16038}{0.1} \times dx \times g \times x = \frac{0.16038}{0.1} \int_0^{0.099} x dx$$

$$\tau = \frac{0.16038 \times 0.099^2}{0.1 \times 2} = 0.0778 \text{ Nm}$$

Consider the general equation of motion for a torsion spring,

$$I\ddot{\theta} + k\theta = 0$$

Consider a general solution,

$$\theta = A \sin(\omega t) + B \cos(\omega t)$$

$$\dot{\theta} = A\omega \cos(\omega t) - B\omega \sin(\omega t)$$

$$\ddot{\theta} = -\omega^2 (A \sin(\omega t) + B \cos(\omega t))$$

Substitute \_\_\_\_\_ in equation \_\_\_\_\_

$$I(-\omega^2 (A \sin(\omega t) + B \cos(\omega t))) + K(A \sin(\omega t) + B \cos(\omega t)) = 0$$

$$I\omega^2 = k$$

$$\omega = \sqrt{\frac{k}{I}} = \sqrt{\frac{0.027864}{6.852 \times 10^{-4}}} = 9.018 \text{ rad/s}$$

$$\text{In equation } \text{_____ substitute } \theta = \frac{3\pi}{2}; \dot{\theta} = 0; t = 0$$

$$\frac{3\pi}{2} = A(0) + B(1)$$

$$B = \frac{3\pi}{2}$$

$$0 = A(1)(\omega) - B(0)$$

$$A = 0$$

Substitute these results in \_\_\_\_\_

$$\theta = B \cos(\omega t)$$

$$\text{Put } \theta = 0; B = \frac{3\pi}{2}$$

$$0 = \frac{3\pi}{2} \cos(\omega t)$$

$$\omega t = \frac{\pi}{2}$$

$$t = \frac{\pi}{2\omega} = \frac{\pi}{2 \times 9.018} = 0.1741 \text{ s}$$

Substitute value of  $t$  and  $\omega$  in \_\_\_\_\_

$$\dot{\theta} = -\frac{3\pi}{2} \times 9.018 \times \sin(9.018 \times 0.174)$$

$$\dot{\theta} = -42.49 \text{ rad/s}$$

$$\ddot{\theta} = -9.018^2 \times \frac{3\pi}{2} \times \cos(9.018 \times 0.174)$$

$$\ddot{\theta} = -0.2922 \text{ rad/s}^2$$

## 9.2 Compression Spring

The dynamic analysis comprises two parts – pertaining to respectively the action of the compression spring and that of the torsional spring. Following are the calculations of the compression spring dynamics. Using usual notations,

$$\tau = 880.79 = \frac{8FDk}{\pi D^3}$$

$$\Rightarrow F = \frac{880.79 \times \pi \times 1.499^3}{8 \times 10.433 \times 1.218} = 91.157 \text{ N}$$

$$K = \frac{F}{y} = \frac{91.15}{205} = 444.63 \text{ N/m}$$

Using second order differential equation governing spring forces,

$$m \times \frac{d^2(m)}{dx^2} + c \times \frac{d(m)}{dx} + k \times x = 0$$

Assuming a negligible damping condition,

$$m \times \frac{d^2(m)}{dx^2} + k \times x = 0$$

$$x = a \cos(\omega t) + b \sin(\omega t)$$

$$\Rightarrow \frac{d(x)}{dt} = -\omega(a \sin(\omega t) - b \cos(\omega t))$$

$$\Rightarrow \frac{d^2(x)}{dx^2} = -\omega^2(a \cos(\omega t) + b \sin(\omega t))$$

$$\omega = \sqrt{\frac{k}{m}} \Rightarrow \omega = \sqrt{\frac{4 \times 444.63}{8}} \Rightarrow \omega = 14.91 \text{ rads}^{-1}$$

Applying boundary conditions of  $x = 0.205 \text{ m}$  at  $t = 0 \text{ s}$ , and  $v = 0 \text{ m/s}$  at  $t = 0 \text{ s}$ ,

$$a = 0.205 \text{ m}; b = 0 \text{ m}$$

At 25% of maximum compression,

$$0.051 = 0.205 \times \cos(14.91t) \Rightarrow t = 0.0884 \text{ s}$$

Therefore, the spring takes 0.0884 s to reach 25% of maximum compression. At that instant,

$$a = \frac{d^2(x)}{dt^2} = 11.39 \text{ ms}^{-2}$$

Therefore force on blocking plate,  $F = m \times a = 8 \times 11.39 = 91.12 \text{ N}$

Force on each blocking part,  $F_{each} = \frac{91.12}{8} = 11.39 \text{ N}$

To find the velocity of the spring when complete deformation occurs,

$$\frac{1}{2} \times k \times x^2 = \frac{1}{2} \times m \times v^2$$

$$\Rightarrow v = \sqrt{\frac{444.63 \times 0.205^2}{8}} = 1.528 \text{ ms}^{-1}$$

Angular velocity,

$$\omega = 42.49 \text{ rad/s}$$

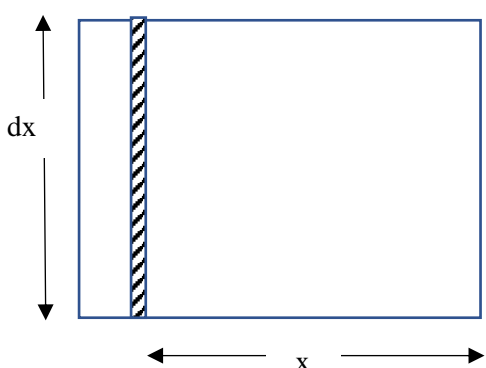
$$\Rightarrow v = \omega R = 42.49 \times 0.1 = 4.249 \text{ m/s}$$

Angular acceleration,

$$\alpha = 0.2922 \text{ rad/s}^2$$

$$\Rightarrow a = \alpha R = 0.02922 \text{ m/s}^2$$

To find impulse force on box consider,



If the hinge axis is the left edge of the lid depicted,

$$P = \int_0^{10} v dm, \text{ where, } v = \dot{\theta}x$$

$$\begin{aligned} P &= \int_0^{10} \dot{\theta}x \times \rho \times dx \times t = \rho t \dot{\theta} \int_0^{10} x dx = \rho t \dot{\theta} \times \left(\frac{x^2}{2}\right)_0^{10} \\ &= 2700 \times 6 \times \frac{42.49}{2} \times 10^{-4} \end{aligned}$$

$$\Rightarrow P = 5.162 \frac{k\text{gm}}{\text{s}^2}$$

Therefore, the impulsive force acting on the box is  $5.162 \text{ kgm/s}^2$ .

It is assumed that the impulsive force lasts for 0.5

Therefore  $\Delta t = 0.5 \text{ sec}$

We know that  $F = \frac{P}{\Delta t}$  hence  $F = \frac{5.162}{0.5} N$

$F=10.252 N$

## 10 Contact Analysis and Finite Element Analysis

### 10.1 Introduction to Contact Analysis

By using the 2<sup>nd</sup> order differential equations, we have found the forces acting on the different parts which undergo collision during the antenna deployment mechanism. The parts which undergo a collision amongst them are:

1. Base of the antenna hub and the Blocking part
2. The surface of the lid and the right side of the box
3. Contact between the columns and the base of the antenna hub
4. Contact between the top surface of the columns and the blocking part
5. Contact between the male and female locks

The contact analysis is very important because it helps us deduce the frictional forces and the pressure forces acting on the different components of the mechanisms due to contact between them. The contact analysis was done on Ansys static structural. There are six types of contacts present in Ansys Static structural they are as follows:

1. Bonded contact -In this type of contact there is no gap between the parts that are in contact and there is no relative motion between the bodies which are under contact (sliding is not allowed and the coefficient of friction is infinite)
2. No separation contact-In this type of contact there are no gaps between the elements which are in contact but there is a relative motion between the components (sliding is allowed but a coefficient of friction exists as there is no gap between the surfaces)
3. Frictionless contact –In this type of contact there are gaps between the elements which are in contact, and sliding is allowed (i.e. there is no coefficient of friction between these surfaces as there is a gap between the two elements)
4. Rough contact-In this type of contacts a gap exists between the two bodies which are in contact but relative motion between them is not possible as the coefficient of friction is infinitely high.
5. Frictional contact – In this type of contact there is a gap that exists between the two bodies that are in contact and there is sliding between their surfaces but is

restrained by frictional forces as a coefficient of friction exists between the two surfaces.

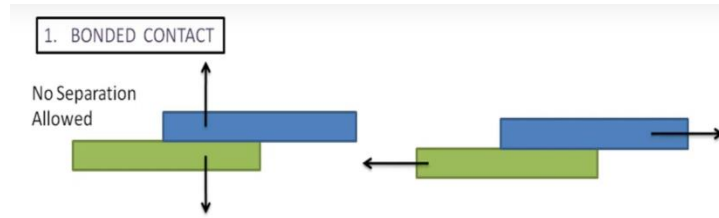


Figure 10.10.1: Bonded Contact

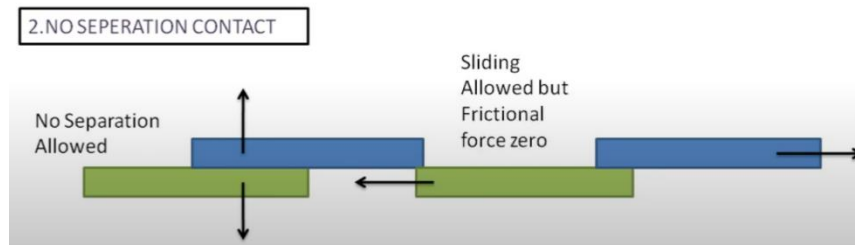


Figure 10.10.2: No Separation Contact

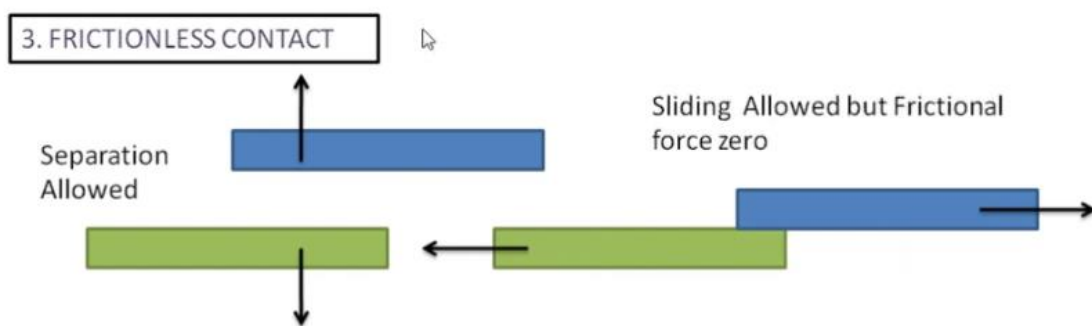


Figure 10.10.3: Frictionless Contact

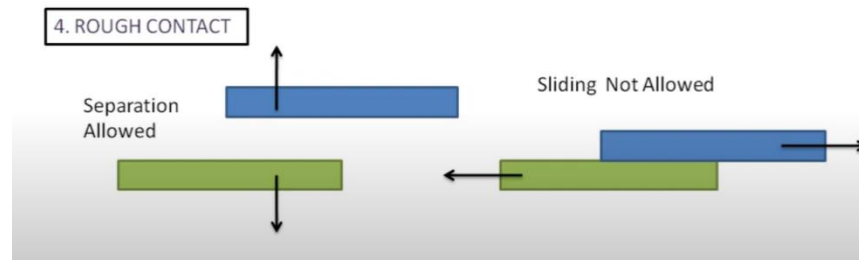


Figure 10.10.4-Rough contact depiction

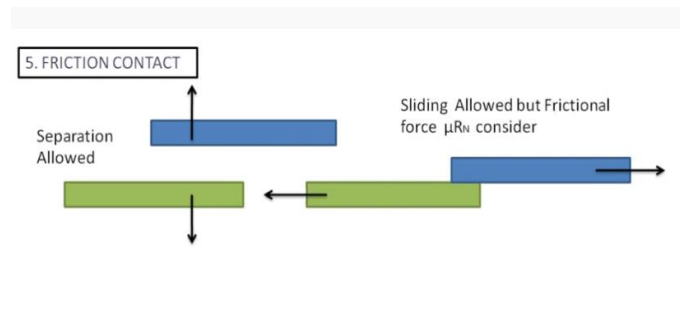


Figure 10.5-Frictional contact depiction

*Note - Whenever there is a contact between two bodies, one of them is considered the contact body (the criteria to classify it as contact body is as follows - if the bodies are made of different materials, then the material with higher strength is considered as the contact body, if the bodies are made of the same material, then the body causing the collision is known as the contact body).*

*The other body is known as target body and this body (the criteria to choose a body as target body is as follows - if the two bodies are made of different material, then the material having the lower strength is considered as the target body; if they are made of the same body then the body undergoing the collision i.e. The stationary body is considered to be the target body)*

### 10.1.1 Contact Analysis of Antenna Hub, Base and Blocking Part

The acceleration at  $t=0.0884$  sec is  $11.39 \text{ m/s}^2$  (obtained by solving the second order differential equation) when multiplied with the mass of the antenna hub that is 8 kg we

get the total force acting on the blocking part that is 91.12 N and a bonded contact exists between the base of the antenna hub and the blocking part.

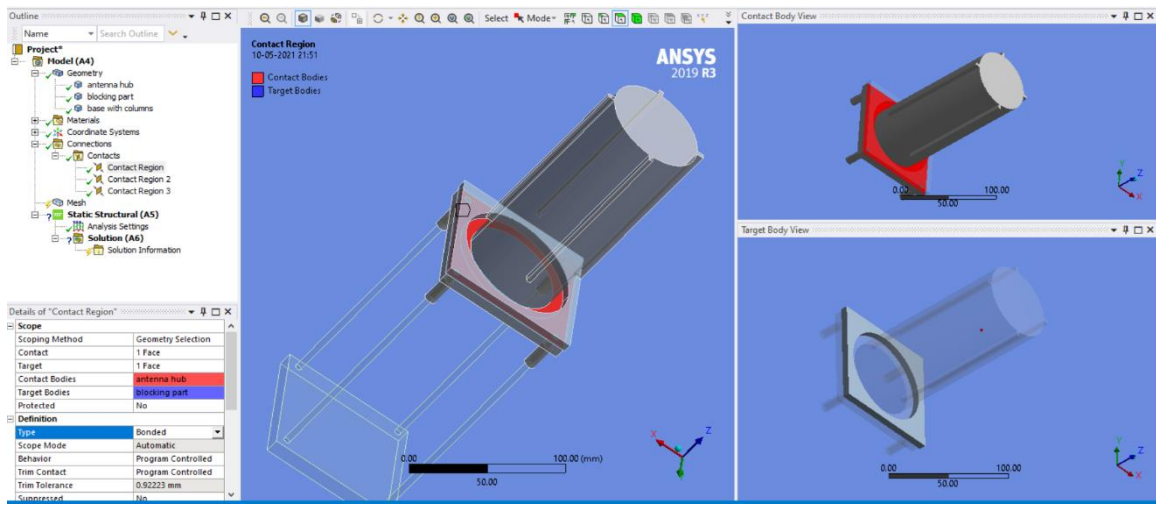


Figure 10.10.6: Contact Analysis Between Base and Blocking Part

In the above figure the body marked in red is the contact body and the body in grey is the target body. Here the antenna hub's base is the contact body and the blocking part is the target body.

### 10.1.2 Contact Analysis between Columns and Base of the Antenna Hub

The holes of the antenna hub and the columns have a surface contact between them. This contact is a frictionless contact because the DU bushes are present, so the stresses due to the frictional forces are zero. But stresses are developed due to pressure forces and the FEA will be shown later in the chapter.

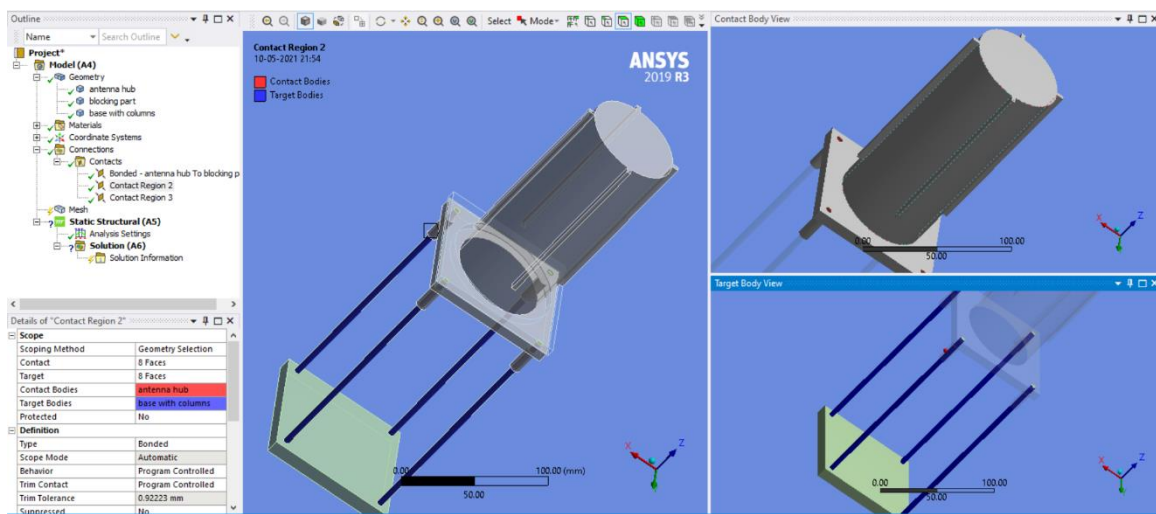


Figure 10.10.7: Contact Analysis between Columns and Antenna Hub

In the above image the columns are the contact bodies and the inner surface of the holes are the target body. As mentioned earlier there exists a frictionless type of contact between the two bodies.

### 10.1.3 Contact Analysis between Columns and Blocking Part

There is no force present between the columns and the blocking part. The blocking part sits on the columns and there exist a bonded contact between them so there is no gap or friction between the two surfaces.

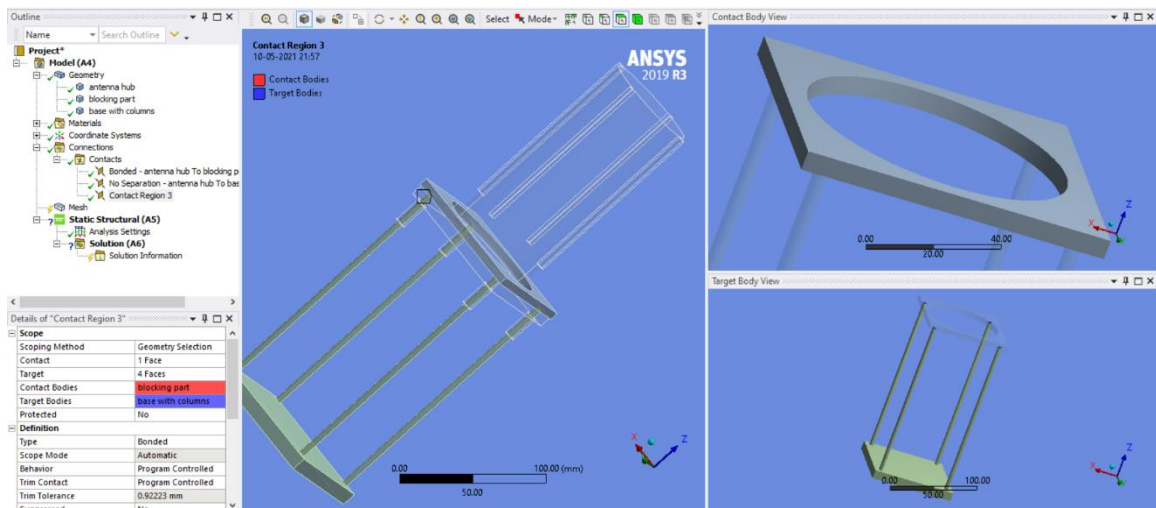


Figure 10.10.8: Contact Analysis between Columns and Blocking Part

Here the contact body is the blocking part and the target body is the columns and as mentioned earlier there exists a bonded contact between them

### 10.1.4 Contact Analysis between Flexible Plate and Female Locks

As mentioned in earlier, the assembly of male and female locks are done on the base and underneath the blocking part respectively when there is a collision between the base of the antenna hub and the blocking part the locking parts snap with each other and a bonded contact exists between them this is understood as these are locks and a bonded contact has to exist between them but for this action to take place there are flexible plates which are assembled inside the box and contact analysis of this is very important as the success of the locks depends on the snapping action of the flexible plate and the male locks thus the contact analysis of the female locks with the flexible plate was done

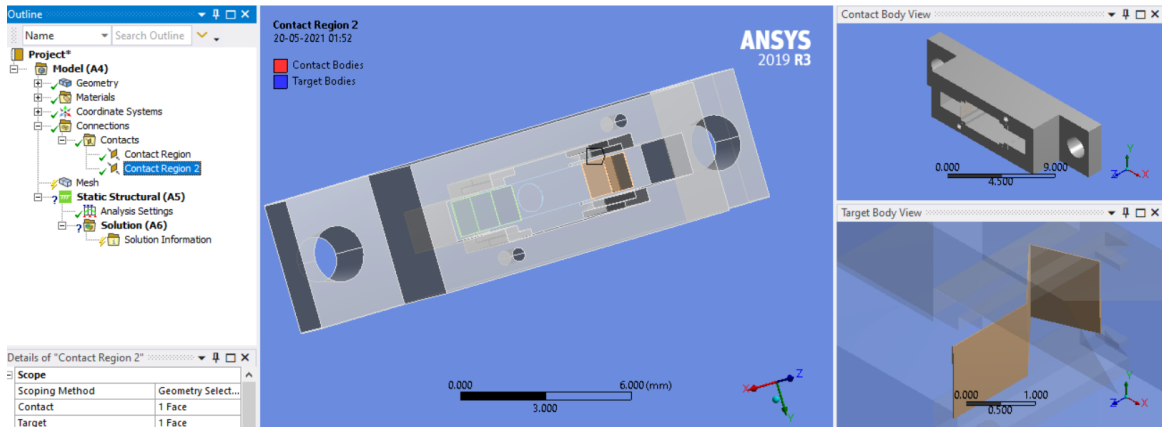


Figure 10.10.9: Contact Analysis between Female Lock and Flexible Plate

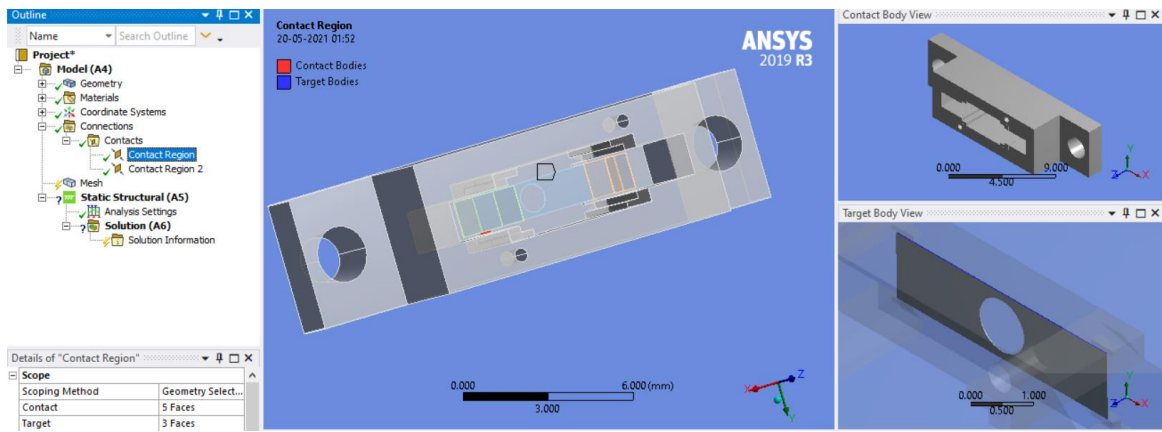


Figure 10.10.10: Contact Analysis between Flexible Plate's Bottom End and Female Lock

The above images show the contact patches between the walls of the female lock and the flexible plate and a bonded contact exists between the flexible plate and the inner walls of the locking mechanism.

### 10.1.5 Contact Analysis between Box and Lid

The torsion springs on the hinge pin are loaded by 270 degrees. When the locks on the box are released, it opens the lid from zero degrees to 270 degrees and the lid collides with the right side of the box. An impulsive force acts on the box as shown in the calculations. Therefore, a contact analysis has to be done between the box and the lid to fully analyze the effect of the impulsive force on the box and the lid.



Figure 10.10.11: Contact Analysis between Box and Lid

The above image shows the contact analysis of the lid and the box. The box is the target body and the lid is the contact body. The contact present between them is a rough contact. The sliding action cannot take place but the two bodies can be separated.

## 10.2 Finite Element Analysis

From all the physical calculations and contact analysis we exactly know the forces and the regions where these forces are acting. The mechanism can then undergo static structural analysis in order to decide the best material for the project. The choice was between the two materials which showed promising results - Aluminium alloy 7075 which has zinc as the primary alloying element and Structural Steel (S460) which has 0.12% carbon in it. In order to justify the best material a detailed analysis of both the materials is shown.

### 10.2.1 Materials under Consideration

The properties of Aluminium alloy 7705, Structural steel (S460 which has 0.12% carbon) and Beryllium Copper are shown in the figures, Beryllium Copper was used only to manufacture the springs the other two materials are compared and the best material is chosen.

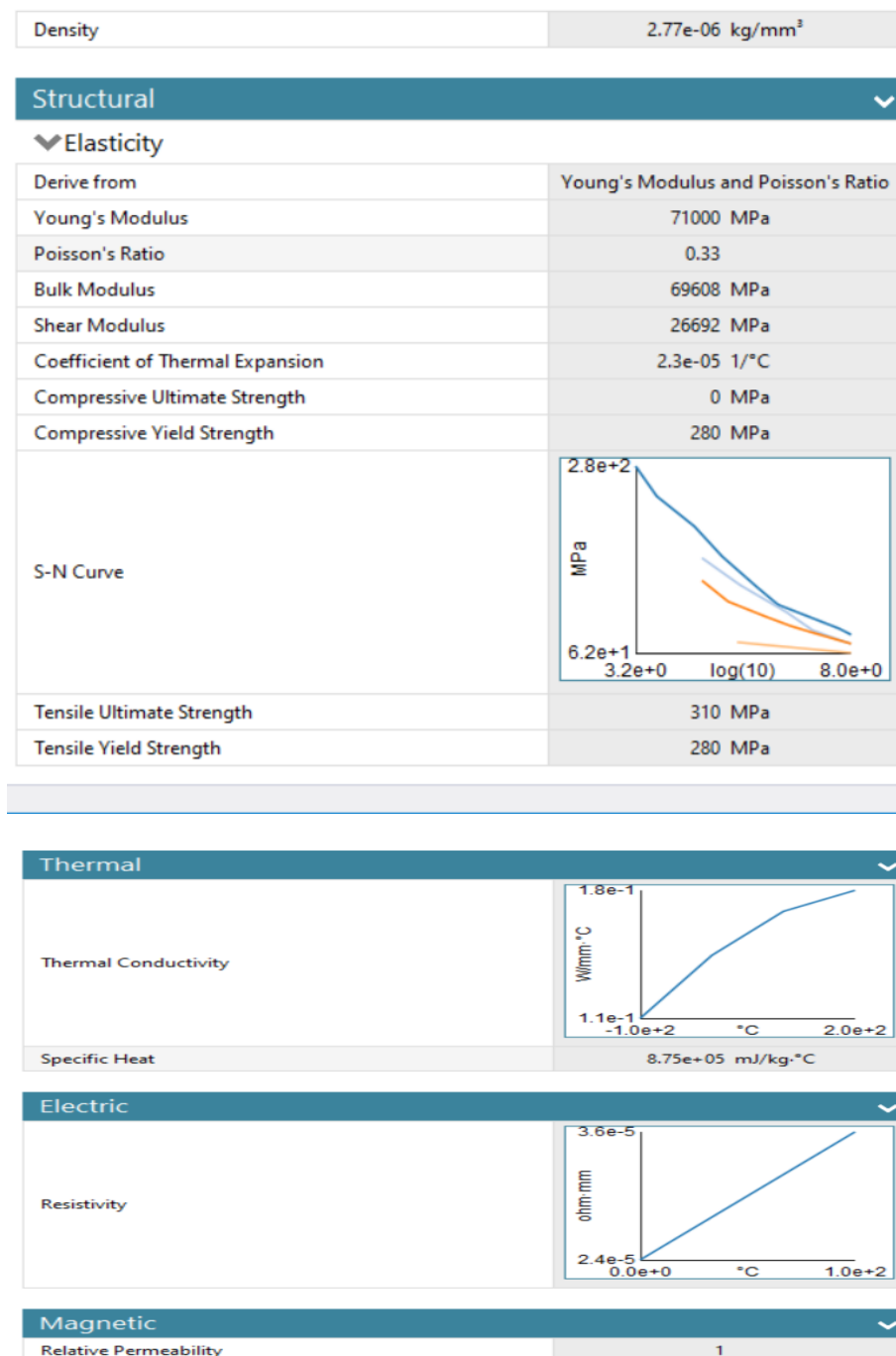


Figure 10.10.12: Properties of Aluminium alloy 7705

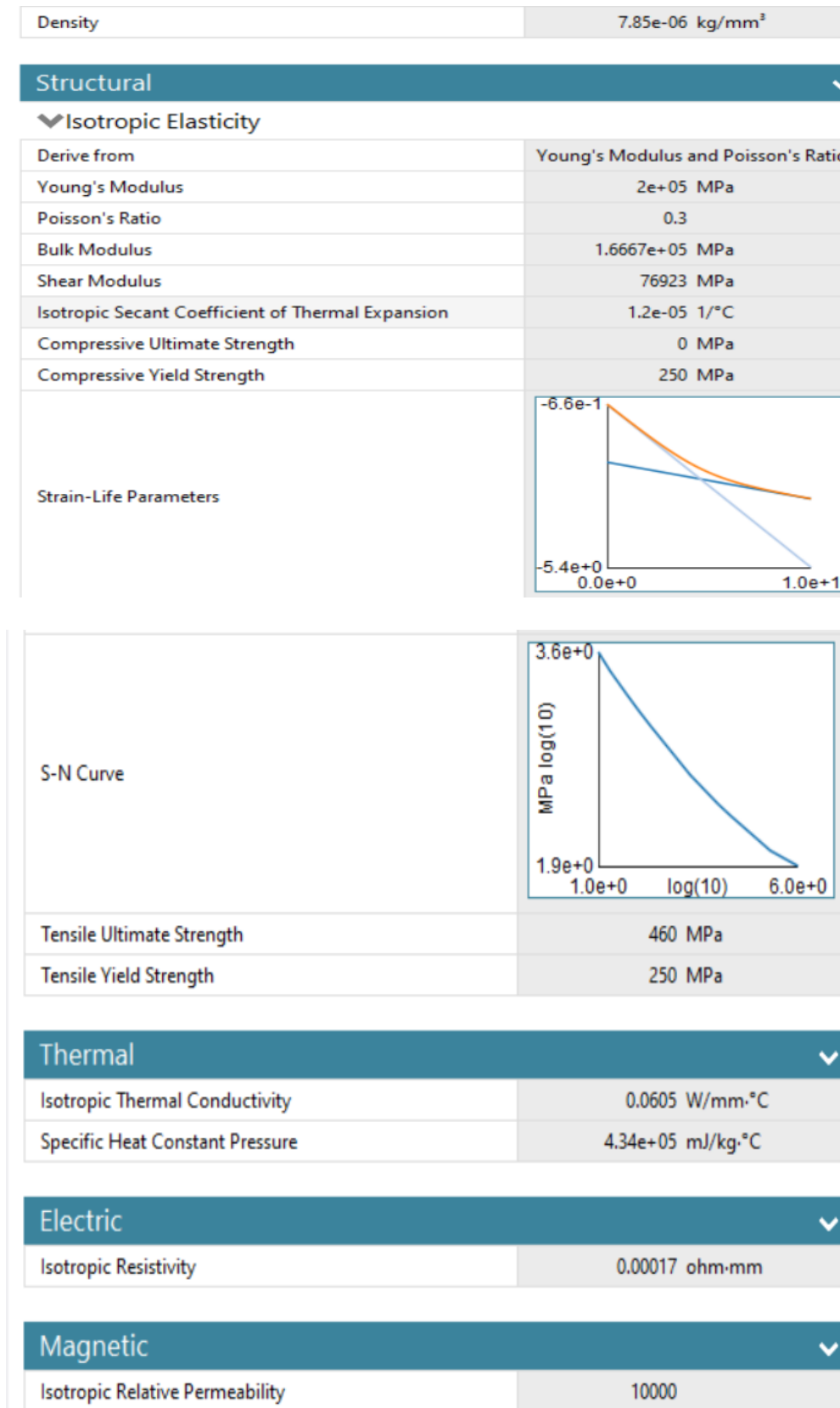


Figure 10.10.13: Properties of Structural Steel S460

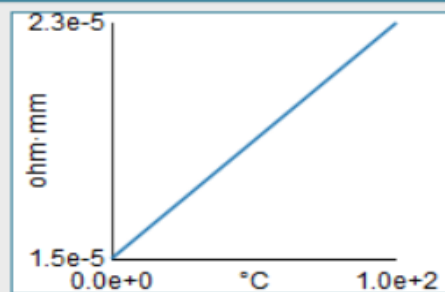
Density	8.3e-06 kg/mm <sup>3</sup>
<b>Structural</b>	
▼ Isotropic Elasticity	
Derive from	Young's Modulus and Poisson's Ratio
Young's Modulus	1.1e+05 MPa
Poisson's Ratio	0.34
Bulk Modulus	1.1458e+05 MPa
Shear Modulus	41045 MPa
Isotropic Secant Coefficient of Thermal Expansion	1.8e-05 1/°C
Compressive Ultimate Strength	0 MPa
Compressive Yield Strength	280 MPa
Tensile Ultimate Strength	430 MPa
Tensile Yield Strength	280 MPa
<b>Thermal</b>	
Isotropic Thermal Conductivity	0.401 W/mm·°C
Specific Heat Constant Pressure	3.85e+05 mJ/kg·°C
<b>Electric</b>	
Isotropic Resistivity	
<b>Magnetic</b>	
Isotropic Relative Permeability	1

Figure 10.10.14: Properties of Beryllium Copper

### 10.2.2 FEA of the lid

The lid and the box undergo a collision due to which an impulsive force of 10.324 N acts on it for a time interval of 0.5 sec. The lid has to be tested for this force because it must have the ability to withstand this force. In order to analyze the lid first, the fixed supports had to be inserted. Fixed support indicate to the system that the force won't be experienced at that location. The hinge axis and the edges of the hinge were considered as the fixed supports and a force of 10.324 N was applied on the plane surface of the lid and the following results were obtained as shown in the figures.

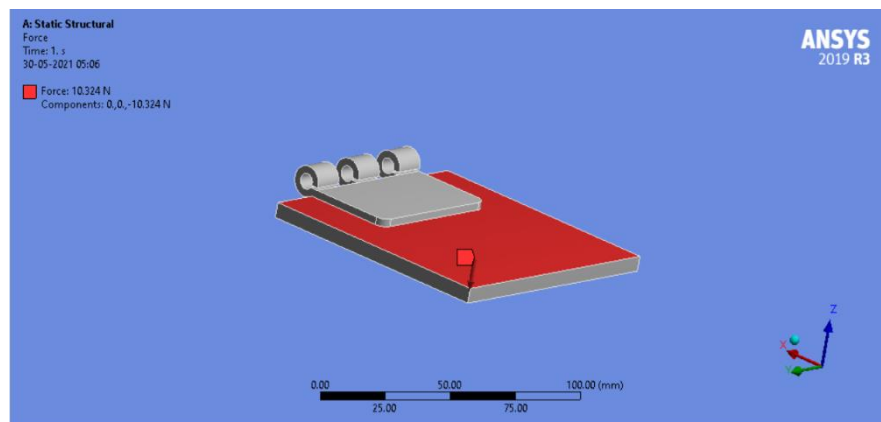


Figure 10.10.15-Application of force and support structures on lid

The above image shows the application of 10.324 N on the lid and also shows the way the force is applied and the graphs related to it

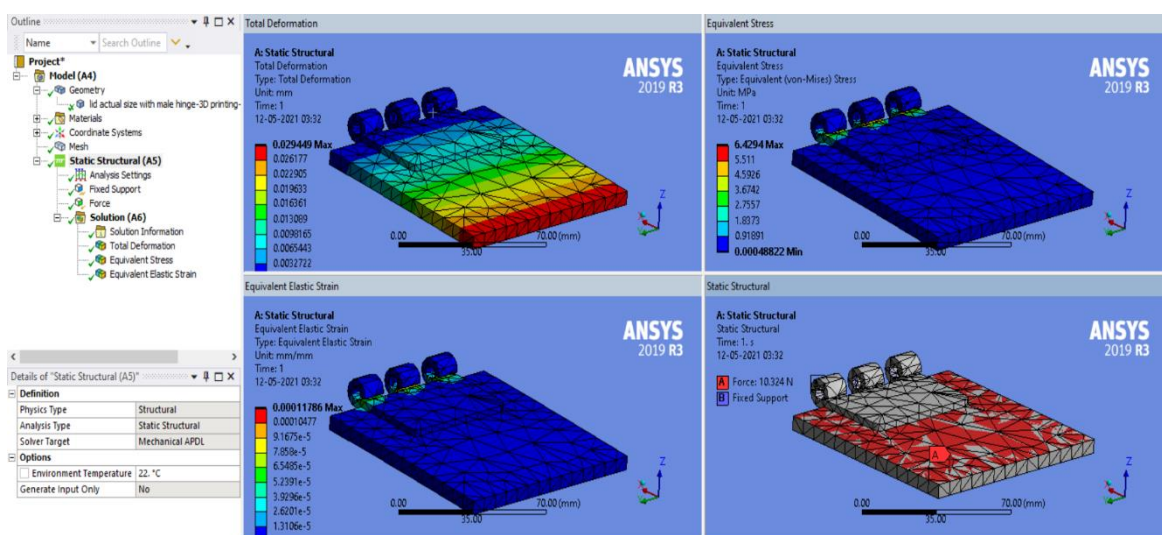


Figure 10.10.16: Results of FEA of Lid Made of Aluminium

The above image shows the total deformation, equivalent stress and strain and the application of force. The max values of the equivalent stress are 6.429 MPa. This shows that the design is safe. The compressive yield strength of Aluminium is 280 MPa. If we take a factor of safety of 0.5, the max stress the material can experience is 140 MPa and the obtained value is well below it.

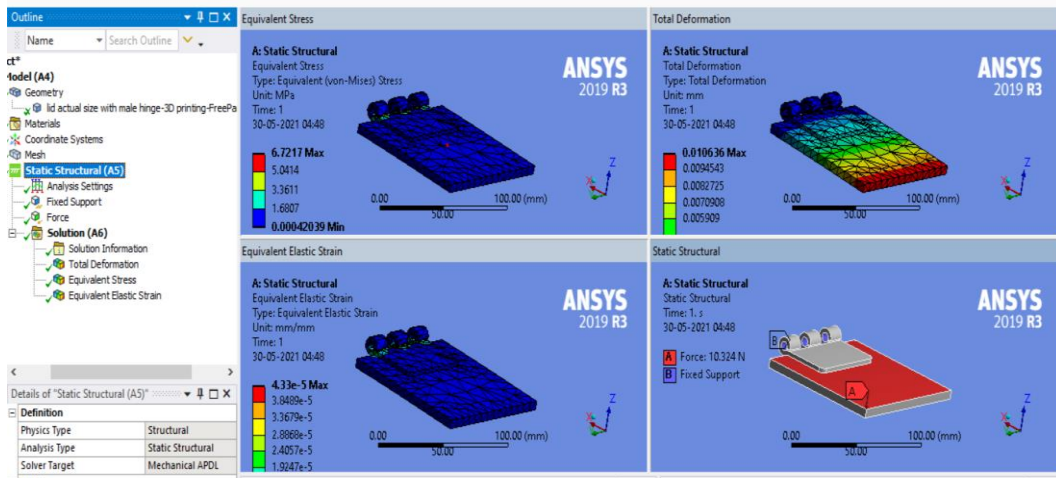


Figure 10.10.17: Result of FEA of Lid Made of Structural Steel

The above image shows the total deformation, equivalent stress and strain and the application of force. The max values of the equivalent stress are 6.7217 MPa this shows that the design is safe the compressive yield strength of Structural Steel is 250 MPa if we take a factor of safety of 0.5 the max stress the material can experience is 125 MPa and obtained value is well below it.

From the comparison, it can be inferred that aluminum is a better material to use than structural steel because it is lighter, it has a higher compressive yield strength, it is flame resistant and more robust even though there isn't a lot of difference in the FEA of the components. Lightness and Flame Resistivity play a vital factor in selecting Aluminium as the material so that if an unforeseen event occurs in space the parts made for aluminum have a higher chance of survival.

### 10.2.3 FEA of the pin

The pin is a part of the hinge, the hinge on the whole experiences a torque of 131 N-mm because of the torsional loading of the torsion springs. These values are taken from the torsion spring calculations. As the hinge experiences all its force on its pin (except during

loading of the torsion spring), it is sufficient to analyze the pin of the Hinges, this saves compilation time while maintaining design safety.

The pin must be able to handle the applied torque. The FEA is done on the pin by taking a torque of 131 N-mm acting on it. While applying this force the two top surfaces of the cylindrical pin are fixed.

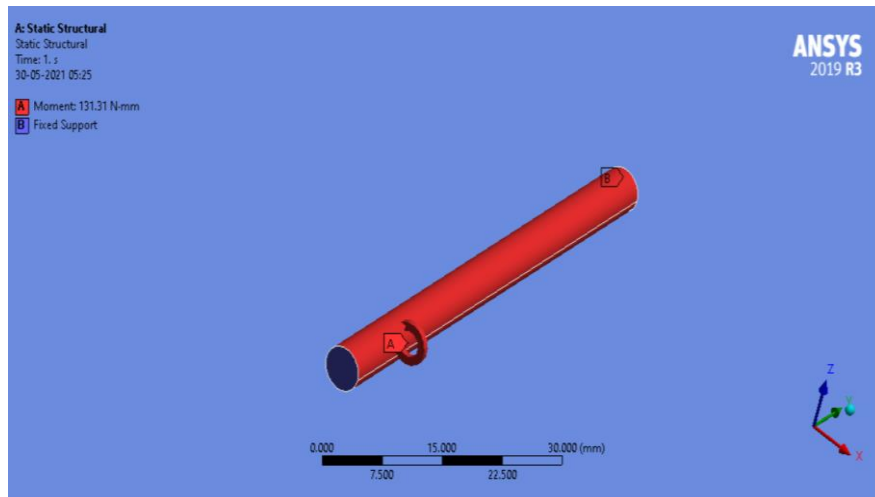


Figure 10.10.18-Application of Torque on Hinge Pin

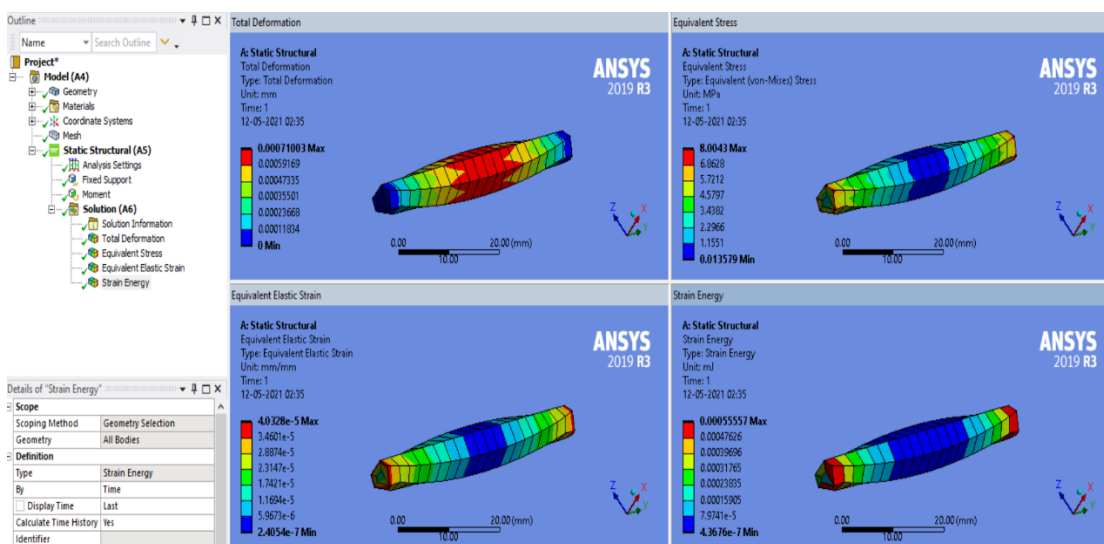


Figure 10.10.19: Results of FEA of Hinge Pin using Structural Steel

When a torque of 131 N-mm acts on the pin the equivalent stress developed is 8.0043 MPa, the yield strength of Aluminium is 280 MPa. Taking a factor of safety of 0.5, the max allowable stress is 140 MPa therefore the designs are safe.

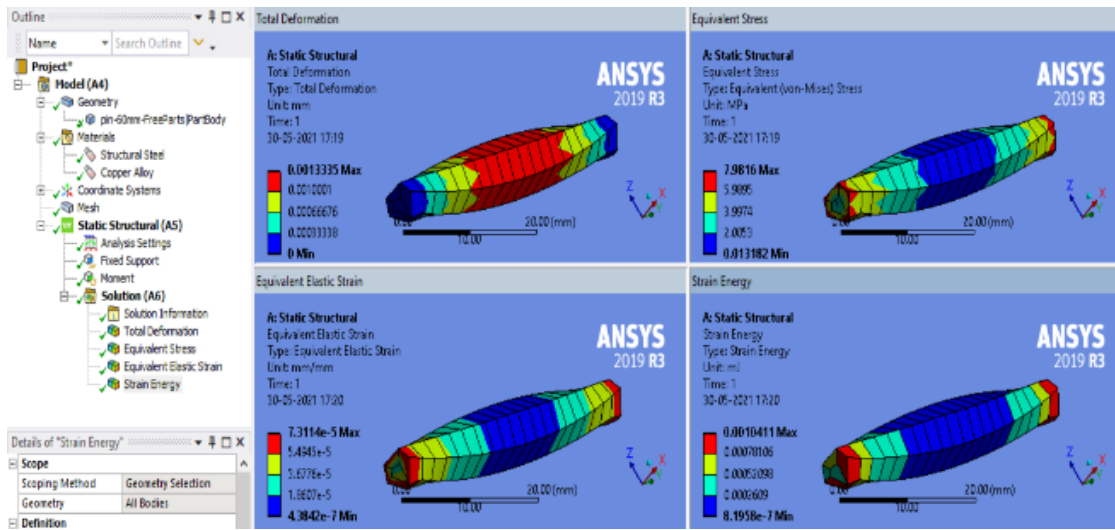


Figure 10.10.20: Result of FEA of Pin Made of Beryllium Copper

When a torque of 131 N-mm acts on the pin made from Beryllium Copper the above results are obtained. The max stress acting on the material is 7.98 MPa. It is almost similar to structural steel. The tensile yield strength of Beryllium Copper is 280 MPa. Therefore the designs are safe.

The inference from these results is as follows. It was decided that Beryllium Copper is the better material to use, even though both the materials cope with the stresses really well. Beryllium Copper has the unique ability of withstanding cold welding which is a phenomenon that occurs in space when two metal surfaces touch in space.

#### 10.2.4 FEA of Torsion Springs

The torsion springs play an important role in opening the lid. These springs are loaded from 0 degrees to 270 degrees and when the loading is released the lid opens up. A torque of 131 N-mm is required to load these springs. The FEA results are obtained by fixing one end of the spring and then giving a torque of 131 n-mm to the other end.

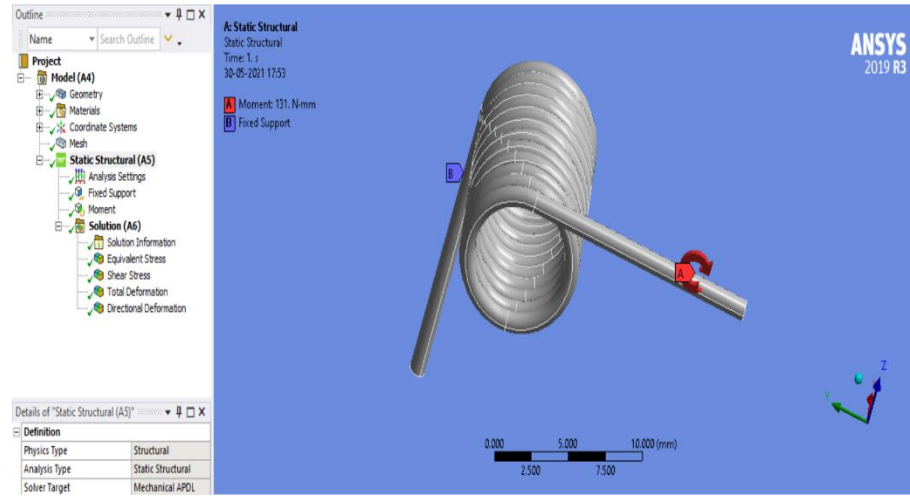


Figure 10.10.21: Application of Torque and Fixed Supports on Torsion Springs

The above figure represents the way the torque is applied on the spring. The FEA is done on Beryllium Copper and Structural Steel the following results are shown in the figure

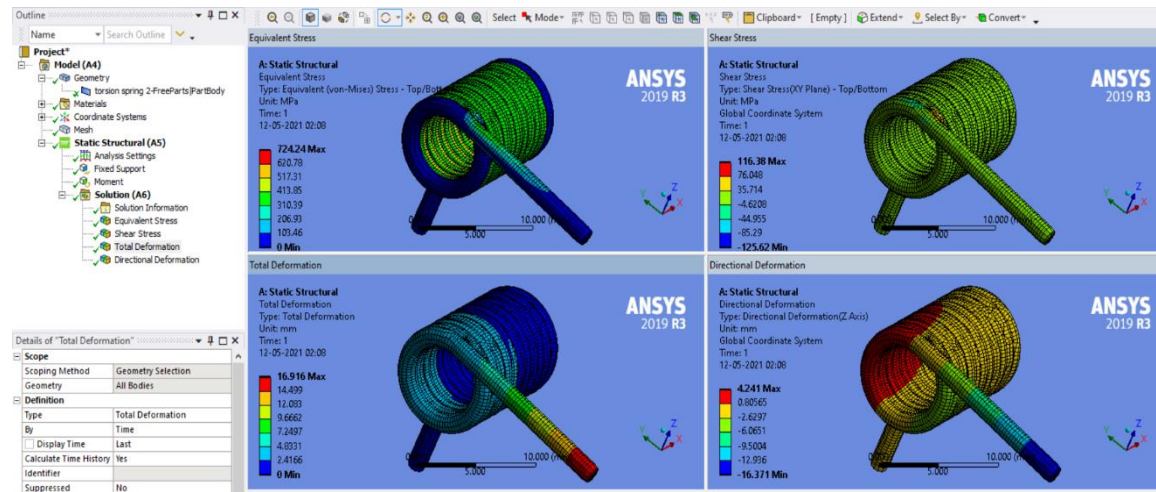


Figure 10.10.22: Result of FEA of Torsion Springs Made of Beryllium Copper

The above picture shows the different results of the FEA on the torsion springs for Beryllium Copper. The total deflection is 16.916 mm which corresponds to the physical calculations of the torsion springs. The total shear force acting on the spring is 116.38 MPa, these values are below the safe stress of the material.

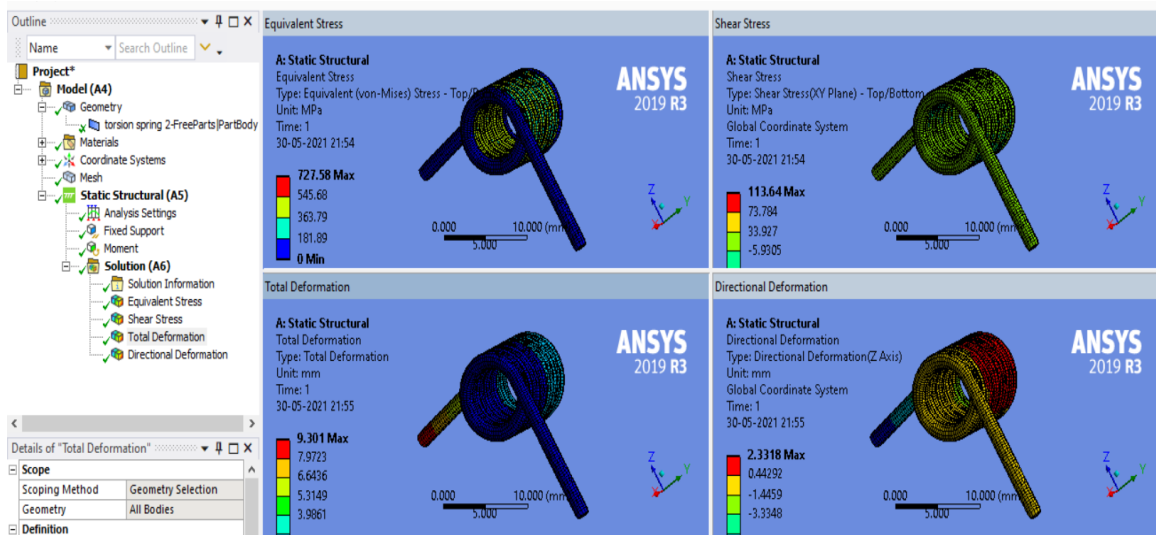


Figure 10.10.23: Result of FEA of Torsion Spring Made of Structural Steel

The above image shows the results for the FEA of torsion spring made of Structural steel. The shear stress developed is 113.64 MPa and the total deformation is 9.301 mm. Inferences from these results are as follows: even though the shear stress developed and the total deflection in Structural Steel (spring steel) is less than Beryllium Copper, the latter is preferred because it has the unique ability of not undergoing cold welding, given that both can safely undergo required loading.

### 10.2.5 FEA of the Box

The lid hits the box and an impulsive force of 10.324 N is generated and the designs of the box are checked for these forces as this is the max force acting on it. The other walls of the box and the edges of the hinges are considered as hinge supports. The below figure shows the fixed supports and the application of force.

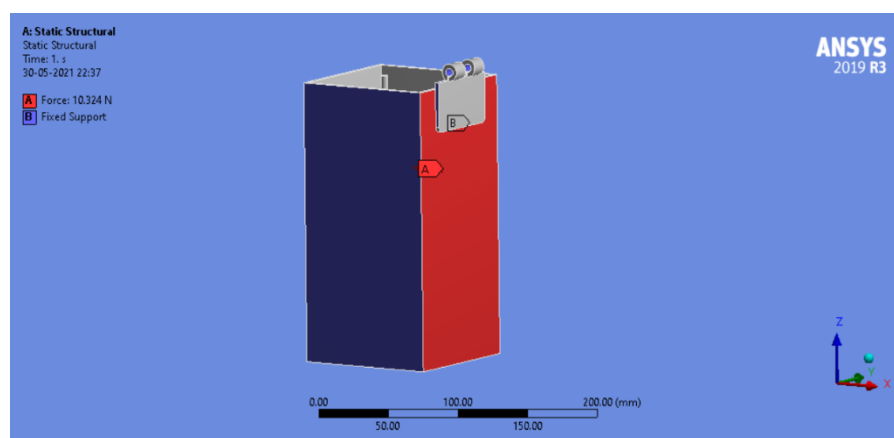


Figure 10.10.24: Support Structures and Application of Force on Box

The fixed supports are shown in blue. Here the effect of the force is minuscule on these fixed supports; the face under loading is shown in the color red.

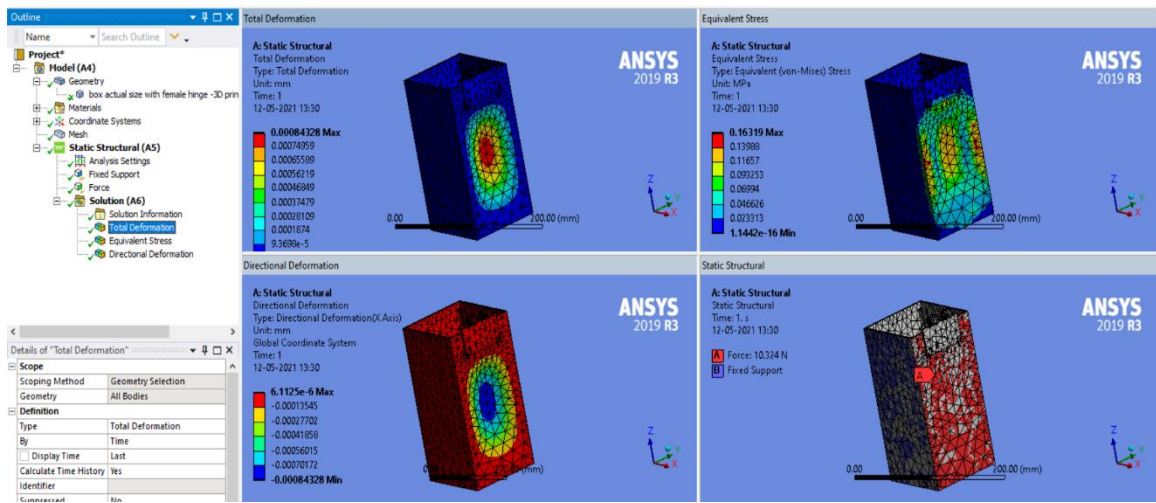


Figure 10.10.25: Result of FEA of Box Made of Aluminium

The above image shows the FEA of the box made of Aluminium. The deformation is of the order  $10^{-6}$ . This shows that the effect of the impulsive force on the box is minuscule. But for the same force the lid experiences a much larger deformation and stress because the edges of the hinges present on the lid also experiences it whereas the hinges of the box don't experience this force. Therefore, the stresses on the box are of the magnitude 0.16319 MPa.

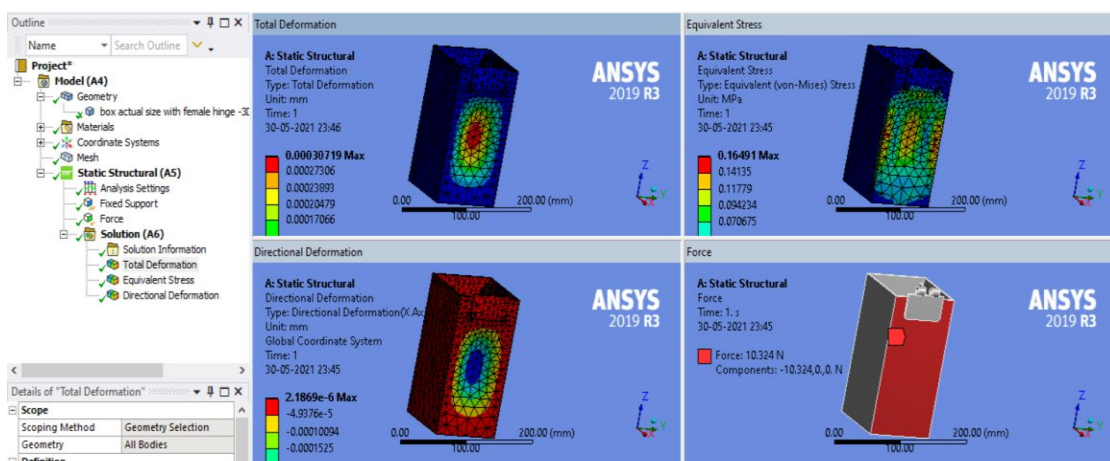


Figure 10.10.26: Result of FEA of Box Made of Structural Steel

The stresses and the total deformation acting on the box made of structural steel is very similar to the box made of Aluminium and as mentioned earlier the effect of the force on the box is minuscule. Inference from the comparison – It doesn't matter which material is used to build the box as the effect of the forces acting on the box is negligible but Aluminium is chosen over structural steel because it is more robust than stainless steel. If an unforeseen event happens in space a box made of Aluminium has a greater chance of surviving it.

### 10.2.6 Antenna Hub FEA

From the physical calculations it can be seen that the force acting on the antenna hub is in the downward direction and has a magnitude of 91.12 N. For safety considerations the analysis is done by applying a force twice the magnitude. The supporting structures for the springs are considered as fixed supports and the force of 182.24 N is applied to the top surface of the base. The below figure shows the application of forces and supports.

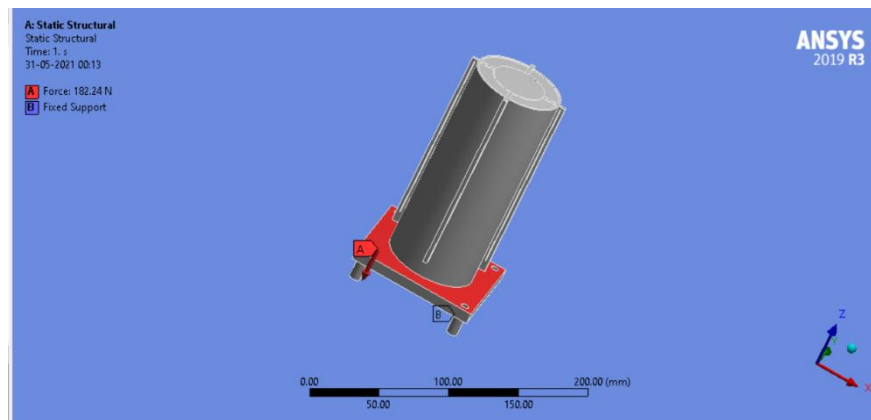


Figure 10.10.27: Application of Support Structures and Force on Antenna Hub

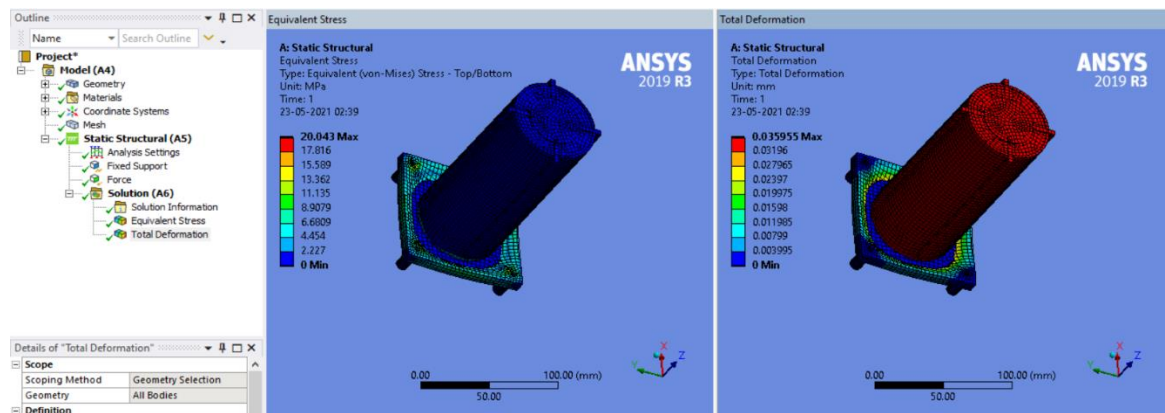


Figure 10.28: FEA of Antenna Hub - Aluminium

From the image it can be seen that the base of the antenna hub experiences a significant amount of stress and the antenna hub undergoes maximum deflection. The value of the stress is of the order 20 MPa as shown in the figure but the safe working stress is of the order 140 MPa, and therefore ensures safety.

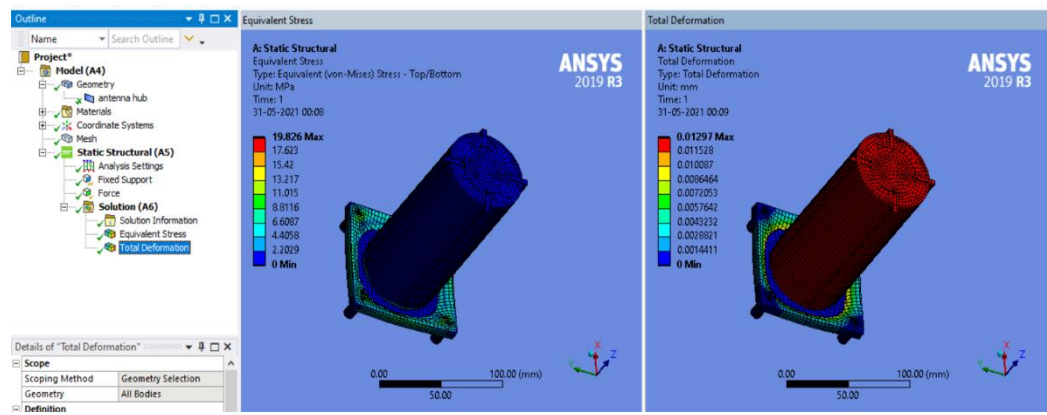


Figure 10.29: FEA of Antenna Hub – Structural Steel

The above figure shows the FEA of the antenna hub made of structural steel. The values of the stresses are well below the safe stresses and the values of the stresses and the deformation for antenna hub made of structural steel is very similar to that of Aluminium. Inference from the comparison – even though the values of the stresses and deformation for both the components are very similar to each other and well below their respective safe stresses, Aluminium is chosen over structural steel because of its lightness and flame resistivity.

### 10.2.7 FEA of the Compression Springs

Compression springs are responsible for the movement of the antenna hub and the base plate assembly from its initial position to the final position.

When the antenna hub is in its initial position the compression spring of total length 230mm is compressed to a length of 25mm. Therefore, the total deflection on the spring is 205mm. This deflection is applied as a displacement in the static structural environment by fixing one end of the spring, and the various stresses and strain acting on the spring are calculated by the software.

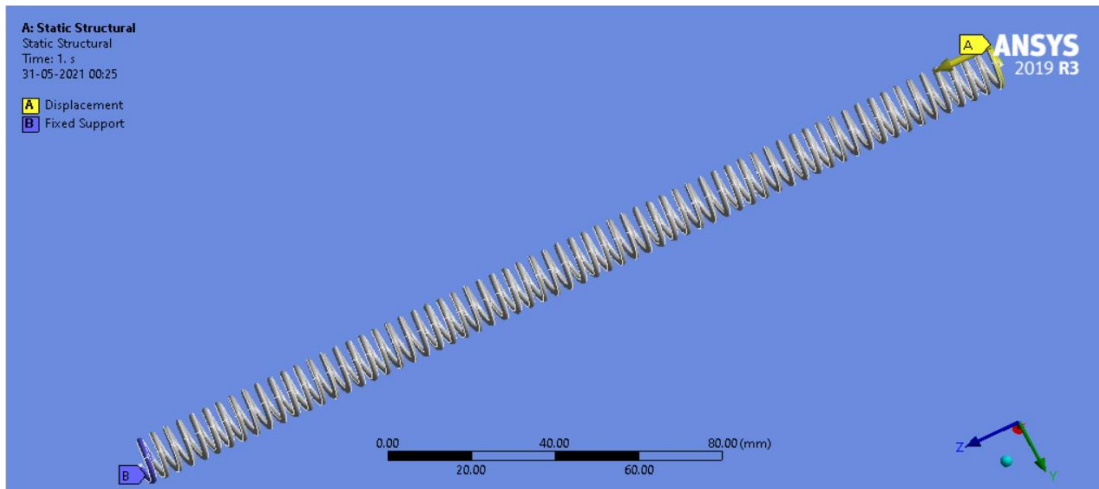


Figure 10.3010.28: Structural Support and Forces on Compression Springs

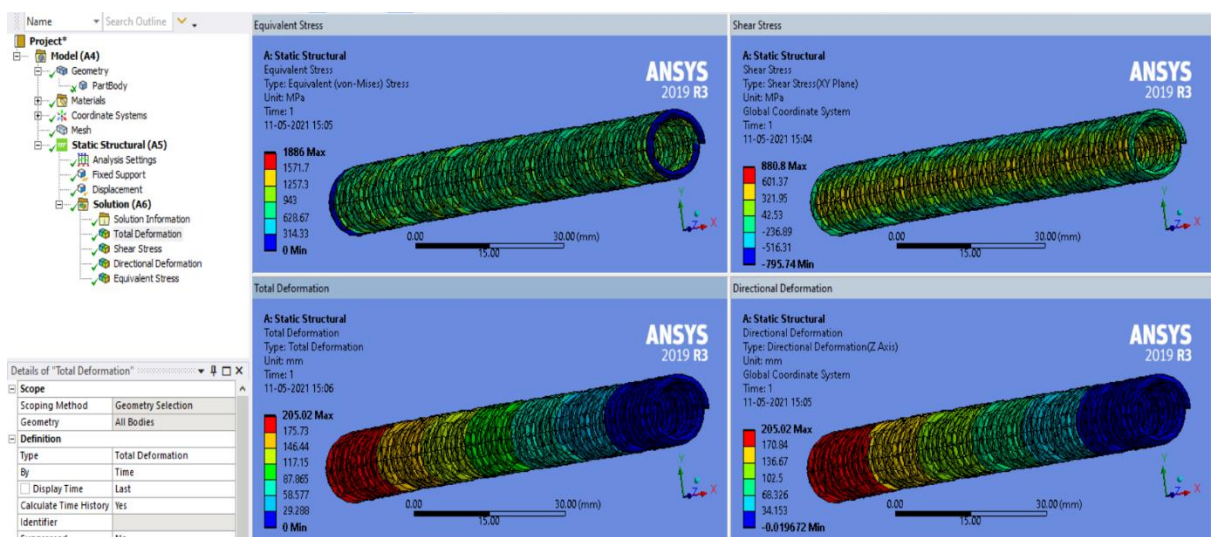


Figure 10.31: Compression Spring FEA - CuBe

The shear stress acting on the springs are of the order 880.8 MPa. There was a discrepancy with the physical calculations of the spring and the FEA as the stresses in the analysis were far greater. Therefore, design had to be done in such a way that it could withstand the stresses from the FEA. The stiffness of the existing springs was increased so that the axial force acting on the spring did not cause the springs to fail.

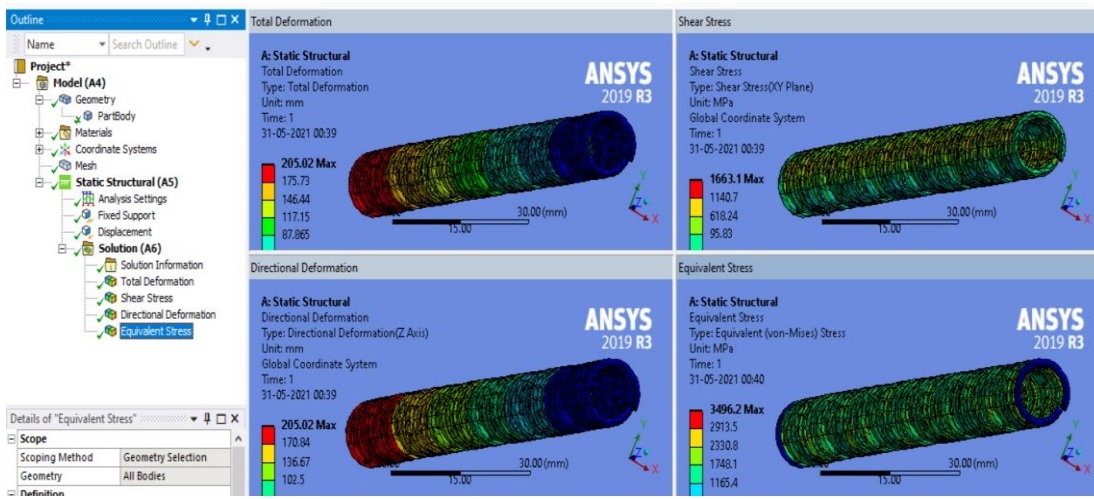


Figure 10.32: Compression Spring FEA – Spring Steel

The above image shows the FEA of the spring made of spring steel. It can be observed that the shear stresses and the equivalent stresses are far greater than the spring made of Beryllium Copper and the springs undergoing failure is a greater possibility.

Inferences from the comparison – it can be inferred that a spring made of spring steel is more vulnerable to failure than the spring made of Beryllium Copper under the same loading conditions. Therefore, Beryllium Copper was used to manufacture the springs.

### 10.2.8 FEA of the Blocking Part

As mentioned earlier, a blocking part is used to prevent the antenna hub from ejection to outer space. Therefore, it experiences the same force of 91.12 N but in the opposite direction. FEA is done by applying a force twice the magnitude of the actual force, hence a force of 182.24 N is applied on the blocking part in the upward direction.

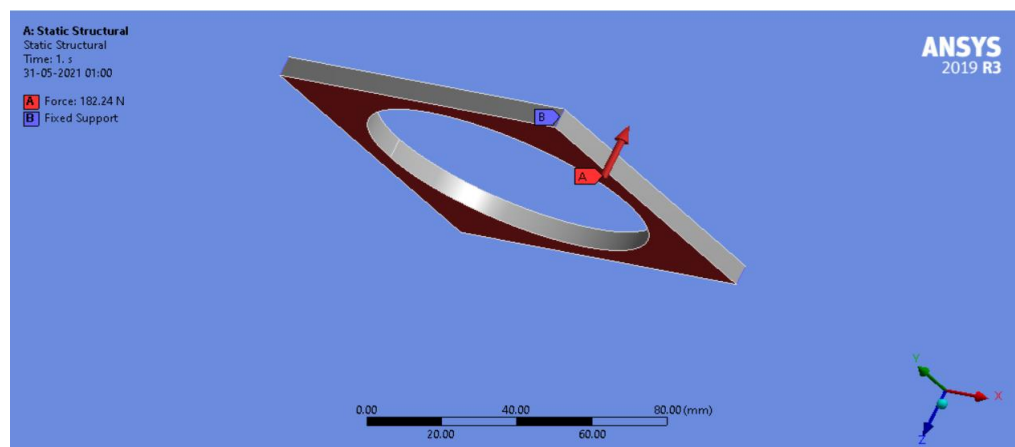


Figure 10.33: Supports and Forces on Blocking Plate

The above image shows application of force and supports on the blocking part. The force acts on the bottom face and the corners of the blocking part are fixed.

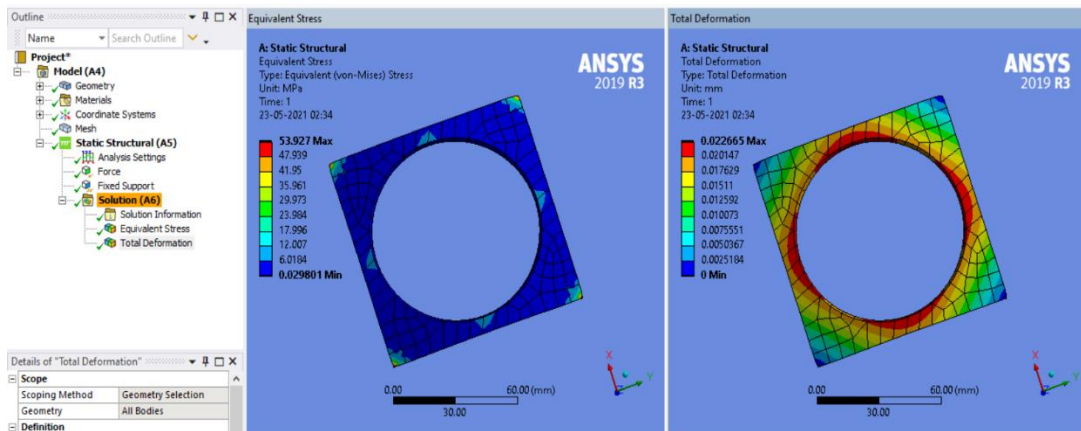


Figure 10.34: Blocking Part FEA - Aluminium

The above figure shows the results for the analysis of the blocking part using Al. The value of the stresses is well under the safe stress conditions. In order to damp these forces RVT compounds are used. These compounds absorb the forces acting on the blocking part and prevent the forces dissipating to other components of the antenna deployment mechanism.

The Results of the FEA of the blocking part made of Structural Steel gives the same result as the blocking part made of Aluminium and the stresses are well under the safe working stress conditions, as shown.

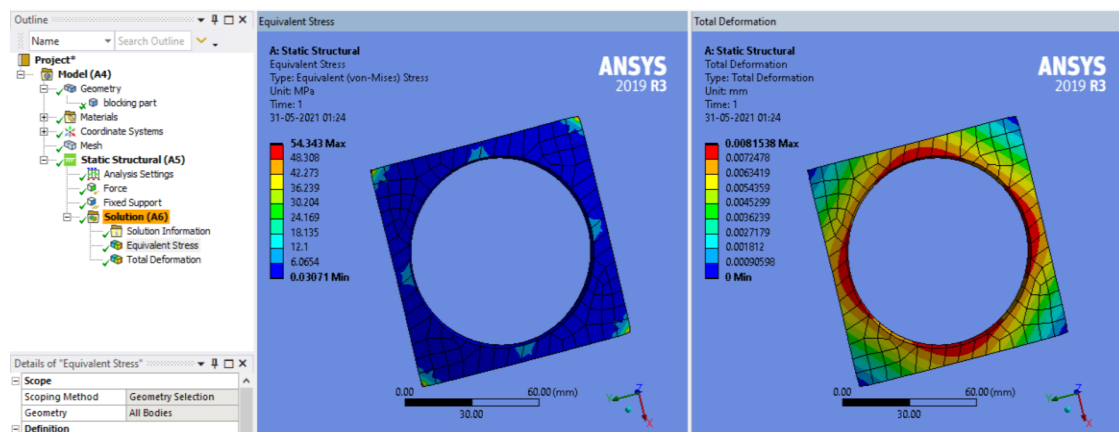


Figure 10.34: Blocking Plate FEA - SS

Inference from the comparison – even though both the materials Aluminium and Structural Steel can withstand the stresses due to the impact forces, Aluminium is preferred over structural steel because of its weight and flame resistivity.

### 10.2.9 Analysis of Contact Regions

There are contact patches between the columns and the holes of the antenna hub. There are certain pressure stresses acting on them. The frictional stresses on the columns are zero because of the presence of DU Bushes. The following image show the pressure stresses between the columns and the holes of the antenna hub.

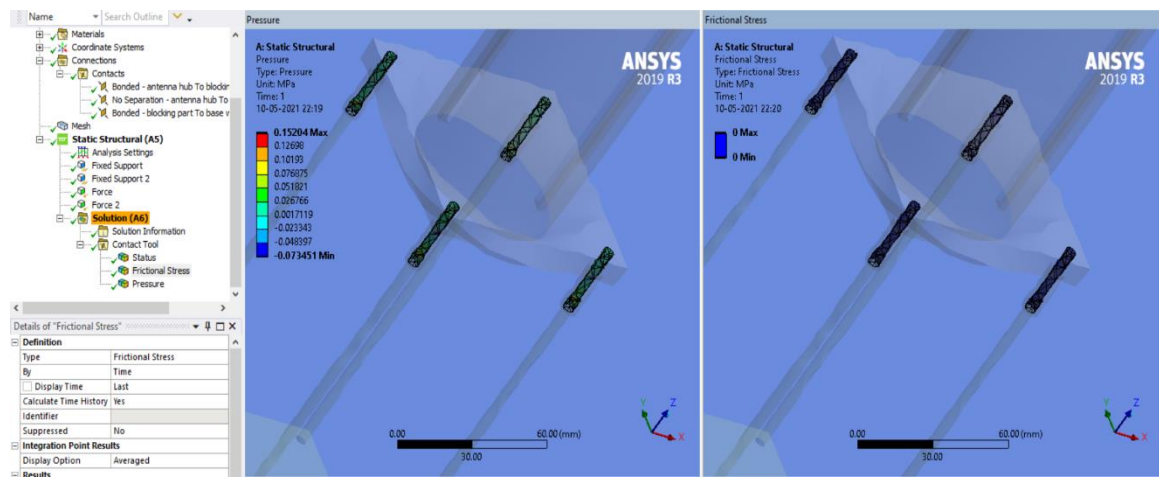


Figure 10.36: Pressure Stresses between Columns and Hub Holes

There are pressure stresses and frictional stresses developed when there is a collision between the base of the antenna hub and the blocking part. The below images shows the effect of these stresses between the contact region.

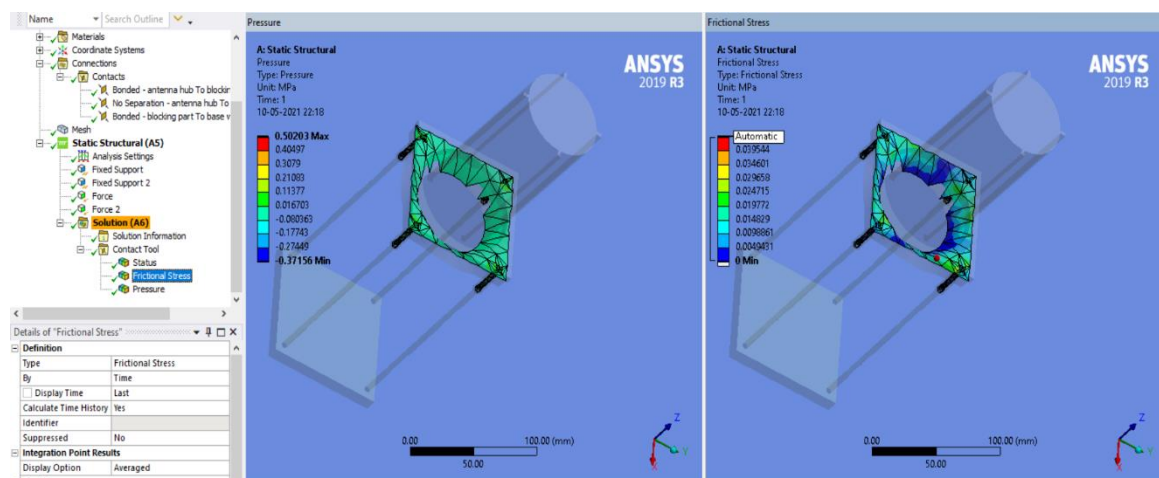


Figure 10.37: Pressure Stresses between Blocking Plate and Hub Base

These stresses do not significantly change between materials; so the values of the pressure stresses between the columns and the holes of the antenna hub, and the value of pressure and frictional stresses between the base of the antenna hub and the blocking part will have the same values irrespective of the material. Therefore, similar values are

obtained for both Aluminium and Structural Steel. The results of the analysis of structural steel is shown in the figure.

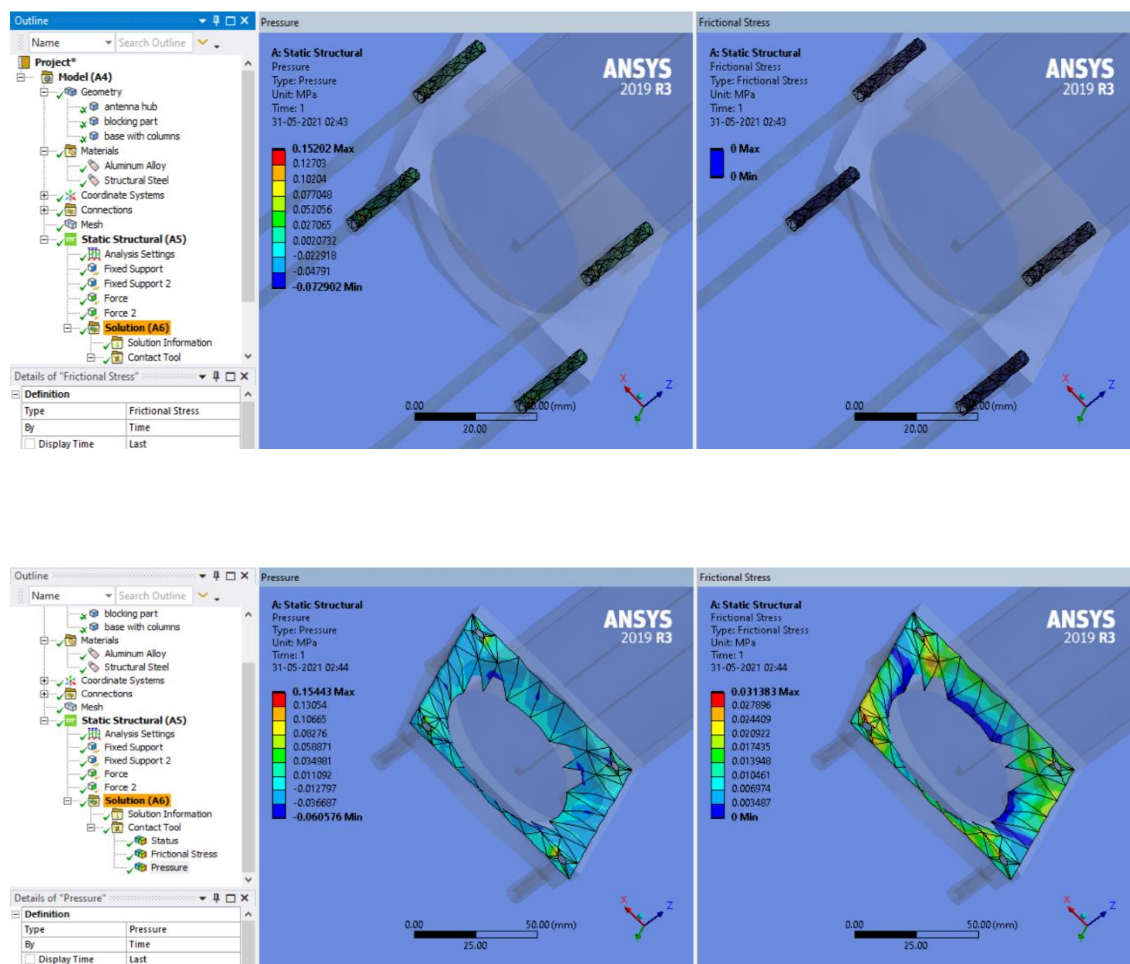


Figure 10.38: Contact Analysis - SS

### 10.2.10 FEA of Locking Mechanism

There are eight pairs of male and female locks and each pair experiences  $\frac{1}{8}$ th of the force experienced by the blocking part (the force experienced by the blocking part is divided between these eight locks).

The FEA is done by applying a force of 11.39 N on both the male and female locks but the opposite direction. The application of the forces and support structures on the male and female locks are shown in the figure.

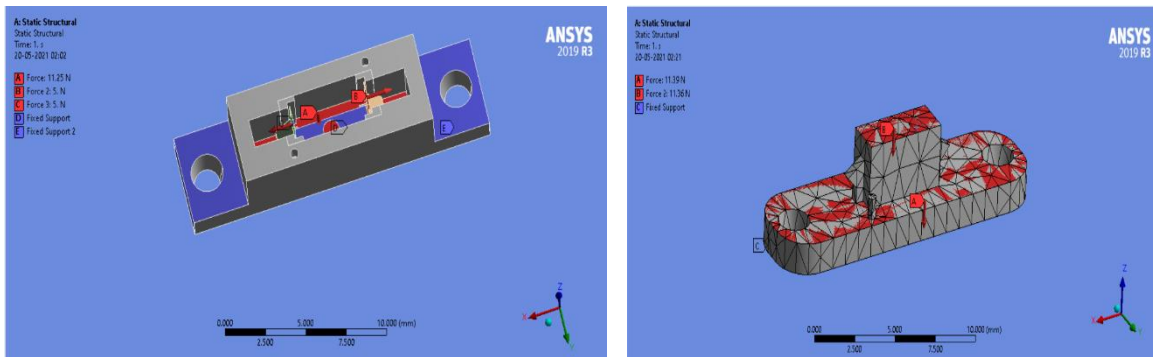


Figure 10.39: Support and Forces on Female Locks and male locks respectively

The locks are made of Aluminum because Steel isn't strong enough to handle the stresses developed on these locks. These locks are very small so 11.39N is a significantly large force acting on these locks.

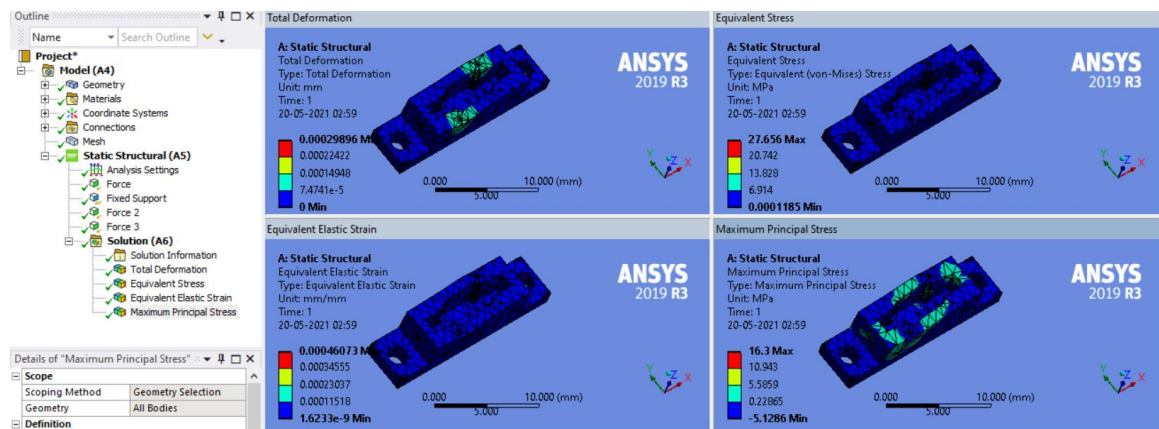


Figure 10.40: Female and male Locks FEA - Aluminium

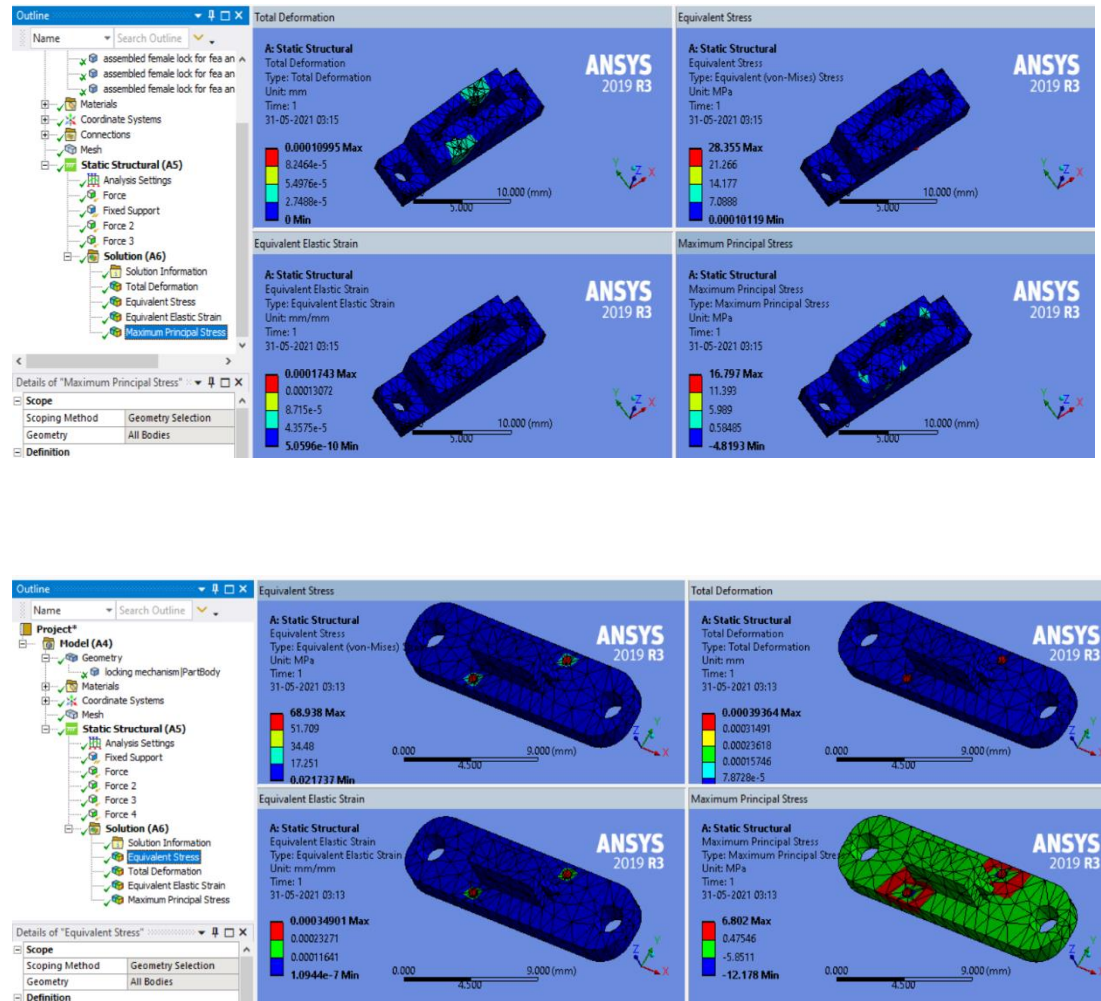


Figure 10.41: Female and Male Locks FEA - SS

Inference From the comparisons - the stresses on the two materials are not very different, but Aluminium is chosen over Structural Steel for its lightness.

## 11 Fabrication of Antenna Deployment Mechanism

The material chosen to build the parts of the antenna deployment mechanism is Aluminum. But before fabricating the parts with Aluminum, a prototype was built to establish proof of concept, using PLA.

### 11.1 FEA of PLA – Polylactic acid

As PLA is used to fabricate the prototype, the FEA of all the parts made of PLA is shown below, along with PLA's material properties, to prove structural stability of the same.

**Engineering Data: Material View**

**PLA**

**Structural**

**Isotropic Elasticity**

Derive from	Young's Modulus and Poisson's Ratio
Young's Modulus	46.5 MPa
Poisson's Ratio	0.3
Bulk Modulus	38.75 MPa
Shear Modulus	17.885 MPa

**Mechanical Properties**

	Metric
Hardness, Shore A	67 - 85
Hardness, Shore D	48 - 87
Ball Indentation Hardness	105 - 190 MPa
Tensile Strength, Ultimate	0.160 - 3000 MPa
	5.00 - 42.0 MPa @Temperature 30.0 - 110 °C
Film Tensile Strength at Yield, MD	19.0 - 54.0 MPa
Film Tensile Strength at Yield, TD	14.0 - 48.0 MPa
Tensile Strength, Yield	8.00 - 103 MPa
	46.0 - 49.0 MPa @Temperature 30.0 - 110 °C
Film Elongation at Break, MD	2.0 - 4550 %
Film Elongation at Break, TD	2.0 - 3980 %
Elongation at Break	0.50 - 700 %

Figure 11.1: Material Properties of PLA

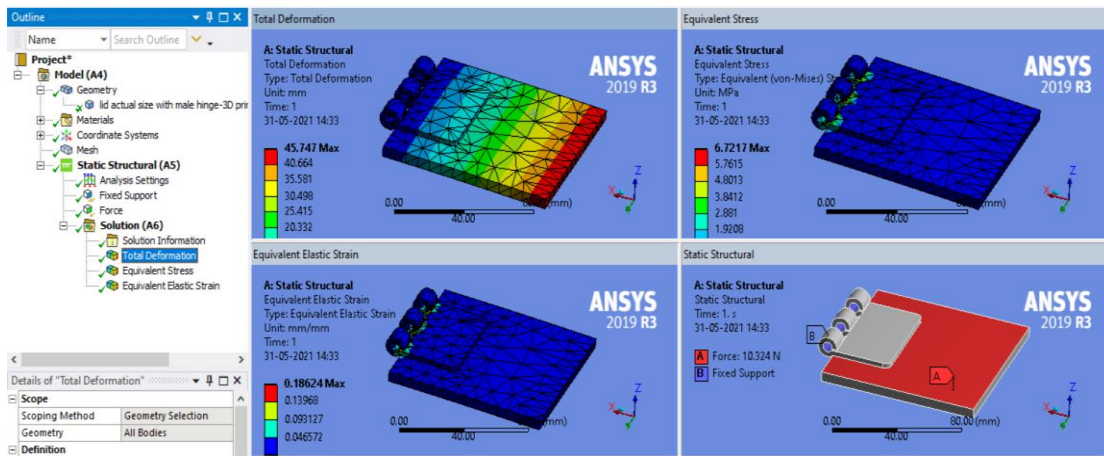


Figure 11.2: FEA of Lid using PLA

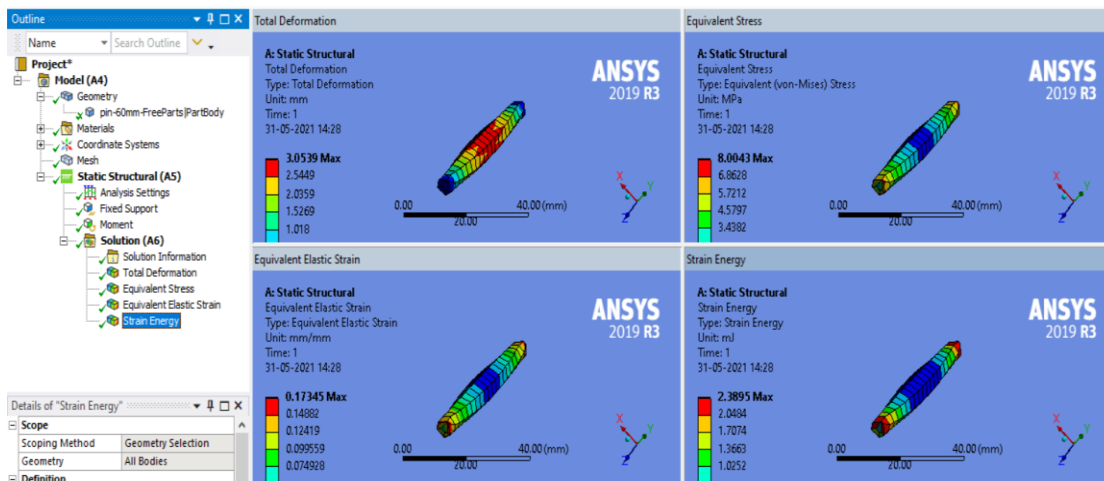


Figure 11.3: FEA of Hinge Pin using PLA

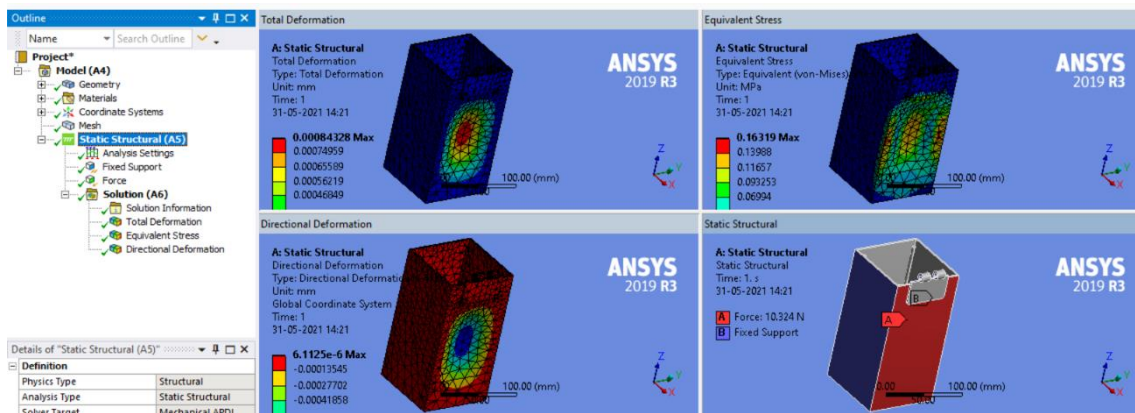


Figure 11.4: FEA of Box using PLA

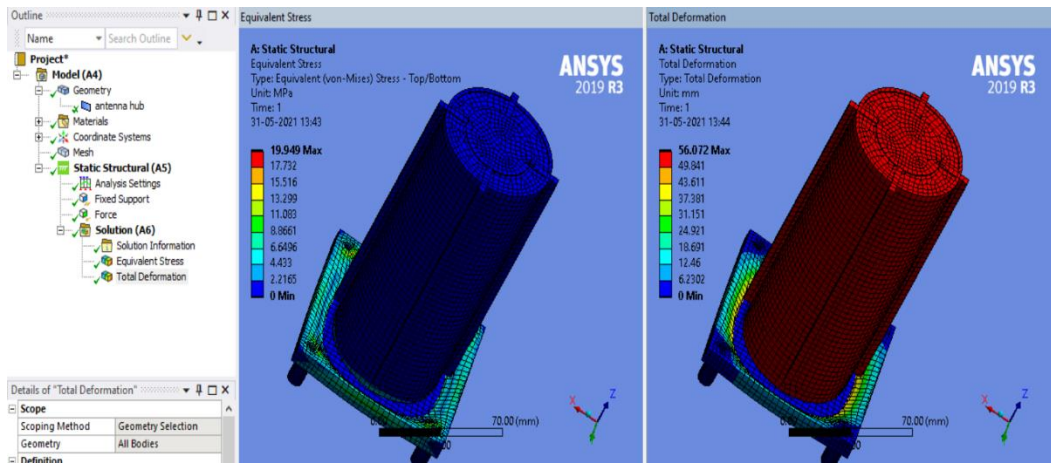


Figure 11.5: FEA of Antenna Hub using PLA

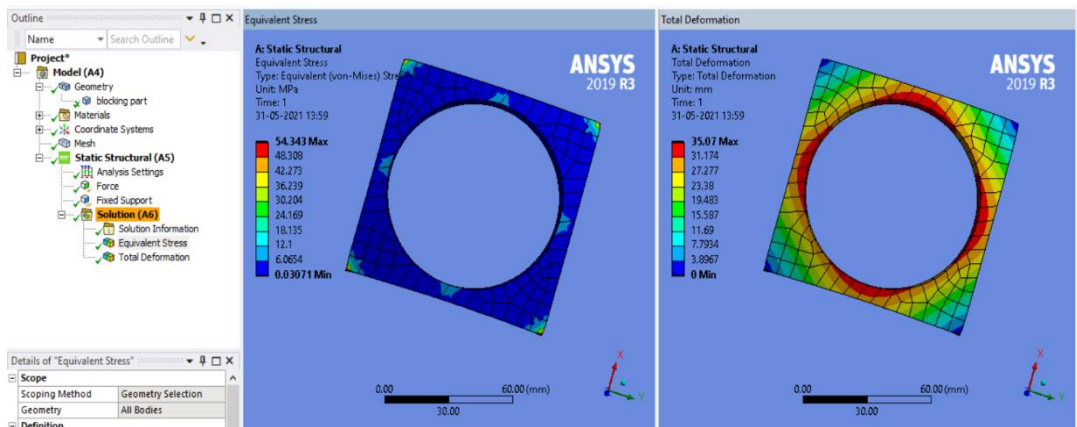


Figure 11.6: FEA of Blocking Plate using PLA

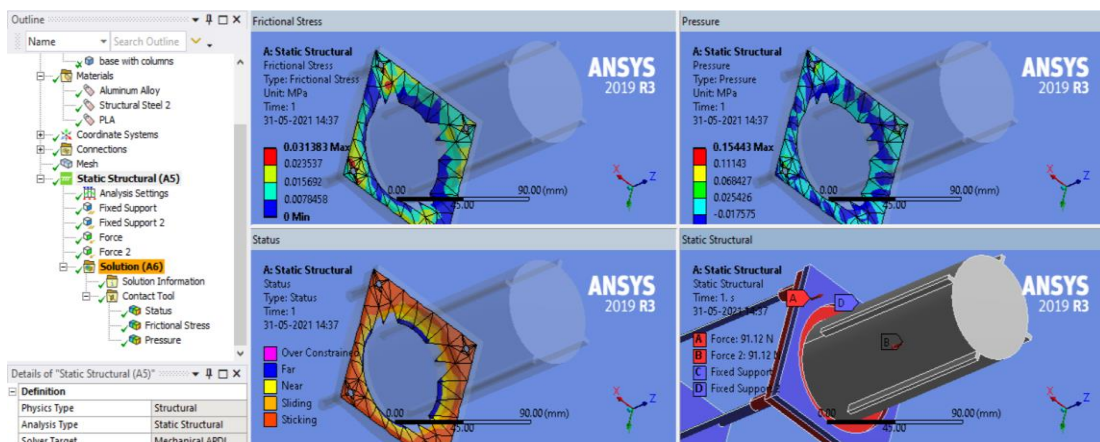


Figure 11.7: FEA of Contact Regions using PLA

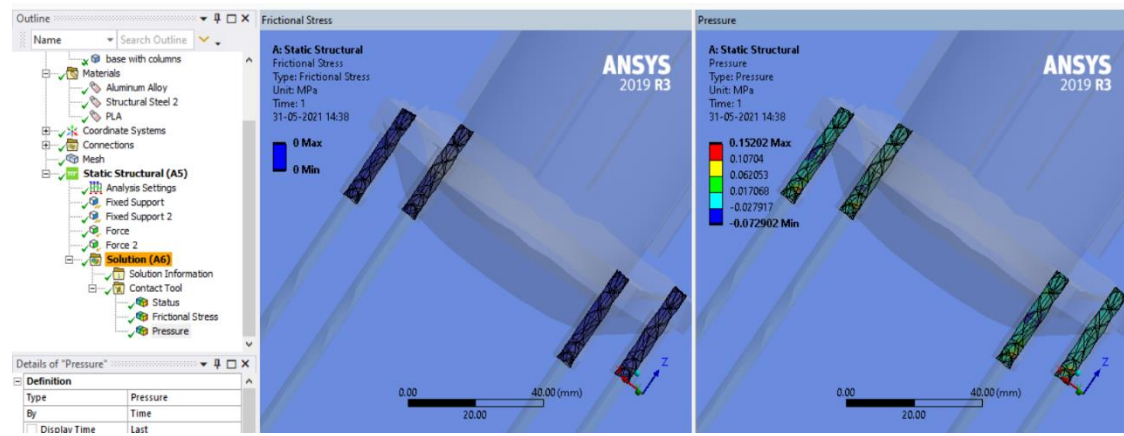


Figure 11.8: FEA of Contact Regions using PLA 2

The above results all fall within the maximum yield strength of PLA - 55.5 MPa. Therefore, PLA can be used to build the prototype, which helps validate the mechanism.

The torsion springs and the compression springs are all made of Beryllium Copper. The application of the supports and forces and the results of their FEA are all shown previously.

## 11.2 Additive Manufacturing & Assembly of Components

FDM was used to print the model of the Antenna Deployment Mechanism using PLA material. FDM (Fused Deposition Modelling) falls under the material extrusion category of 3D printing technology. In an FDM printer, the filament is pushed into the hot extruder. The filament is heated first and then deposited through the nozzle onto a build platform in a layer-by-layer process to form the complete object.

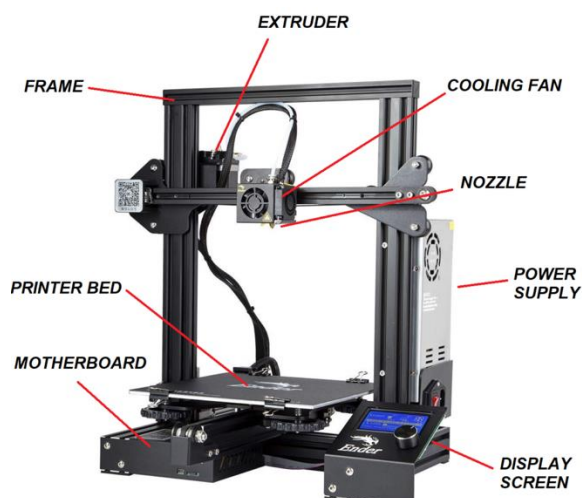


Figure 11.9: FDM Printer

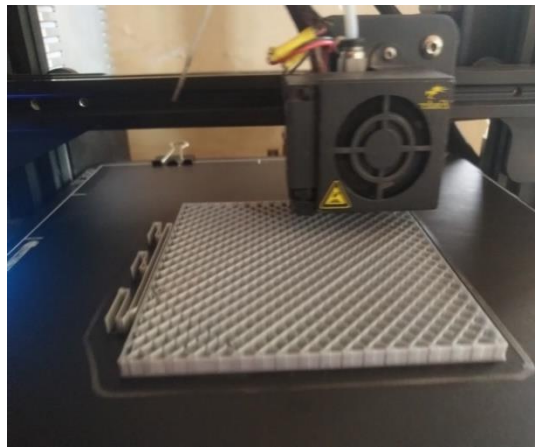


Figure 11.27: Printing of Base

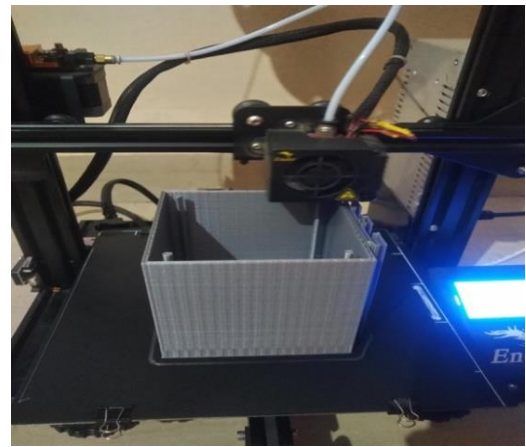


Figure 11.18: Printing of Box

The 3D designs were made on CATIA and Fusion 360 and converted to STL format for the FDM printer to read. The base of the box is first printed followed by the walls of the box and the columns present in the interior of the box. Similarly, the other 4 components - namely the lid with hinges, antenna hub on the base plate, blocking part and pin - were printed. The fabricated components are shown in the figures below. The remaining parts are either off-the-shelf components, or are readily available through orders to makers.



Figure 11.54: Fabricated Box w/ Male Hinge



Figure 11.45: Fabricated Lid w/ Female Hinge



Figure 11.36: Fabricated Hinge Pin

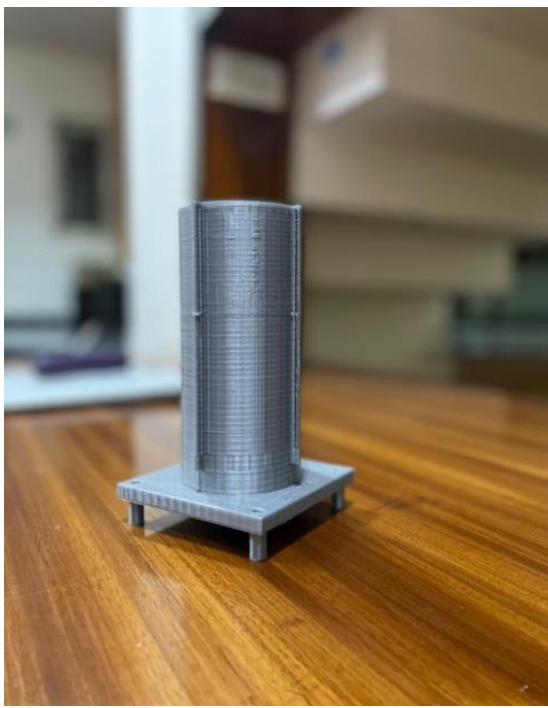


Figure 11.89: Fabricated Antenna Hub



Figure 11.63: Assembled Box & Lid

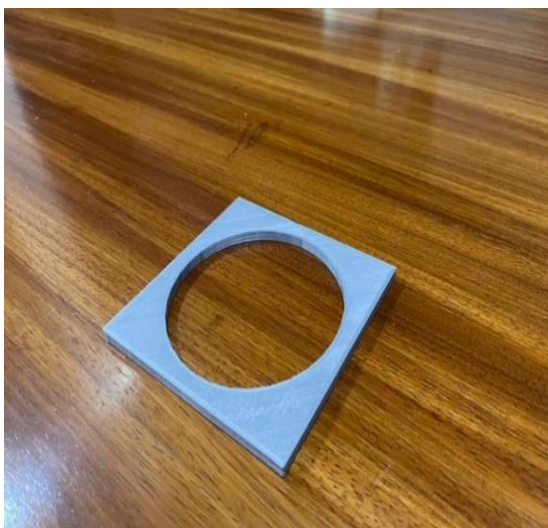


Figure 11.72: Fabricated Blocking Plate



Figure 11.81: Fabricated Components

## 12 Result and Discussion

The project had the initial objective of designing and manufacturing a deployment mechanism for satellite antennae. In that regard, the designs obtained were thorough, robust and fully functional. The static structural and dynamic analyses performed on them ensured their guaranteed performance under the operational conditions. The proof of concept in the form of a PLA prototype demonstrates the feasibility of the concept and its conformity to required configurations.

On the basis of meeting the objectives set out in the beginning, the success of the methodology followed, and the culmination of the project into a working model suitable for adaptation into CubeSat's of a variety of sizes and functionalities, the project may be deemed a successful endeavor.

## 13 Conclusion and Scope for Future Work

Due to modularity of the thus discussed antenna deployment model, it can be integrated in larger cube sets. For example, the 2U CubeSat can be placed in a 12U cube sat. Newer, more modular and inexpensive innovations in design and material science reduce costs and increase productivity achievable pre-launch.

Scope for future work includes developing autonomous systems that don't require interface with controllers during performance, research in newer/better materials used and the properties they may afford, and achieving a multiplicity of functional operations. It is possible with the foundational design of a deployment system, such as the one under discussion, to then build on it to achieve specificity in terms of required functionality, as well as advancement of the possible functionalities. Technologies that aid larger satellites, accompany interplanetary missions, as well as achieve hitherto unaccomplished miniaturizations are possible with a foundational deployment scheme.

In conclusion, the project was a successful starting step towards more advanced satellite-making. In achieving a basic deployment mechanism for antennae adaptable to other satellite booms, this project establishes a solid footing in the realm of space exploration using CubeSat's.

## 14 References

1. [Doncaster, B., et. al., "SpaceWorks' 2017 Nano/Microsatellite Market Forecast", Proceedings of the AIAA/USU Conference on Small Satellites, Swiftly Session 2, SSC17, 2017]
2. [Adamowski, J., "SmallSat Market Forecast to Exceed \$30 Billion in Coming Decade", Space News, 9th, August 2017, Online]
3. [Murphrey, T. et. al., "High Strain Composites," Proceedings of the 2nd AIAA Spacecraft Structures Conference, 2015 AIAA SciTech Conference, Session on Composite Materials for Spacecraft Structures, AIAA 2015-0942, Kissimmee, FL.]
4. [Wikipedia page on "High Strain Composite Structure", authored primarily by B. Davis 2014, [https://en.wikipedia.org/wiki/High\\_strain\\_composite\\_structure](https://en.wikipedia.org/wiki/High_strain_composite_structure)]
5. [Storable Tubular Extensional Member Device, US Patent #3434674]
6. [Annon, "Tubular Spacecraft Booms (Extendible, Reel Stored)," tech. Prep. SP8065, NASA, Feb 1971]
7. [Cox, K., et. al., "Flight Build of a Furled High Strain Composite Antenna for CubeSats," | Proceedings of the 5th AIAA Spacecraft Structures Conference, 2018 AIAA SciTech Conference, Session on Composite Materials for Spacecraft Structures, AIAA 2018-1678, Kissimmee, FL.]
8. [Mechanism Design & Flight Build of Furled High Strain Composite Antenna for CubeSats]
9. [Bruce Davis\*, Ryan VanHalle\*, Kevin Cox\* and Will Francis\* AIAA SciTech Forum 8-12 jan 2018]
10. [CubeSats 10: Basic Concepts and Processes for First-Time CubeSat Developers | E-pamphlet on NASA Website]
11. [CubeSat Design Specifications | [www.cubesats.org](http://www.cubesats.org)]